# SYNTHETIC, PHYSICAL, AND PHOTOLYTIC PROPERTIES OF LINEAR, BRANCHED, AND CYCLIC OLIGOGERMANES

By

SANGEETHA P. KOMANDURI

Bachelor of Science in Specialized Chemistry
University of Illinois at Urbana-Champaign
Urbana-Champaign, Illinois
2013

Submitted to the Faculty of the
Graduate College of the
Oklahoma State University
in partial fulfillment of
the requirements for
the Degree of
DOCTOR OF PHILOSOPHY
July, 2018

SYNTHETIC, PHYSICAL, AND PHOTOLYTIC

PROPERTIES OF LINEAR AND CYCLIC

OLIGOGERMANES

Dissertation Approved:

Dr. Charles S. Weinert

Dissertation Adviser

Dr. Allen W. Apblett

Dr. Richard A. Bunce

Dr. Toby L. Nelson

Dr. John N. Veenstra

# ACKNOWLEDGEMENTS

This work is dedicated to the many people who have supported and helped me during my time as a graduate student. First and foremost, I'd like to thank my committee members Dr. Bunce, Dr. Apblett, Dr. Nelson, and Dr. Veenstra for their assistance and the knowledge they have imparted onto me over the years. In addition to their help in the classroom, their advice has been vital. Of course the biggest influence on my time here has been my research advisor Dr. Weinert. He has provided me with the mentorship and practical knowledge which I have used daily in and outside of the lab. None of this work could have been completed without his valuable guidance and consistent help, all which has molded me into an independent researcher.

Within the laboratory and the chemistry department at OSU, my colleges, friends, and staff members have given me great support during the technical aspects of my research. My lab mates Alex Shumaker, Miguel Leal, and Ardalan Hayatifar are the research family who encouraged, taught, and gave me the structural criticism to push me further and improve my skills. Along with my fellow colleges I'd also like to thank former students Kimberly Roewe, Aaron Schrick, Evangeline Renuko, Wes Honeycutt, Eric Butson, Claire Spice, Chen, and Heather Storm who have aided me both mentally and technically throughout this process. In addition to my lab mates in the states, I would also like to give my appreciation to our collaborators in Graz, Austria. My gratitude to Melanie Wolf, Beate Steller, Micheal Traxler, Astrid Falk, Ana Torvisco, Elli Schwarz, Judith Biedermann, and others at Graz Technical University who gave advice, company, and stimulating conversations on a regular basis. I'm also very grateful to Dr. Frank Uhlig for providing me the unique opportunity to study and work in his laboratories.

Finally, I'd like to give thanks to my parents and family who have been by my side and assisted me to achieve more. Their constant reinforcement during the challenges has given me the motivation to pursue my PhD and has bolstered my drive. I'd like to partially dedicate this work to my late father, who has always instilled the value of hard work in any task I undertake. My mother, on the other hand, has been my rock all throughout my studies. Her continued love and support have been immeasurable, and without either of them I would not be where I am today. I am sincerely thankful for my family, both academic and personal, who have helped me along this journey to accomplish my goals now and in the future.

Name: SANGEETHA P. KOMANDURI

Date of Degree: JULY, 2018

Title of Study: SYNTHETIC, PHYSICAL, AND PHOTOLYTIC PROPERTIES OF LINEAR, BRANCHED, AND CYCLIC OLIGOGERMANES

Major Field: CHEMISTRY

Abstract:

The following dissertation focuses on the synthesis and characterization of unique linear, branched, cyclic germanium compounds to further the knowledge and scope of organometallic chemistry of the element. In chapter II a 2-germanium atom end capping reagent was used for synthesis of longer linear oligomer using monohydride $Ph_3GeGePh_2H$. This species was observed to be thermally unstable upon heating the material to 200 °C. Thermal decomposition products were identified as $Ph_3GeH$ and assumed germylene ($Ph_2Ge$:), which subsequently polymerized. Reactions were monitored by NMR ($^1H$ and $^{13}C$) spectroscopy and characterized using X-ray crystallography.

A series of linear oligomers $R_3Ge(GePh_2)_nGeR_3$ ($n$ = 0 or 1), were synthesized and subsequently photolyzed. The photodecomposition pathways of these compounds were analyzed after exposure to UV-C light (280-100 nm) in the presence of acetic acid, acting as a germylene trapping agent. Resulting photoproducts showed germylene ($Ph_2Ge$:) extrusion and germyl radical formation ($R_3Ge\cdot$) to yield $R_2Ge(H)OAc$ and $R_3GeOAc$, $R_3GeH$ and $R_3GeGeR_3$ respectively. Photoproducts were identified by 1H NMR, electron impact gas-chromatography (EI-GC/MS), and high resolution accurate mass-mass spectrometry (HRAM-MS).

Three branched oligogermanes $(Me_3Ge)_3GePh$, $(Me_2Bu^tGe)_3GePh$, $(Me_2PhGe)_3GePh$, and $(Bu^n_3Ge)_3GePh$ were synthesized and characterized. All species were prepared and characterized by NMR ($^1H$, $^{13}C$, and $^{73}Ge$) and HRAM-MS. The varying substituent composition on the peripheral $R_3Ge$- groups provided insight on the electronic properties studied by cyclic/differential pulse voltammetry (CV and DPV) and UV-visible spectroscopy.

Chapter V describes the synthesis of a series $Pr^i_3Ge(GePh_2)_nGePr^i_3$ ($n$ = 0-3) linear oligomers. Compounds were characterized using NMR ($^1H$ and $^{13}C$), UV-vis, and CV/DPV. A bathochromic shift was seen *via* Ge – Ge chain elongation, and species became easier to oxidize. Crystals of the pentagermane showed dichroism and luminescence, the smallest discrete oligomer to exhibit polymeric like properties.

The final chapter focuses on the synthesis of perarylated cyclotetra- $(Ar_2Ge)_4$ and cyclopentagermanes $(Ar_2Ge)_5$ (Ar = 2,5-xylyl), using $Ar_2GeCl_2$ as the precursor. These species were selected to increase solubility in ring opening reactions with an alkali metal. Crystals were only obtained in experimental conditions for $(Ar_2Ge)_4$. However, the expected product turned out to be a germyl-substituted cyclogermane $ClGeAr_2(Ge_4Ar_7)$, the first compound of its class to be synthesized.

TABLE OF CONTENTS

Chapter Page

LIST OF TABLES

LIST OF FIGURES

Figure Page

LIST OF SCHEMES

# CHAPTER I

## INTRODUCTION

The element germanium was first discovered in 1886 by Clemons Winkler in the mines near Freiberg, Saxony as the silver-rich mineral argyrodite $Ag_8GeS_6$.[1-2] Originally proposed by Dmitri Mendeleev, germanium was predicted to possess comparable properties to silicon and therefore was called ekasilicon.[3] It has five naturally occurring isotopes $^{70}Ge$, $^{72}Ge$, $^{73}Ge$, $^{74}Ge$, and $^{76}Ge$ and organometallic derivatives are generally found in +4 or +2 oxidation states.[4-5] Germanium is a metalloid and an indirect band gap semiconductor and belongs to group 14. It was therefore used in the development of the first transistor in 1947, and this is arguably one of the most important electronic events of the 20$^{th}$ century, as it paved the way for integrated circuits and microprocessors which are the basis for all modern electronics. Pure germanium was used as a semiconductor until the mid 1960s when it was gradually replaced by silicon because of its lower cost.[6-7] Due to its high index of refraction, germanium is now used in IR lenses, microscopes, wide-angle cameras, and fiber optic cables.[8] Some germanium compounds are also used for chemotherapy treatment, as alloying agents, polymerization catalysts, and as a phosphor for fluorescent lamps. Certain germanium compounds also have low mammalian toxicity to target bacterial activity, and have the potential as antibacterial agents.[9-10]

Group 14 elements (C, Si, Ge, and Sn) that are found in the formal (IV) oxidation state have the ability among other main group elements to form oligomers and polymers. Polysilanes

were a new class of inorganic metalloid polymers introduced in the early 1980s.[11] These materials possessed unique electronic and optical properties that are particularly useful for photoresists, photoconductors, and other non-linear optical materials.[12] The chemistry of other group 14 (Si, Sn) oligomers and polymers has been studied to a significant extent.[13-16] However, due to the high cost of starting materials and a dearth of useful synthetic methods, analogous oligogermanes and polygermanes have been yet to be as thoroughly investigated.

Heavy catenated group 14 oligomers are able to exhibit unique optoelectric properties due to their inherent σ-delocalization.[17] First observed in polysilanes, this has also been observed in heavier germanium and tin analogs. This phenomenon results in the electrons in the highest occupied molecular orbital (HOMO) being delocalized across the E – E (E = Si, Ge, or Sn) backbone. Electrons are thus able to move over the entire length of the backbone rather then being localized between two atoms. The σ bonding nature of the HOMO is due to the overlap of the diffuse $sp^3$ orbitals when oriented in a *trans*-coplanar fashion (**Figure 1.1**). Optimal overlap of the $sp^3$ hybridized molecular orbitals is achieved when the atoms are oriented this way, and are delocalized over the entire oligomeric backbone.[18-19] This delocalization imparts oligomeric germanium compounds, which have single E – E bonds, with physical properties that are similar to conjugated unsaturated hydrocarbons while structurally they are analogues of saturated hydrocarbons.[20]

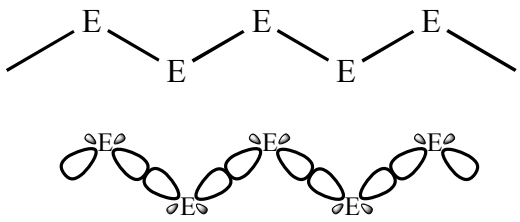


**Figure 1.1:** Orientation of the $sp^3$ orbitals of the HOMO in a *trans*-coplanar fashion.[17]

The interesting physical properties exhibited by discrete germanium oligomers can be manipulated by altering the chain length and/or the substituent composition.[21-22] These optical and

electrical attributes can be probed by ultraviolet-visible spectroscopy (UV-vis) and cyclic/differential pulse voltammetry (CV/DPV) respectively. In these systems the HOMO is σ-bonding in nature while the lowest unoccupied molecular orbital (LUMO) being $\sigma^*$ antibonding in nature. The HOMO-LUMO electron transitions typically involve the promotion of an electron from the $\sigma \longrightarrow \sigma^*$ molecular orbital.[23] Since this transition falls in the ultraviolet region, it can be studied spectroscopically by monitoring the UV-vis absorbance maxima. A bathochromic or red shift, is observed upon elongation of the Ge – Ge backbone.[24-25] This trend is also observed when more electron donating groups are added to the oligomer, but to a lesser extent. The CV/DPV also shows a change in the oxidation potential of catenated species, where when the degree of catentation is increased the oligomer becomes easier to oxidize.[26-27] Also adding more electron donating substituents decreases the oxidation potential. Discrete group 14 oligomers can possess physical properties comparable to their larger polymeric counterparts, making them useful as small molecular models of these systems and could lead for the development of new conductive and electroluminescent materials.[28-30]

Unlike their hydrocarbon analogs, which are stable at ambient temperatures and under oxygen, germanium – germanium bonds need to be stabilized by the presence of organic functional groups or halogens. Group 14 alkane analogs are often highly reactive and can be pyrophoric in nature. They are also often difficult to purify due to their high sensitivity to both air and moisture. The synthesis of organogermanium compounds began with tetraethylgermane $Et_4Ge$ by Winkler after the initial discovery of germanium in 1887.[31] However, it was not until a few decades later when $Ph_3GeGePh_3$ was prepared as the first recorded compound containing a germanium-germanium bond.[32] Further progress on germanium catenates has been stalled due to the lack of methods for germanium bond formation. Synthesizing Ge – Ge bonds has always been problematic in comparison to the silicon[33-34] and tin[35-36] congeners, as they are often complicated by low yields and formation of product mixtures.[37-39] All these combined factors make working with germanium challenging.

Common methods of germanium-germanium bond formation include Wurtz-type polycondenstation of organogermanium halides reacted with alkali metals[40], thermal decomposition

of germylmercury compounds[41], nucleophilic substitution reactions with triorganogermanium anions and organogermanium halides[42], the insertion of germylenes $R_2Ge$: into Ge – X bonds (X = N, O, or halogen)[43], and the reactions of Grignard reagents with germanium (IV) halides[44]. It is important to point out that the formation of triorganogermanium anions $R_3Ge^-$ in nucleophilic substitution reactions is unique to germanium chemistry and is useful in oligomer preparation, something not observed with Si or Sn.[45] However, most of these methodologies afford low yields and multiple product mixtures.

The most detailed study conducted on linear and cyclic germanium syntheses, spectra, structures, and reactivity was later reported by Dräger in the 1980s. His series of nineteen publications focused on germanium catentates having between two and six germanium atoms in the oligomeric backbone.[46-63] A later synthetic improvement was found using samarium(II) iodide, a mild one-electron reducing agent, to prepare a series of discrete di- and trigermanes with better yields (**Scheme 1.1**).[64-65]

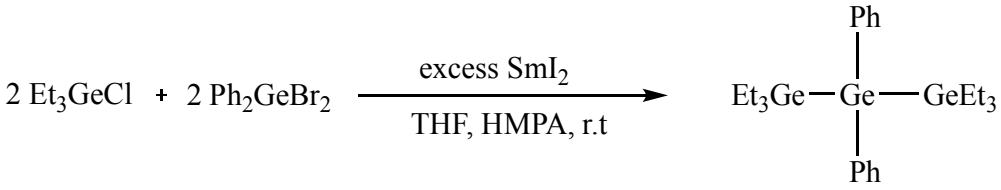


**Scheme 1.1:** Germanium – Germanium bond formation using $SmI_2$.[64]

The hydrogermolysis reaction involves a germanium amide $R_3GeNMe_2$ with a germanium $R_3GeH$ in order to form Ge – Ge bonds in high yields. The analogous hydrostannolysis has been used for the preparation of oligostannanes, yet the reaction conditions were more difficult for germanium species. The early use of the hydrogermolysis reaction was thought to proceed only with the use of an "activated" Ge – H bond by means of an electron withdrawing group (EWG) such as pentafluorophenyl-substituted germanium hydride $(C_6F_5)GeH$.[66] However, this route proved

inefficient for preparing a diverse series of oligogermanes as there is a limitation on the possible substituents used to "activate" the germanium atom.

Weinert *et al*. found that the hydrogermolysis reaction can be used to promote Ge – Ge bond formation without an "activated" germanium-bound hydrogen, but instead by using acetonitrile $CH_3CN$ as the solvent.[67-68] Initially this reaction was conducted in refluxing benzene or toluene; however, no product formation was observed. It was not until acetonitrile $CH_3CN$ was used as the solvent that the digermane $Bu^n_3GeGePh_3$ was isolated in 84% yield, by reacting $Bu^n_3GeNMe_2$ with $Ph_3GeH$.[84] The reaction pathway was studied by NMR, showing the amide reagent is actually converted to an $\alpha$- germyl nitrile ($R_3GeCH_2CN$) intermediate *in situ*, which contains a reactive Ge – C bond. To demonstrate that this intermediate is crucial in the formation of a Ge – Ge bond, acetonitrile-$d_3$ was used to monitor the reaction by $^1H$ and $^{13}C$ NMR.[67] Also the synthesis of the $\alpha$-germyl nitrile was achieved by reacting a trialkylgermanium chloride $R_3GeCl$ with $LiCH_2CN$, when the latter reagent was generated from lithium diispropylamide and $CH_3CN$.[67] The independently prepared $\alpha$- germyl nitrile was then added directly to $Ph_3GeH$, and resulted in the formation of a digermane. This reaction was also repeated with other solvents and a catalytic amount of acetonitrile, but no formation of the digermane was detected. The evidence supports the hypothesis that acetonitrile plays two roles, as both solvent and reagent to form the $\alpha$- germyl nitrile species *in situ*, and makes the formation of the $\alpha$- germyl intermediate the crucial component in Ge – Ge bond formation.[67]

Besides providing better overall yields and product selectivity, the hydrogermolysis reaction can be used to increase the length of catenated species in a step-wise manner and to enable direct control of the composition of organic side groups. Therefore, the hydrogermolysis reaction provides a versatile route to prepare numerous oligomers with different chain lengths and a range of substitution patterns, allowing for the molecule to be specifically tuned to process the desired optical and electronic properties.

The other area of research, important to this work, is the chemistry of germylenes ($:GeR_2$), divalent germanium derivatives. Germylenes, are highly reactive analogues of carbenes, and due to this attribute, they undergo rapid polymerization making them difficult to characterize.[69] These species are in the +2 oxidation state and often require sterically bulky or electron donating ligands to stabilize them for further isolation and characterization (**Figure 1.3**). Germylene monomers have a rich chemistry due to the Ge(II) center having both an electron lone pair and a vacant p-orbital. This allows germylenes to act as a Lewis base, with donating ability from its electron pair in the $sp^2$ hybridized orbital, but also as a Lewis acid, accepting electron density into the empty p-orbital.[70] Advancements in the synthesis and characterization of germylenes can be attributed to spectroscopic methods. However, germlyenes can also be easily identified by several common germlyene and divalent group 14 compound trapping reagents. Such compounds include benzil, 2,3-dimethyl-1,3-butadiene (DMB), $CCl_4$, and acetic acid (AcOH).[71-72]

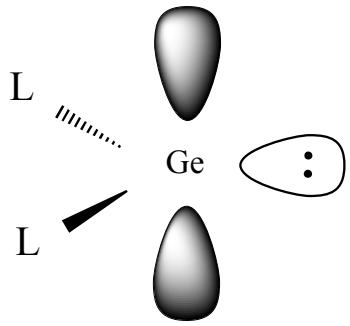


**Figure 1.2:** General structure for a germanium (II) monomer.

The research results described in this dissertation involves the synthesis and characterization of new linear, branched and cyclic germanium compounds and an investigation into their unique chemistry. Chapter II will describe the synthesis and reactivity of a linear digermane $Ph_3GeGePh_2H$, that can be used as a synthetic precursor for the preparation of longer catenated oligogermanes. The strategy employed the monohdyride digermane to act as a potential end cap by reaction with either a

$Me_2N(GePh_2)_nNMe_2$ ($n$ = 3 or 4). In order to yield a hepta- ($n$ = 3) or octagermane ($n$ = 4), this two-germanium atom building block was used in the hydrogermolysis reaction. However, due to the thermal instability of the $Ph_3GeGePh_2H$, decomposition was observed to yield both a germylene ($:GePh_2$) that subsequently underwent polymerization, and triphenyl germane ($Ph_3GeH$). As germylenes themselves can not usually be isolated, the produced $:GePh_2$ was trapped using 1,4-butadiene (DMB) and characterized.

Chapter III describes the photolysis of discrete oligogermanes, including di- and trigermane $Bu^n_3Ge(GePh_2)_nGeBu^n_3$ ($n$ = 0 or 1). The linear catenates were photolyzed by UV-C light (100-280 nm) in the presence of acetic acid as a germylene and germyl radical trapping reagent, resulting in the isolation of $R_2Ge(H)OAc$, $R_3GeOAc$, and $R_3GeH$ photoproducts. In addition, germyl radicals ($R_3Ge\cdot$) that are also formed generate digermanes, that are produced by the combination of two $R_3Ge\cdot$ radicals. The photoproducts were characterized by $^1H$ and $^{13}C$ NMR, gas-chromatography mass spectroscopy (GC-MS), and high resolution accurate mass-mass spectroscopy (HRAM-MS).

The optical and electronic properties of a series of alkylsubstituted branched compounds are the focus of Chapter IV. The oligomers include $(Me_3Ge)_3GePh$, $(Me_2Bu^tGe)_3GePh$, $(Me_2PhGe)_3GePh$, and a previously known $(Bu^n_3Ge)_3GePh$. The effects of varying the substituent pattern in the peripheral $R_3Ge$- group on the physical properties of these compounds were investigated using NMR ($^1H$, $^{13}C$, and $^{73}Ge$), UV-visible spectroscopy, CV/DPV, and HRAM-MS. This represents the first analysis by HRAM-MS of branched germanium species.

Chapters V discusses the synthesis and characterization of a series of isopropyl terminated linear oligogermanes $Pr^i_3Ge(GePh_2)_nGePr^i_3$ ($n$ = 0-3). Their physical properties were also probed by NMR ($^1H$, $^{13}C$), UV-vis, and CV/DPV. The oligogermanes show a successive red shift in their absorbance maxima and become easier to oxidize as their germanium backbone length is increased. The X-ray crystal structure of the pentagermane $Pr^i_3Ge(GePh_2)_3GePr^i_3$ was determined, and it exhibits dichroic and luminescent behavior in solution. The five chained oligomer is the smallest discrete molecule to mimic the properties of larger polygermanes systems.

Lastly, Chapter VI discusses the synthesis of a series of perarylated cyclic $(Ar_2Ge)_4$ and $(Ar_2Ge)_5$ compounds prepared from a dichlorodiarylgermane $Ar_2GeCl_2$ and an alkali metal. These compounds were of interest as precursors for $\alpha,\omega$-dilitihiated polygermanes $Li(GePh_2)_nLi$ ($n$ = 4, 5) by ring opening reactions. Converting these lithiated compounds to synthons for the hydrogermolysis reaction might allow for preparation of longer linear oligogermanes. However, this reaction resulted in multiple bond cleavage of the Ge – Ge bonds. In order to control the interaction with the metal surface, it was desirable to manipulate solubility of the cyclic species, which was is done by changing the aryl substituent from phenyl groups to 2,5-xylyl. The preparation of the $(2,5\text{-xylyl})_2GeCl_2$ precursor needed for both cyclic homologs, $(Ar_2Ge)_4$ and $(Ar_2Ge)_5$, was optimized by a Grignard strategy. However, the expected cyclic tetragermane did not crystallize, but rather crystals of the first observed germyl-substituted cyclotetragermane. This product is suspected to be formed by some type of aryl-migration, but further work must be done to definitively elucidate the reaction pathway.

# CHAPTER II

## SYNTHESIS AND THERMAL DECOMPOSITION OF $Ph_3GeGePh_2H$

### 2.1 Introduction

Oligomeric germanium species have always been more difficult to prepare and characterize due to the weakness of germanium-germanium bonds. In anticipation of using the hydrogermolysis reaction to prepare longer catenated oligogermanes, strategies were explored to prepare larger building blocks to increase chain length. Replacement of aryl substituents at both of two germanium atoms of a digermane, to give a compound with a general formula $Ge_2Ar_4X_2$, is relatively facile. The digermane $(Cl_3CC(O)O)Ph_2GeGePh_2(O(O)CCCl_3)$ **2** was synthesized by Dräger *et al.* from $Ge_2Ph_6$[73] and trichloroacetic (TCA) in reasonable yields. Additionally, $Ge_2Ph_6$ could also be subsequently converted to both $Ge_2Ph_4Cl_2$ and $Ge_2Ph_2Cl_4$ using HCl under pressure.[74] However, generation of the monosubstituted digermanes $Ge_2Ar_5X$ by replacing only one aryl group, proved to be a more difficult synthetic challenge. Preparation of these compounds are of interest as they provide two-atom end-capping synthons for synthesizing long-chain oligogermanes or mixed group 14 element oligomers or polymers. A variety of mono-substituted digermanes have been successfully synthesized by Zaitsev *et al*., including $Ph_2(OTf)GeGeMe_3$[75], $ClPh_2GeGeMe_3$[75], $Ph_2Ge(OTf)GePh_3$[76], $Ph_2Ge(OTf)GeBu^tMe_2$[76], and $ClPh_2GeGePh_3$[76]. All the aforementioned species were fully characterized by spectroscopic techniques.

The digermane $HPh_2GeGePh_2H$ had been synthesized successfully, but product isolation was needed after each subsequent step within the method causing some preparatory complications.[23] The previous literature procedure was altered to ensure facile workup, purity, and higher yields, shown below in **Scheme 2.1**. As the 1,2-dihydro-1,1,2,2-tetraphenyldigermane ($HPh_2GeGePh_2H$) was frequently needed in synthesizing tetragermanes ($R_3Ge(GePh_2)_2GeR_3$ where R = Et, $Bu^n$, $Pr^i_3$), an efficient method of preparation was necessary. It was found that Dräger's method, in addition to preparing **2**, could also synthesize the monosubstituted digermane $Ph_3GeGePh_2(O(O)CCCl_3)$ **3** in a mixture by variation of the experimental conditions. In order for the full conversion of **2** to form from $Ge_2Ph_6$ (**1**), a molar ratio of 5:1 trichloroacetic acid (TCA) to **1** was used in boiling toluene.[73] However, it was observed that a molar ratio of 4.3:1 of TCA:**1** achieves only partial conversion, and produces a mixture of **2** and $Ph_3GeGePh_2(O(O)CCCl_3)$ (**3**) when a solution of hexaphenyldigermane $Ph_3GeGePh_3$ and trichloroacetic acid were heated in toluene for 72 hours at 95 °C.

The mixture of **2** and **3** was converted to the corresponding chloro-substituted species $ClPh_2GeGePh_2Cl$ (**4**) and $Ph_3GeGePh_2Cl$ (**5**) by direct addition of 1.0 M ethereal HCl, and the solution was then heated at 95 °C for 18 hours in a sealed Schlenk tube. The workup consisted removing the solvent *in vacuo*, washing the crude material with several aliquots of hexane to dissolve re-formed $Cl_3CC(O)OH$ and any other soluble impurities, until the supernatant became colorless. The product was isolated as a white product after drying. The ratio of each product in the mixture could not be determined by simple integration of $^1H$ NMR spectra due to signal overlap, but $^{13}C$ NMR identified the presence of both **4** and **5** since there were twelve distinct aromatic resonances observed that matched literature values for both compounds. The initial ground work was expanded upon to rework the products prepared in an attempt to prepare longer precursors.

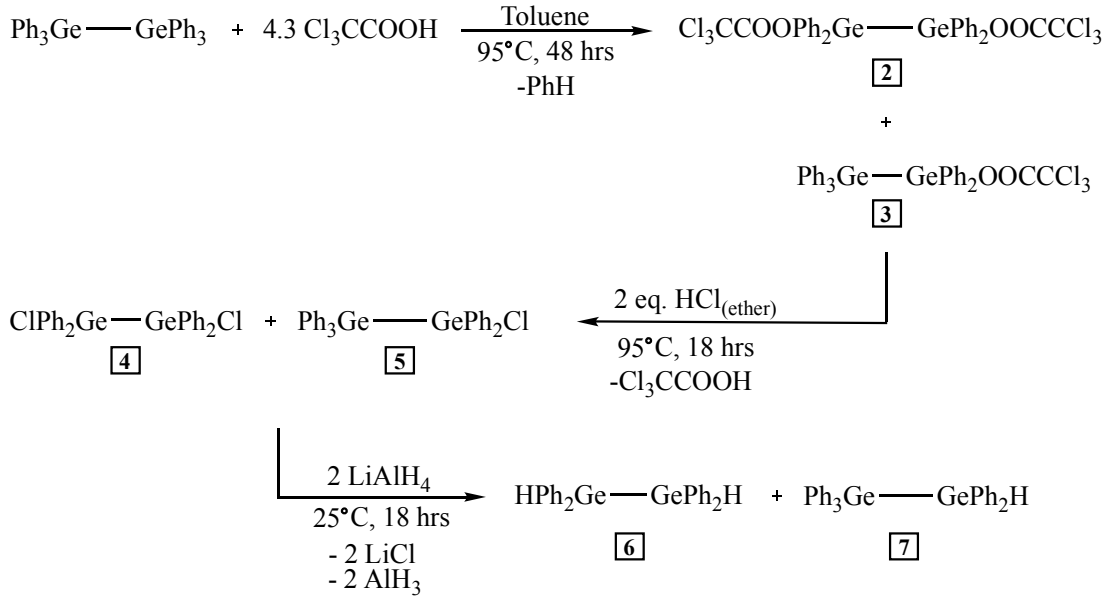


**Scheme 2.1:** Synthetic route of dihydride (**6**) and mono- (**7**) species.

The mixture of **4** and **5** were subsequently used to prepare the corresponding hydrides $HPh_2GeGePh_2H$ (**6**) and $Ph_3GeGePh_2H$ (**7**) using $LiAlH_4$. The $^1H$ NMR spectra of the product mixture contains three signals in the hydride Ge – *H* region (**Figure 2.2**), with peaks at δ 5.57, 5.72, and 5.85 ppm. The peak at δ 5.57 ppm corresponded to $HPh_2GeGePh_2H$ (**6**)[11], and the peak at δ 5.85 ppm is due to a small amount of $Ph_3GeH$ generated during the reaction. The major peak at 5.72 ppm corresponded to the monohydride $Ph_3GeGePh_2H$ (**7**). The mixture of compounds was determined to be composed of roughly 79% **7**, 10% **6**, and 11% $Ph_3GeH$ *via* integration of the resonances. The monohydride **7** was isolated from **6** and $Ph_3GeH$ by crystallization of a saturated toluene solution at -35 °C, giving **7** in of 28% yield based on starting digermane $Ge_2Ph_6$. The NMR of the purified compound was compared to that reported for **7** prepared by a previous method, using $Ph_3GeLi$ with $Ph_2GeHCl$. Upon inspection the spectral data were identical and the purity of **7** was confirmed.

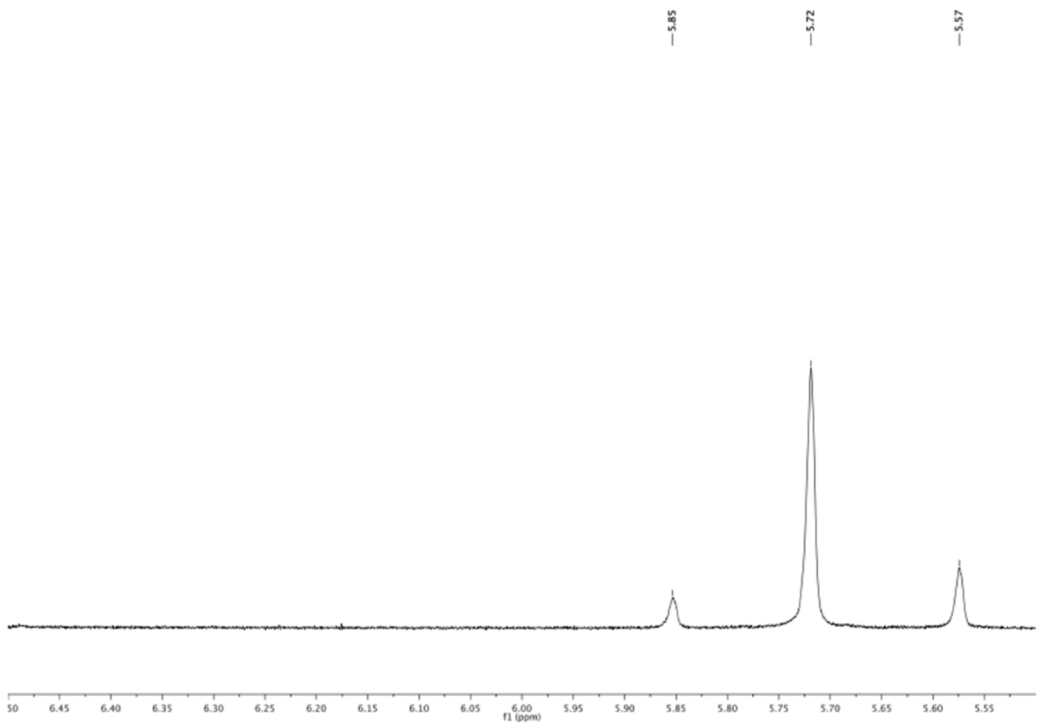


**Figure 2.1:** $^{1}$H NMR spectra of Ge – *H* region after treating mixture of **6** and **7** with $LiAlH_4$.

Suitable crystals for analysis by X-ray diffraction quality crystals of **7** were obtained with two different morphologies, two types of crystals, one set larger and another set smaller. The physically larger crystals (**7a**) have three independent molecules in the unit cell. In all three independent molecules of **7a**, both germanium atoms are disordered over two sites each with an occupancy greater than 97.8% in one position versus the other, such that the occupancy of the second position has little to no effect on the structural parameters, bond distances and bond angles, within each molecule.

The germanium-germanium bond distances in molecules 1, 2 and 3 of **7a** are 2.4219(7), 2.4205(7) and 2.4279(7) Å respectively, with the average bond distance among the three molecules being 2.4234(7) Å. The Ge-H bond distances for independent molecules 1, 2, and 3 are 1.35(4), 1.41(4) and 1.38(4) Å respectively, and average to 1.38(4) Å. The bond distances for Ge-$C_{ipso}$ for molecules 1, 2, and 3 average 1.956(4), 1.956(4), and 1.959(4) Å respectively, and

together average 1.957(4) Å. These Ge-$C_{ipso}$ distances all fall within the range of typical bond distances for germanium-bound phenyl rings. In all three molecules of **7a** the environment around Ge(1) is almost ideal, with the C – Ge – C bond angle averaging to 109.02 °. On the other hand, the environment of Ge(2) is slightly distorted from the idealized tetrahedral geometry, with an average bond angle of C – Ge – C at 106(1) ° due to the presence of the hydrogen atom. The hydrogen atoms were identified crystallographically.

The second smaller set of crystals (**7b**), which crystallized with only one independent molecule in the unit cell, again has disorder of the Ge atoms with the occupancies of one site greater than 97.3%. Ignoring the minimal contribution of the second position of the atoms in **7b**, the Ge – Ge bond distance is 2.4213(5) Å, the Ge – H bond distance is 1.49(3) Å, and the Ge – $C_{ipso}$ bond distances averaging to 1.954(3) Å. The average C – Ge – C bond in **7b** angle at Ge(1) is 108.5(1)° and angle at Ge(2) is 107(1) °. This indicates that both **7a** and **7b** have similar structures, but the distance of the Ge – H bond in **7b** is longer than each of the three Ge – H bonds in **7a**. It was observed that Ge – Ge bond distance in $Ge_2Ph_6$ (**1**) is 2.437(2) Å, but replacing one phenyl group with a less sterically hindered hydrogen atom, a shortening of the Ge – Ge bond is observed by 0.02 Å along with a slight environmental distortion of the hydrogen bound germanium atom. This initial work, in part completed by co-author Schrick, A. C., was further expanded upon below.

**2.2 Results and Discussion**

The synthesis of **7** was undertaken to provide a two-germanium synthon for the preparation of long oligogermane chains, acting as an end capping reagent. This strategy is a 2 + $x$ + 2 method, where $x$ = 3 or 4 germanium atoms in length, referring to the three groups containing two or three germanium atoms combining to form the product. The digermane **7**

($Ph_3GeGePh_2H$) would be added to either $Me_2N(GePh_2)_3NMe_2$ or $Me_2N(GePh_2)_4NMe_2$ amides to synthesize a heptagermane $Ge_7Ph_{16}$ or an octagermane $Ge_8Ph_{18}$, which would be the longest structurally characterized germanes reported to date. In order to prepare the heptagermane, two equivalents of $Ph_3GeGePh_2H$ would be reacted with one equivalent of $Me_2N(GePh_2)_3NMe_2$, and to prepare the octagermane two equivalents of $Ph_3GeGePh_2H$ would be added to one equivalent of $Me_2N(GePh_2)_4NMe_2$. As a proof of concept, **7** was reacted with one equivalent of $Ph_3GeNMe_2$ in $CH_3CN$ to attempt to prepare a known trigermane $Ge_3Ph_8$ for comparison.[61,77] However, after stirring the reaction for 48 hours at 85 °C and removal of the volatiles the product isolated was an intractable mixture. In the $^1H$ NMR spectrum of the product mixture, a resonance at δ 5.85 ppm was identified as $Ph_3GeH$, which suggests that **7** is thermally unstable and decomposes under the above reaction conditions.

In order to confirm this postulate, a sample of **7** was heated alone in acetonitrile for 48 hours. A yellow oil was obtained after volatiles were removed, and its $^1H$ NMR spectrum contained multiple overlapping resonances in the aromatic region as well as a peak at δ 5.85 ppm again indicating the presence of $Ph_3GeH$. The solid **7** was distilled in a Kugelrohr oven at 160 ºC at a pressure of 0.01 torr, and the white solid distilled over and collected in a receiving flask after heating for 2 hours. This solid was identified as $Ph_3GeH$ and was obtained in 87% yield based on **7**. The material remaining in the distillation pot was a thick oil and its $^1H$ NMR spectrum contained numerous overlapping resonances, suggesting the formation of polygermanes.

These observations indicate that **7** is thermally unstable and decomposes both in the solid state and in solution. In order to ascertain the decomposition pathway, a sample of **7** was heated in toluene in a Schlenk tube at 95 ºC in the presence of 10 equivalents on 2,3-dimethyl-1,4-butadiene (DMB). After the reaction mixture was heated for 72 hours the volatiles were removed and the $^1H$ NMR spectrum of the product mixture was recorded. The resulting mixture showed $Ph_3GeH$ and a germacyclopentene **(8)** compound were present along with other polymeric materials shown in **Scheme 2.2**. The identity of compound **8** was confirmed by comparison of the

NMR spectra of known species germacyclopentene species in literature.[78] Previous work done by Mochida *et al.* shows that when simple extrusion of germylenes occurs in the presence of DMB, a germacyclopentene **8** is generated along with a germyl radical.[79] Germylenes are germanium analogues of carbenes having a singlet ground state that have an empty p-orbital and a lone pair on the germanium atom. These species are highly reactive and undergo dimerization, oligomerization, or polymerization.[80] Therefore, it was concluded that the presence of **8** and also of the polymeric material indicated that **7** decomposed *via* extrusion of a germylene $Ph_2Ge$: to generate $Ph_3GeH$. The germylene was subsequently trapped by DMB to produce **8**, but it also underwent rapid polymerization to yield polygermanes $[Ph_2Ge]_n$.

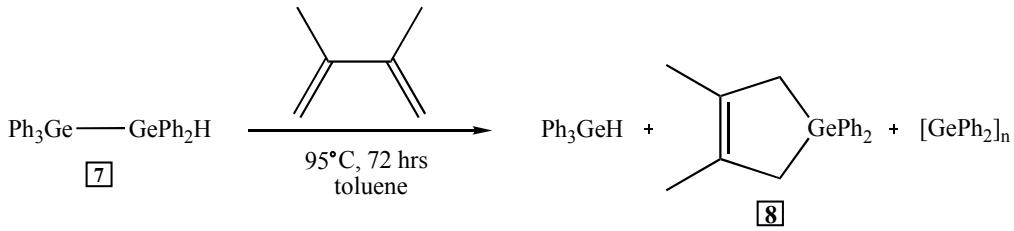


**Scheme 2.2:** Thermal decomposition of $Ph_3GeGePh_2H$ (**7**) with DMB in solution.

## 2.3 Conclusion

Variation of the synthetic method used to prepare $HPh_2GeGePh_2H$ (**6**) lead to a mixture of **6** and $Ph_3GeGePh_2H$ (**7**), when **7** was separated by selective crystallization. Digermane **7** was found to crystallize in two different morphologies, where one unit cell had three unique molecules while the other unit cell contained only one. The average Ge – Ge bond length between the two crystal structures of **7** was 2.4223(5) Å. An attempt was made to use this two-germanium atom synthon as a precursor in the hydrogermolysis reaction to prepare long chain linear oligogermanes. However, the experimental conditions caused the oligomer to undergo a thermal decomposition to yield $Ph_3GeH$ and germylene $Ph_2Ge$:, the latter of which polymerizes.

## 2.4 Experimental

*General Considerations*

All manipulations were carried out using standard Schlenk, syringe, and glovebox techniques. Reagents including $Cl_3CCOOH$, $LiAlH_4$, $LiNMe_2$, and 2,3-dimethyl-1,3-butadiene, and 1.0 M $HCl_{(ether)}$ were received from Aldrich. The digermane $Ge_2Ph_6$ was commercially available from Gelest. All reagents were used without further purification. Solvents were dried using a Glass Contour solvent purification system. NMR spectra of $^1H$ and $^{13}C$ were acquired using a Bruker Avance 400 MHz spectrometer operating at 400 and 100 MHz respectively. A Varian 800 FTIR spectrophotometer was used to acquire infrared spectra. Elemental analyses were carried out by Gailbraith Laboratories.

*Synthesis of $ClPh_2GeGePh_2Cl$ (**4**) / $Ph_3GeGePh_2Cl$ (**5**)*

A Schlenk tube was charged with 1.00 g (1.64 mmol) of $Ge_2Ph_6$ (**1**) that was dissolved in 15 mL toluene. To this was added a suspension of 1.15 g (7.04 mmol) trichloroacetic acid in 10 mL of toluene. The reaction mixture was sealed in the Schlenk tube with a Teflon plug and heated at 95 ºC for 72 h, at which time the solution was free of solid material. The solution was allowed to cool and 2.5 equiv. of a 1.0 M ethereal HCl solution (4.11 mL, 4.11 mmol) was added *via* syringe. The Schlenk tube was sealed and the reaction mixture was heated for a further 18 h at 95 ºC. The reaction mixture was transferred by cannula into a Schlenk flask and the volatiles were removed *in vacuo* to yield a white solid that was washed with hexane (3 x 15 mL) and dried under vacuum to yield 0.390 g of a solid product. $^1H$ ($CDCl_3$, 25 ºC) δ 7.58 – 7.46 (m, aromatic hydrogens), 7.44 – 7.40 (m, aromatic hydrogens), 7.38 – 7.30 (m, aromatic hydrogens) ppm. For **4**: $^{13}C$ NMR ($CDCl_3$, 25 ºC) δ 135.5 (*ipso*-$C_6H_5$), 133.9 (*o*-$C_6H_5$), 130.6 (*p*-$C_6H_5$), 128.8 (*m*-$C_6H_5$). For **5**: $^{13}C$ NMR ($CDCl_3$, 25 ºC) δ 137.9 (*ipso*-Cl($C_6H_5$)$_2$GeGe$Ph_3$), 135.4 (*ipso*-

$ClPh_2GeGe(C_6H_5)_3$), 135.0 (*o*-$Cl(C_6H_5)_2GeGePh_3$), 133.8 (*o*-$ClPh_2GeGe(C_6H_5)_3$), 129.9 (*p*-$Cl(C_6H_5)_2GeGePh_3$), 129.4 (*p*-$ClPh_2GeGe(C_6H_5)_3$), 128.6 (*m*-$Cl(C_6H_5)_2GeGePh_3$), and 128.5 (*m*-$ClPh_2GeGe(C_6H_5)_3$) ppm.

*Synthesis of $HPh_2GeGePh_2H$ (**6**) / $Ph_3GeGePh_2H$ (**7**)*

The mixture of **4** and **5** (0.360 g) was dissolved in 10 mL of THF, and to this, was added a suspension of $LiAlH_4$ (0.062 g, 1.63 mmol) in 10 mL of THF. The reaction mixture was stirred for 18 h at 25 ºC and the volatiles were removed *in vacuo*. The resulting solid was washed with 3 x 15 mL of hot benzene and the combined washes were filtered though Celite. The volatiles from the filtrate were removed *in vacuo* to yield a mixture of **6** and **7** along with a trace amount of $Ph_3GeH$ (0.33 g total material). Pure **7** was obtained from the product mixture by recrystallization from a concentrated toluene solution at – 35 ºC (0.240 g, 28 % based on 1). For **6**: $^1$H NMR ($C_6D_6$, 25 ºC) δ 7.54 – 7.50 (m, 8H, *o*-$C_6H_5$), 7.08 – 7.04 (m, 12H, *m*-$C_6H_5$ and *p*-$C_6H_5$), 5.57 (s, 2H, Ge – *H*) ppm. $^{13}$C NMR ($C_6D_6$, 25 ºC) δ 136.0 (*ipso*-$C_6H_5$), 135.7 (*o*-$C_6H_5$), 129.1 (*p*-$C_6H_5$), 128.7 (*m*-$C_6H_5$) ppm. For **7**: $^1$H NMR ($C_6D_6$, 25 ºC) δ 7.59 (d, $J$ = 8.0 Hz, 6H, *o*-$(C_6H_5)_3GeGePh_2H$), 7.54 (d, $J$ = 6.1 Hz, 4H, *o*-$Ph_3GeGe(C_6H_5)_2H$), 7.10 – 7.03 (m, 15H, *p*-$(C_6H_5)$ and *m*-$(C_6H_5)$), 5.72 (s, 1H, Ge – *H*) ppm. $^{13}$C NMR ($C_6D_6$, 25 ºC) δ 137.5 (*ipso*-$HPh_2GeGe(C_6H_5)_3$), 135.9 (*ipso*-$H(C_6H_5)_2GeGePh_3$), 135.8 (*o*-$HPh_2GeGe(C_6H_5)_3$), 135.5 (*o*-$H(C_6H_5)_2GeGePh_3$), 129.2 (*p*-$HPh_2GeGe(C_6H_5)_3$), 129.1 (*p*-$H(C_6H_5)_2GeGePh_3$), 128.8 (*m*-$HPh_2GeGe(C_6H_5)_3$), 128.7 (*m*-$H(C_6H_5)_2GeGePh_3$) ppm. Anal. Calcd. for $C_{30}H_{26}Ge_2$: C, 67.76; H, 4.93. Found: C, 67.87; H, 4.89.

*Thermal decomposition of **7** in $CH_3CN$ solution*

A Schlenk tube was charged with **7** (0.050 g, 0.094 mmol) and $CH_3CN$ (10 mL) was added. The Schlenk tube was sealed and heated in an oil bath at 85 ºC for 48 h. The reaction

mixture was transferred *via* cannula into a Schlenk flask and the volatiles were removed *in vacuo* to yield a yellow oil that was analyzed by $^{1}$H NMR spectroscopy in benzene-$d_6$.

*Thermal decomposition of solid **7***

A round-bottomed flask was charged with **7** (0.100 g, 0.188 mmol) and was connected to a receiving bulb cooled to –78 ºC. The flask was heated to 160 ºC in a Kugelrohr oven for 2 h under vacuum (0.01 torr). After such time, a white solid had collected in the receiving bulb, and was identified as $Ph_3GeH$ (0.049 g, 86%) by $^{1}$H and $^{13}$C NMR spectroscopy (benzene-$d_6$) by comparison of the spectra to an authentic sample.

*Thermal decomposition of **7** in toluene in the presence of DMB*

A Schlenk tube was charged with **7** (0.075 g, 0.14 mmol) in toluene (15 mL), and 2,3-dimethyl-1,3-butadiene (0.120 g, 1.46 mmol) was added to the solution. The Schlenk tube was sealed and the reaction mixture was heated to 95 ºC for 72 h. The reaction mixture was transferred to a Schlenk flask and the volatiles were removed *in vacuo* to yield a colorless oil. The $^{1}$H and $^{13}$C NMR spectra in benzene-$d_6$ were acquired.

# CHAPTER III

## PHOTODECOMPOSITION PATHWAY OF LINEAR OLIGOGERMANES $Bu^n_3GeGePh_2GeBu^n_3$ AND $Bu^n_3GeGePh_3$: PHOTOPRODUCT IDENTIFICATION BY SPECTROSCOPIC AND SPECTROMETRIC METHODS

### 3.1 Introduction

The photochemistry of catenated group 14 compounds is of interest due to their unexpected reactivity and product generation. This process can be used to convert one type of catenate to another, but also can be used for the generation of reactive intermediates include silylenes, germylenes, stannylenes. The group 14 element centered radical species produced photolytically can subsequently be trapped and characterized.[81-83] The photochemistry of conjugated organopolysilane systems have received considerable attention, but photochemical studies on germanium analogues are substantially more scarce. The photochemistry of the cyclotrigermane $(Mes_2Ge)_3$ is the most intensively studied germanium compound. This species is observed to photochemically convert to a generate both a germylene $Mes_2Ge$: and a digermene $Mes_2Ge{=}GeMes_2$, and the chemistry of both photoproducts has been rigorously investigated.[84] Other than a few other studies, the photochemistry of linear oligogermanes have been limited. Examples include the photolysis of permethylated oligogermanes $Me(GeMe_2)_nMe$ ($n$ = 3-6)[84-85] and polygermanes $(R_2Ge)_n$ ($R_2$ = $Et_2$, $Bu^n_2$, $Hex_2$, PhMe).[86-88]

Linear oligogermanes have been shown to decompose by homolytic scission of the Ge – Ge bond to yield germyl radicals, by germylene extrusion with concomitant chain contraction, or by a combination of both processes. A study of the photoproducts generated after photolysis of three linear phenylated trigermanes $(PhMe_2Ge)_2GeMe_2$, $(Me_3Ge)_2GeMePh$, and $(Me_3Ge)_2GePh_2$ has been conducted, where the photochemical products of the organic substituted trigermanes were observed by trapping experiments, matrix isolation, and laser flash photolysis techniques. The photolytic experiments revealed that both the simple extrusion of germylenes and the formation of germyl radicals and digermyl radicals.[79] Trapping agents, such as 2,3-dimethyl-1,3-butadiene (DMB) or $CCl_4$, were added to the reaction mixture prior to irradiation and the photolytically produced germylenes $R_2Ge$: (R = Me or Ph) to be trapped with 18-32% conversion with the concomitant formation of digermanes (**Scheme 3.1**).[79] Reaction of the germylenes with the trapping agents, DMB or $CCl_4$, gives a germacyclopentene or trichloromethylchlorogermane respectively.

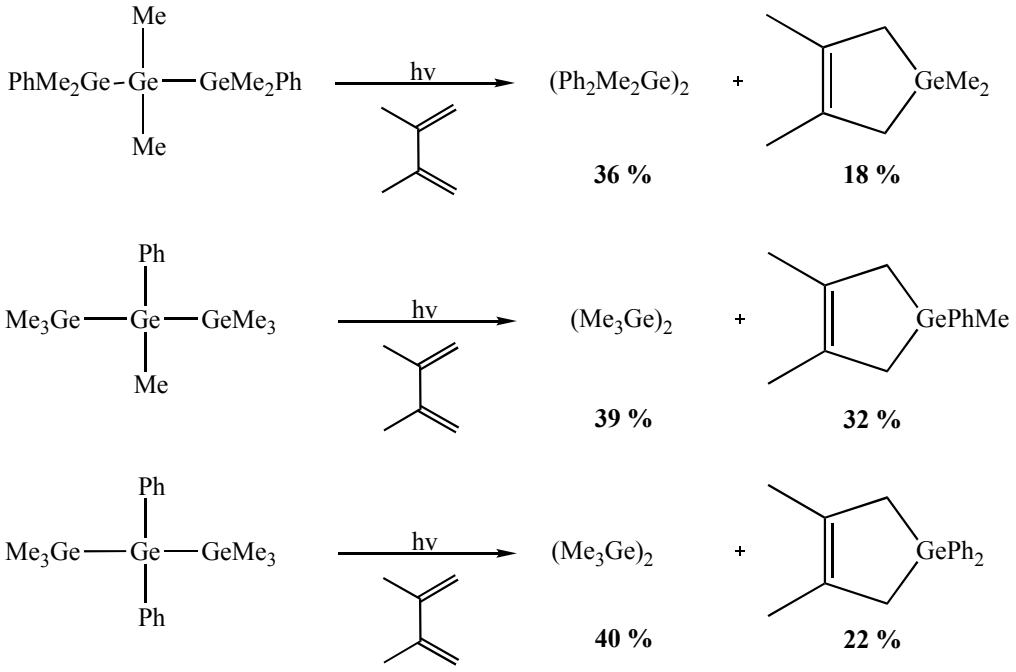


**Scheme 3.1:** Photolysis of three linear trigermanes with trapping agent DMB.[79]

The formation of digermanes $(PhMe_2Ge)_2$ and $(Me_3Ge)_2$ after photolysis indicates the formation of germyl radicals, which then recombine to yield the oligomers shown. The germacyclopentenes generated clearly indicates the extrusion of germylenes before being trapped by the DMB reagent. The trigermanes were also photolyzed in the presence of $CCl_4$ (**Scheme 3.2**). This experiment provides further evidence that both germyl radicals and digermyl radicals are generated during homolytic cleavage of the Ge – Ge bonds of the trigermanes. These radicals abstract chlorine atoms from the $CCl_4$ to generate chlorogermanes and chlorodigermanes. The formation of dichlorogermanes ($R_2GeCl_2$) is a clear indicator that germylenes are forming and then inserting into the C – Cl bond of $CCl_4$. This yields a trichloroalkylchlorogermane ($Cl_3CGeR_2Cl$) that is thermally unstable and decomposes to dichlorogermane and dichlorocarbene.[79]

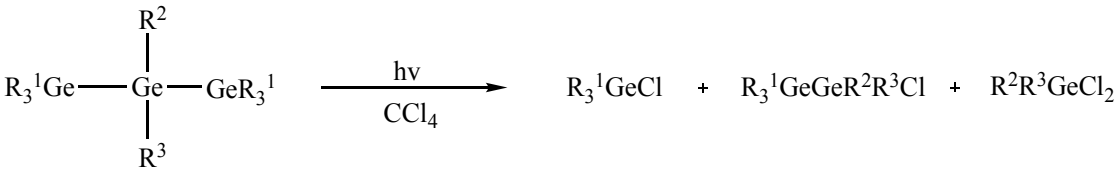


$R_3^1Ge-Ge(R^2)(R^3)-GeR_3^1 \xrightarrow[CCl_4]{h\nu} R_3^1GeCl + R_3^1GeGeR^2R^3Cl + R^2R^3GeCl_2$

**Scheme 3.2:** Photolysis of linear phenylated trigermanes in the presence of $CCl_4$.[79]

A later study was conducted by Leigh and coworkers, looking into the chemistry of germylenes with the goal of detecting the parent germylene ($:GeH_2$) directly and studying its reactivity in solution. This was done with laser flash photolysis methods on dihydro-3-methyl-4-phenyl-1-germacyclopent-3-ene in cyclohexane-$d_{12}$ and using acetic acid (AcOH) as the germylene trapping agent. Reactions were monitored by $^1H$ NMR and by the formation of 2-methyl-3-phenyl-1,3-butadiene and $AcOGeHL_2$ (L = H or D), resulting form the insertion of the O – H bond. This shows the ability of AcOH to be used as a germlyene trapping agent (**Scheme 3.3**).[78]

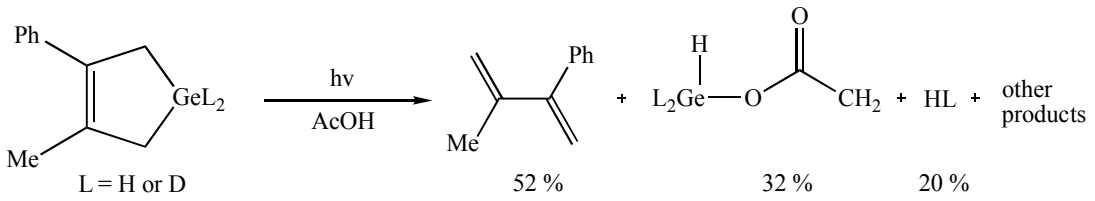


**Scheme 3.3:** Photolysis of dihydro-3-methyl-4-phenyl-1-germacyclopenten-3-ene with trapping agent AcOH.[78]

The photochemistry of heteroleptic oligogermanes, where the substituent patterns are different at various germanium atoms, have not been extensively examined. In this work, two $Bu^n$/Ph substituted oligogermanes, $Bu^n_3GeGePh_2GeBu^n_3$ (**1**) and $Bu^n_3GeGePh_3$ (**2**), were photolyzed in the presence of acetic acid and the photoproducts were identified. If germylene $:GeR_2$ formation occurred, it would be observed *via* the generation of a trapped photoproduct $R_2Ge(H)OAc$.[78] The trigermane was chosen as it contained internal $GePh_2$ and terminal $GeR_3$ fragments, in contrast to the digermane. These experiments were conducted to determine the decomposition pathways and to identify the photoproducts generated. It was postulated that the photolysis of **1** would produce photoproducts which resulted from both radical and germylene formation during the photolysis reaction. The photoproducts $Bu^n_3GeH$ and $Bu^n_3GeOAc$ would be produced from the generation of tributylgermyl radicals, while the formation of $Ph_2Ge(H)OAc$, and possibly $Bu^n_2Ge(H)OAc$ would result from the extrusion of germylenes $Ph_2Ge:$ and $Bu^n_2Ge:$ respectively. Any trapped $Ph_2Ge:$ would be identified as $Ph_2Ge(H)OAc$ and would also indicate the source of the germylene coming from the central germanium atom of **1**. Similarly, formation of $Bu^n_2Ge(H)OAc$ would indicate that $Bu^n_2Ge:$ was extruded from either of the terminal germanium atoms of **1**. The possibility of ligand scrambling might also result in mixed-ligand radicals or germylenes being produced, which could also be trapped and identified. All photoproducts obtained from **1** were characterized by $^1H$ NMR spectroscopy, gas

chromatography electron impact mass spectrometry (GC-MS), and high resolution accurate mass mass spectrometry (HRAM-MS). The photochemistry of **2** was also investigated in a similar fashion.

### 3.2 Results and Discussion

Both trigermane **1** and digermane **2** were synthesized using the hydrogermolysis shown in **Scheme 3.4**.[67] The reaction involves reacting a trialkylgermanium amide in $CH_3CN$ that is converted to an $\alpha$-germyl nitrile species *in situ*. This activated nitrile compound reacts with the a trialkyl germanium hydride species to complete the Ge – Ge bond formation. The compounds were photolyzed using UV-C light (100-280 nm) in the presence of acetic acid as the trapping agent. The oligogermanes were photolyzed under two different experimental conditions. One method used two equivalents of AcOH irradiated at regular intervals over a span of 120 minutes, and the second method used ten equivalents of AcOH continuously irradiated for 18 hours. The postulated germylene trapping products, $Ph_2Ge(H)OAc$ (**3**) and $Bu^n_2Ge(H)OAc$ (**4**), were independently synthesized from the corresponding germanium hydrochloride $R_2GeHCl$ species by reaction with silver acetate.[89] The other acetate, $Bu^n_3GeOAc$ (**5**), was prepared from $Bu^n_3GeCl$ and silver acetate (**Scheme 3.5**). Each photoproduct containing an acetate group will show unique resonances corresponding to the methyl group of the acetate. The $^1H$ NMR spectrum of the photolysis showed peaks at $\delta$ = 1.97, 1.86, and 1.90 ppm, corresponding to the methyl groups $Ph_2Ge(H)OAc$ (**3**), $Bu^n_2Ge(H)OAc$ (**4**), and $Bu^n_3GeOAc$ (**5**) respectively. The Ge – *H* bond resonances in **3** results in the observation of a singlet at $\delta$ = 6.72 ppm, and a pentet at $\delta$ = 5.71 ppm ($J$ = 3.9 Hz) was observed for **4**. After photolysis, the photoproducts of trigermane **1** were observed to be $Bu^n_3GeH$, $Bu^n_3GeOAc$, $Ph_2Ge(H)OAc$, and the digermane $Bu^n_6Ge_2$. The photoproduct mixture indicates that upon irritation, the Ge – Ge singles bonds are cleaved homolytically to generate a germylene $Ph_2Ge$: and two $Bu^n_3Ge\cdot$ radicals. Under identical

experimental conditions, the photoproducts of digermane **2** were identified as $Bu^n_3GeH$, $Bu^n_3GeOAc$, $Ph_3GeH$, $Ph_3GeOAc$, and the digermanes $Bu^n_6Ge_2$ and $Ph_6Ge_2$.

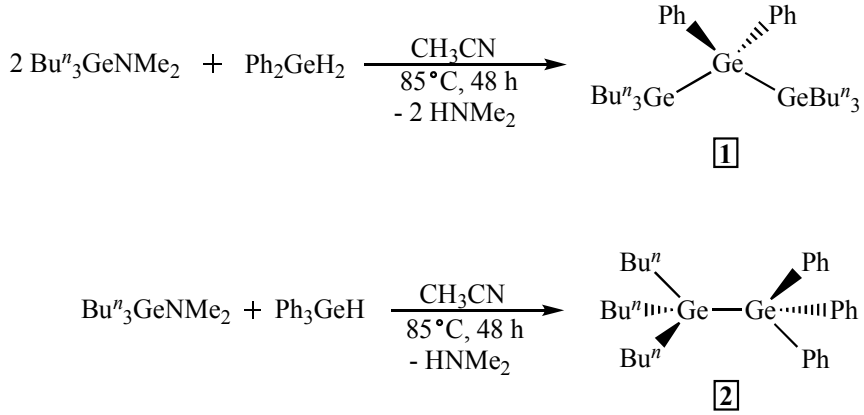


**Scheme 3.4:** Synthesis of $Bu^n_3GeGePh_2GeBu^n_3$ (**1**) and $Bu^n_3GeGePh_3$ (**2**) *via* hydrogermolysis.

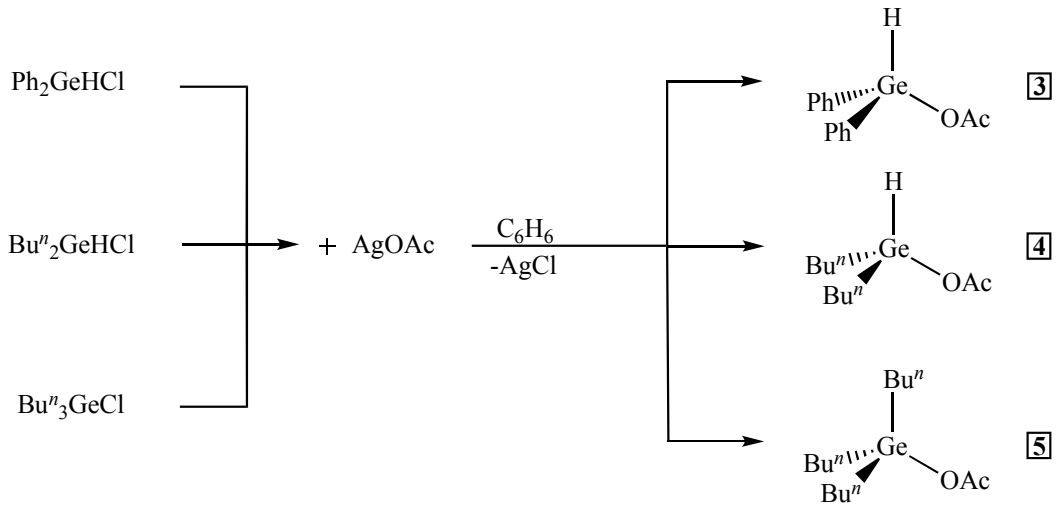


**Scheme 3.5:** Independent synthesis of possible photoproducts after the photolysis of **1**.

In order to monitor the photolysis reaction on an NMR scale, the trigermane (**1**) was dissolved in cyclohexane-$d_{12}$ in a quartz NMR tube. The sample was irradiated intermittently with

UV-C light after the addition of two equivalents of AcOH. After each subsequent exposure to the light source, a $^1$H NMR spectra was taken of the sample. Spectra were taken at varying times, with the final spectral data after 3 hours shown in **Figure 3.1**. After 3 minutes of initial radiation of UV-C light, a noticeable decrease in the intensity of glacial AcOH signals at δ 12.00 and 1.93 ppm along with a gradual growth of a multiplet at δ 3.79 ppm and a singlet at δ 1.88 ppm was seen. The new peaks continued to increase in intensity as the photolysis progressed. After 15 minutes an additional two singlets appeared at δ 6.52 and 1.99 ppm corresponding to germanium-bound hydrogen and the methyl group of the acetate of the acetoxydiphenyl germane $Ph_2Ge(H)OAc$ (**3**). All four signal intensities at δ = 6.52, 3.79, 1.99, and 1.88 ppm continued to increase until a total irradiation time of 120 minutes, after which no further changes were observed in the $^1$H NMR spectrum. Residual AcOH was detected by the presence of a small singlet remaining at 1.93 ppm, while the O – *H* signal at 12.00 ppm had broadened into the baseline. In order to ensure no other photoproducts were produced later the reaction was monitored for an additional 3 hours, which resulted in no further changes in the spectral data.

a) t = 0 min

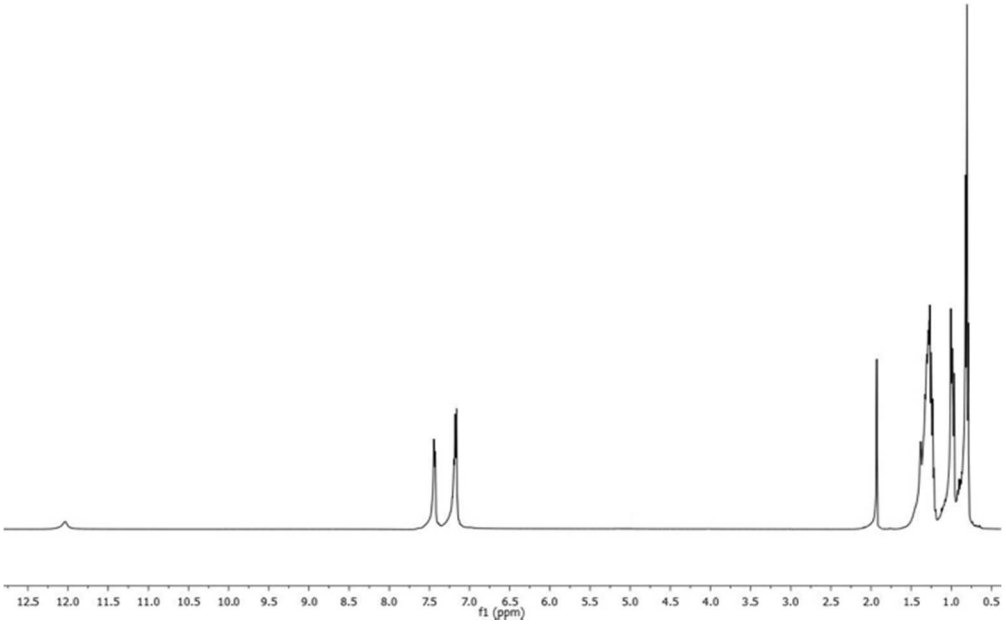

b) t = 15 min

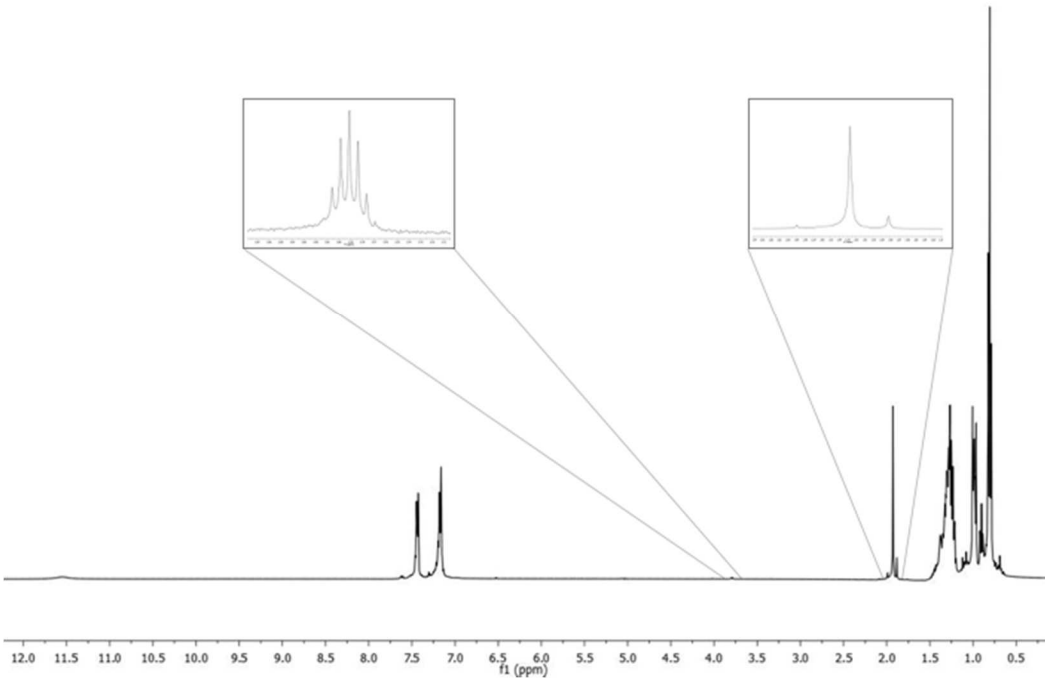


c) t = 30 min

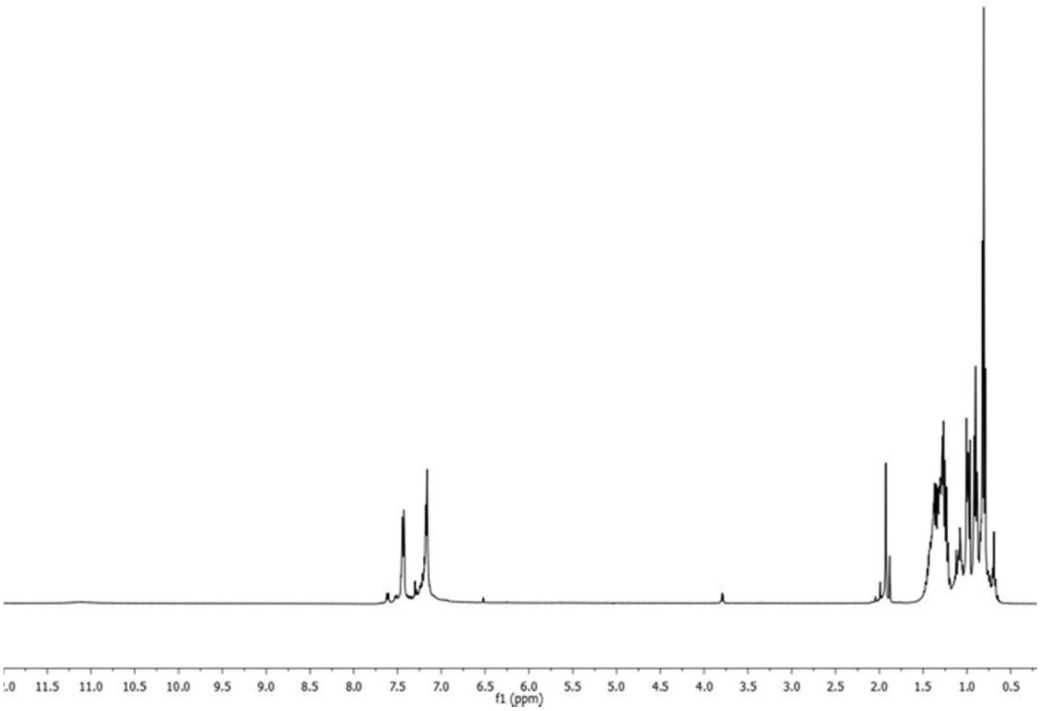

d) t = 90 min

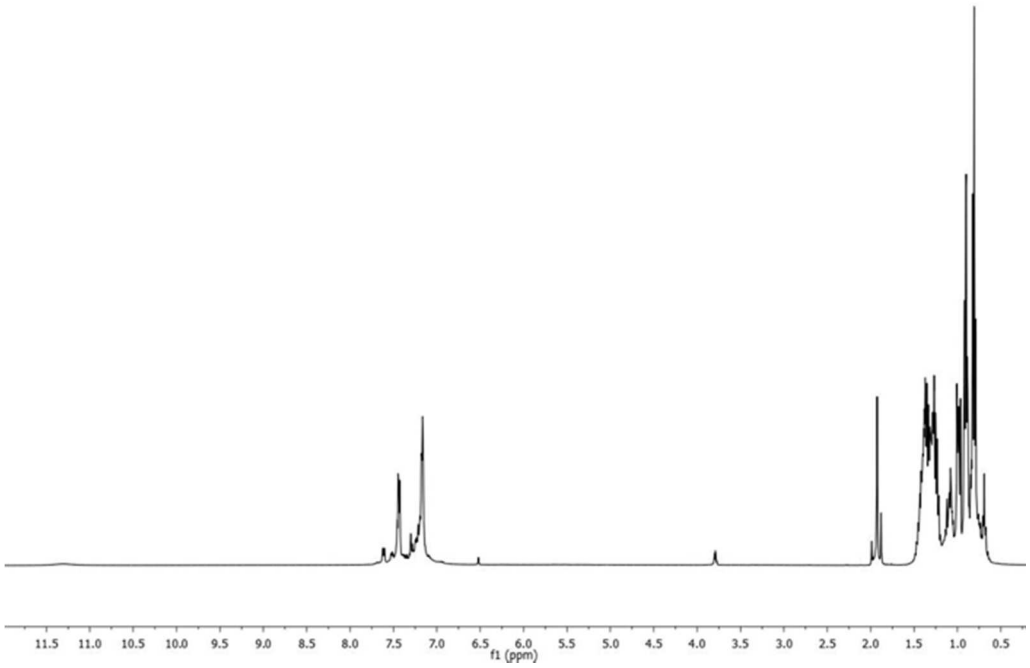


e) t = 3 hours

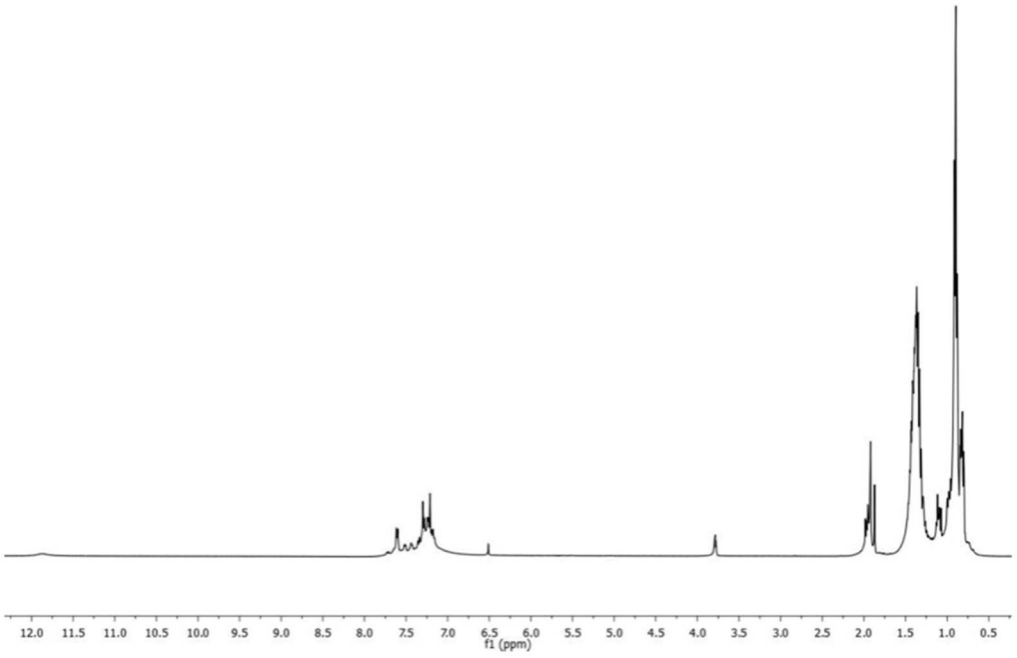


**Figure 3.1:** Timed $^{1}H$ NMR (**a-e**) experiment monitoring the photolysis process of $Bu^{n}_{3}GeGePh_{2}GeBu^{n}_{3}$ (**1**) in the presence of AcOH in cyclohexane-$d_{12}$.

A bulk photolysis of **1** was conducted in addition to the timed NMR experiment by irradiating the sample continuously for 18 hours with UV-C light in THF in the presence of ten equivalents of acetic acid (AcOH). In order to remove excess AcOH, to prevent over saturation of the $^1$H NMR spectrum, an aqueous work up was done after irradiation. The remaining thick liquid was dissolved in benzene (15 mL), the acetic acid was extracted using deionized water (3 x 10 mL), and the organic layer was dried to yield the photoproducts. The NMR spectrum of the product was taken in benzene-$d_6$, that exhibited a complex pattern of peaks in both the alkyl and aryl regions, indicating the formation of multiple photoproducts. Two clear singlets were visible at $\delta$ = 6.72 and 1.78 ppm, again revealing the presence of **3**, and additional singlets at $\delta$ = 1.90 and a septet at $\delta$ = 4.02 ppm ($J$ = 3.0 Hz). Based on these results and the timed NMR scale reaction, it was postulated that the singlet and septet at $\delta$ 1.90 and 4.02 ppm, could be due to the presence of seven possible photoproducts. One option is that both peaks are due to the generation of acetoxydibutyl germane $Bu^n_2Ge(H)OAc$ (**4**), the germylene trapping product of $Bu^n_2Ge$: that could be extruded from the terminal $Bu^n_3Ge$ groups of **1**. The other possibility would have the septet attributed to the presence of $Bu^n_3GeH$ (**6**), while the singlet resulted from another acetate containing product. The identity of the septet was ascertained by comparing it to that in the $^1$H NMR spectrum of a commercial sample of **6**, where the two spectra were identical. This confirms the hypothesis that the singlet was indeed a result of a separate photoproduct. This photoproduct signal at $\delta$ 1.90 ppm was a match for the independently synthesized $Bu^n_3GeOAc$ (**5**), that exhibited an identical singlet at the same chemical shift for the protons in the methyl group of the acetate. Therefore, it was determined that during the photolysis reaction germylene extrusion occurred at the interior germanium atom, and radical formation was observed at the terminal germanium atoms to generate **5** and **6**, respectively.

The photoproduct mixture from **1** was also analyzed using GC-MS, with electron impact used as the ionization technique, to further identify the products. However, as this is a hard

ionization method, the parent ion $M^+$ was expected to be absent although fragments of the compound would appear. Germanium has a unique isotope patterning in the mass spectrum of compounds of this element due to its having five naturally occurring isotopes ($^{70}$Ge, $^{72}$Ge, $^{73}$Ge, $^{74}$Ge, and $^{76}$Ge), making it easily decipherable in the mass spectra. The GC trace in **Figure 3.2** of the photoproducts showed five peaks with retention times of 10.9, 16.4, 23.7, 29.9, and 44.9 minutes (**Table 3.1**). Due to thermal conditions used for the GC column the phenyl-substituted germanes, thermally decompose, and were not observed even though they were present in the product mixture. The largest peak, which eluted off the column first $t_r$ = 10.9 min, corresponded to fragments from $Bu^n_3GeH$. The main peaks and their assignments that contain germanium in the MS were *m/z* = 189 ($Bu^n_2GeH^+$), 133 ($Bu^nGeH_2^+$), and 75 ($GeH^+$) amu. There were also two lesser peaks with *m/z* = 132 ($Bu^nGeH^+$) and 75 ($GeH^+$), which are due to the fragmentation of the $Bu^n_2GeH^+$ ion. When compared to commercially pure $Bu^n_3GeH$, the mass spectrum and retention times were identical, demonstrating that the first eluted compound was **6**.

Elution of the second compound came at a retention time of 16.4 minutes, with the main peaks containing germanium in the MS as follows: *m/z* = 223 ($Bu^n_2GeO(H_3O)^+$), 167 ($Bu^nHGeO(H_3O)^+$), and 131 ($Bu^nGe^+$) amu. This fragmentation is likely due to the formation of $Bu^n_3GeOGeBu^n_3$, generated by the insertion of oxygen within the germanium-germanium bond of $Bu^n_6Ge_2$ under the experimental conditions. The third compound eluted at $t_r$ = 23.7 minutes on the mass spectrum had peaks at *m/z* = 265, 209, and 153 amu corresponding to the $Bu^n_2Ge(C_2H_3O_2)(H_2O)^+$, $Bu^nGe(C_2H_3O_2)(H_2O)H^+$, and $Ge(C_2H_3O_2)(H_2O)H_2^+$ ions, respectively. This fragmentation pattern indicated that this compound was $Bu^n_3GeOAc$.

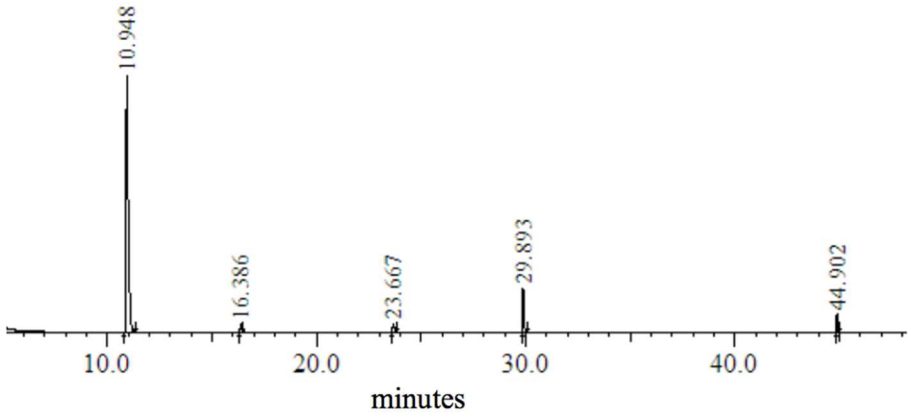


**Figure 3.2**: GC-MS of the photoproducts of $Bu^n_3GeGePh_2GeBu^n_3$ (**1**) with 10 eq. AcOH.

$t_r$ = 10.9 min

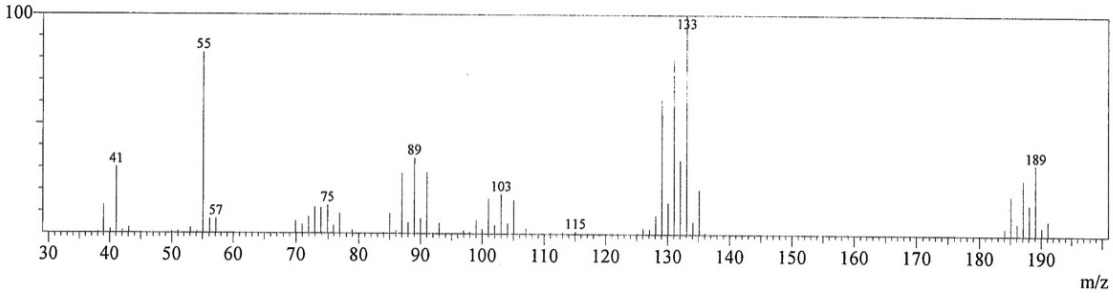


$t_r$ = 29.9 min

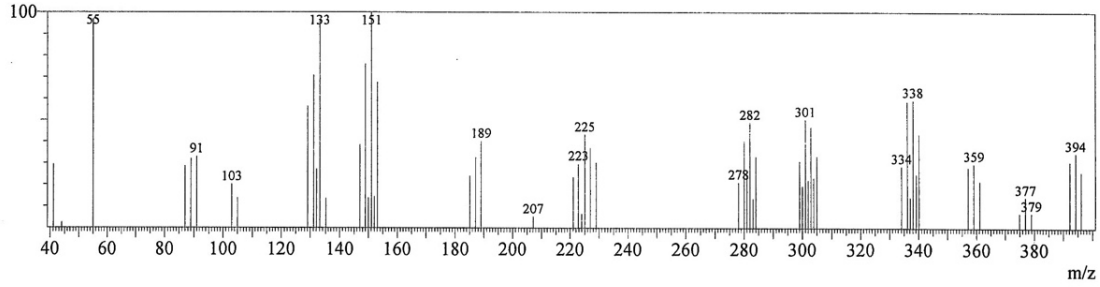

$t_r$ = 44.9 min

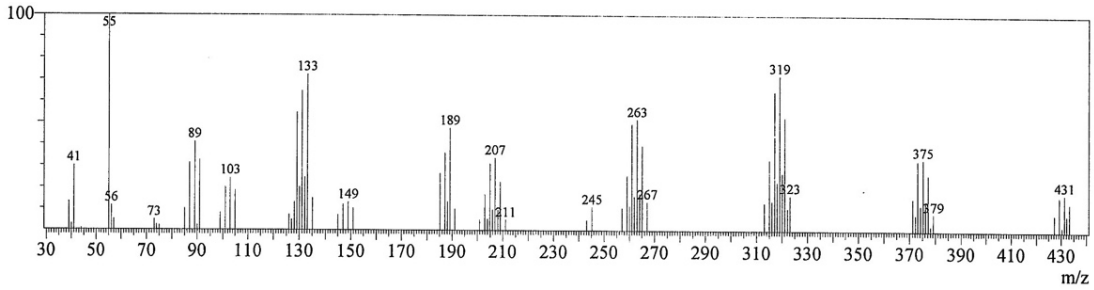


**Figure 3.3:** MS of the major components eluted at 10.9 min (top), 29.9 min (middle), and 44.9 min (bottom) of the photoproducts $Bu^n_3GeGePh_2GeBu^n_3$ (**1**) with AcOH.

| | Area % | *m/z* | Assignment |
|---|---|---|---|
| $Bu^n_3GeH$ (**6**) | 85.6 | 189 | $Bu^n_3GeH^+$ |
| ($t_r$ = 10.9 min) | | 133 | $Bu^n_3GeH_2^+$ |
| | | 75 | $GeH^+$ |
| $Bu^n_3GeOGeBu^n_3$ | 1.8 | 223 | $Bu^n_2GeO(H_3O)^+$ |
| ($t_r$ = 16.4 min) | | 167 | $Bu^nHGeO(H_3O)^+$ |
| | | 131 | $Bu^nGe^+$ |
| $Bu^n_3GeOAc$ (**5**) | 2.5 | 265 | $Bu^n_2Ge(C_2H_3O_2)(H_2O)^+$ |
| ($t_r$ = 23.7 min) | | 209 | $Bu^nGe(C_2H_3O_2)(H_2O)H^+$ |
| | | 153 | $Ge(C_2H_3O_2)(H_2O)H_2^+$ |
| $Bu^n_3GeGeBu^n_3$ (**7**) | 7.6 | 431 | $Bu^n_5Ge_2^+$ |
| ($t_r$ = 29.9 min) | | 375 | $Bu^n_4Ge_2H^+$ |
| | | 319 | $Bu^n_3Ge_2H_2^+$ |
| | | 263 | $Bu^n_2Ge_2H_3^+$ |
| | | 207 | $Bu^nGe_2H_4^+$ |
| $Bu^n_3GeGePh_2GeBu^n_3$ (**1**) | 2.5 | 394 | $Bu^n_3GeGePh^+$ |
| ($t_r$ = 44.9 min) | | 338 | $Bu^n_3HGeGePh^+$ |

| | | |
|---|---|---|
| | 282 | $Bu^n_2H_2GeGePh^+$ |
| | 225 | $HGeGePh^+$ |

**Table 3.1:** Electron impact GC-MS data for photolyzed trigermane $Bu^n_3GeGePh_2GeBu^n_3$ (**1**).

The second most abundant compound in the photoproduct mixture and, the fourth overall compound eluted off the column, had a retention time of 29.9 minutes. The MS peaks corresponded closely to hexabutyldigermane (**7**), an authentic sample was also run for comparison, that confirms $Bu^n_3Ge\cdot$ radical formation during the photolysis.[90] Along with germlyene formation, subsequent recombination of these radicals was occurring as they come together to form $Bu^n_3GeGeBu^n_3$. The main peaks containing germanium in the MS at $t_r$ = 29.9 minutes were as follows: *m/z* = 431 ($Bu^n_5Ge_2^+$), 375 ($Bu^n_4Ge_2H^+$), 319 ($Bu^n_3Ge_2H_2^+$), 263 ($Bu^n_2Ge_2H_3^+$), and 207 ($Bu^nGe_2H_3^+$) amu. This fragmentation and isotope pattern was indicative of the presence of two germanium atoms with the successive loss of four -$Bu^n$ groups from the $Bu^n_5Ge_2^+$ ion. This denoted the presence of the digermane **7** within the photoproduct mixture. Further confirmation was obtained from the GC-MS of a synthetically prepared sample of $Bu^n_3GeGeBu^n_3$[48] which also showed the same retention times and mass spectrum.

The mass spectrum of the fifth species eluted ($t_r$ = 44.9 min) contained peaks at *m/z* = 394, 338, 282, and 225 amu. The fragment assigned to *m/z* = 394 amu was $Bu^n_3GeGePh^+$, which was formed by losing one terminal $Bu^n_3Ge$ and one -Ph ligand from the starting material **1**. The other peaks with *m/z* = 338, 282, and 225 amu resulted from successive loss of all three -$Bu^n$ groups *via* fragmentation of $Bu^n_3GeGePh^+$. All five photoproducts were identified from the mixture of compounds from the photolysis of $Bu^n_3GeGePh_2GeBu^n_3$ (**1**), the most abundant species in the GC trace were $Bu^n_3GeH$ (**6**) and digermane $Bu^n_3GeGeBu^n_3$ (**7**). There was no evidence of the formation of $Ph_2Ge(H)OAc$ (**3**) due to thermal decomposition.

The photolysis product mixture of **1** was also analyzed *via* High Resolution Accurate Mass Mass Spectrometry (HRAM-MS). The samples were opened on the bench top, dissolved in 1 mL of acetonitrile, diluted, and solution injected *via* electrospray in acetonitrile with 0.1% formic acid. Electrospray ionization (ESI) technique is one of the softest ionization methods, using electrical energy to assist the transfer of ions from solution into the gaseous phase before being subjected to mass spectrometric analysis. This method was used in an attempt to observe parent ion and possible ligand scrambling, as well as and to determine whether photoproducts were being formed photolytically or as a result of the process itself. The HRAM-MS of **1** showed six intense peaks with *m/z* = 230.0964, 245.1425, 270.0337, 286.1588, 305.0385, and 346.0652 amu (**Table 3.2** and **Figure 3.4**) These values were assigned to $Bu^n_2GeH(CH_3CN)^+$, $Bu^n_3Ge^+$, $Ph_2GeH(CH_3CN)^+$, $Bu^n_3Ge(CH_3CN)^+$, $Ph_3Ge^+$, and $Ph_3Ge(CH_3CN)^+$ ions, respectively. Two other weaker signals with *m/z* = 565.1749 and 731.2704 amu, respectively, corresponded to $Bu^n_3GeOGeBu^n_3H^+$ and parent ion $Bu^n_3GeGePh_2GeBu^n_3(H_3O)^+$. The first ion, was a product of oxygen insertion between the germanium bonds of $Ge_2Bu^n_6$ under experimental MS conditions, while the second ion indicates unphotolyzed starting trigermane.

| | Observed | Calculated | $\Delta_{mass}$ (ppm) | Assignment |
|---|---|---|---|---|
| **1** (photolysis w/ 10 eq. AcOH) | 230.0964 | 230.0959 | 2.173 | $Bu^n_2Ge(CH_3CN)H^+$ |
| | 286.1588 | 286.1585 | 1.048 | $Bu^n_3Ge(CH_3CN)^+$ |
| | 270.0337 | 270.0333 | 1.481 | $Ph_2Ge(CH_3CN)H^+$ |
| | 305.0385 | 305.0380 | 1.639 | $Ph_3Ge^+$ |

| | | | | |
|---|---|---|---|---|
| | 346.0652 | 346.0646 | 1.733 | $Ph_3Ge(CH_3CN)^+$ |
| | 565.1741 | 565.1741 | 1.415 | $Bu^n_3GeOGeBu^n_3H^+$ |
| | 731.2704 | 731.2861 | 21.47 | $Bu^n_3GeGePh_2GeBu^n_3(H_3O)^+$ |
| **1** unphotolyzed | 368.2119 | 368.2116 | 1.629 | $Bu^n_3Ge(CH_3CN)_3^+$ |
| | 594.2128 | 594.2119 | 1.514 | $Bu^n_3GeGePh_2(CH_3CN)^+$ |
| | 999.4687 | 999.4536 | 15.11 | $Bu^n_3GeGePh_2GeBu^n_3(CH_2CN)_7^+$ |
| $Ph_2Ge(H)OAc$ (**3**) | 229.0065 | 229.0067 | 0.8733 | $Ph_2GeH^+$ |
| | 270.0329 | 270.0333 | 1.481 | $Ph_2Ge(CH_3CN)H^+$ |
| | 473.0180 | 473.0261 | 17.12 | $Ph_3Ge_2(CH_3CN)(H_2O)_3H^+$ |
| $Bu^n_2Ge(H)OAc$ (**4**) | 230.0968 | 230.0959 | 3.911 | $Bu^n_2Ge(CH_3CN)H^+$ |
| | 393.1447 | 393.1428 | 4.832 | $Bu^n_4Ge_2(H_2O)H^+$ |
| $Bu^n_3GeOAc$ (**5**) | 428.2320 | 428.2327 | 6.134 | $Bu^n_3GeGeOAc(CH_3CN)_3H^+$ |
| | 327.1342 | 327.1850 | 155.2 | $Bu^n_3Ge(CH_3CN)_2^+$ |
| $Bu^n_3GeH$ (**6**) | 286.1582 | 428.2317 | 6.134 | $Bu^n_3GeGe(CH_3CN)^+$ |
| | 505.2684 | 505.2683 | 0.1979 | $Bu^n_3GeOGeBu^n_3H^+$ |

**Table 3.2:** HRAM-MS data for photolyzed (**1**).

**a)** $Bu^n_3Ge(CH_3CN)H^+$

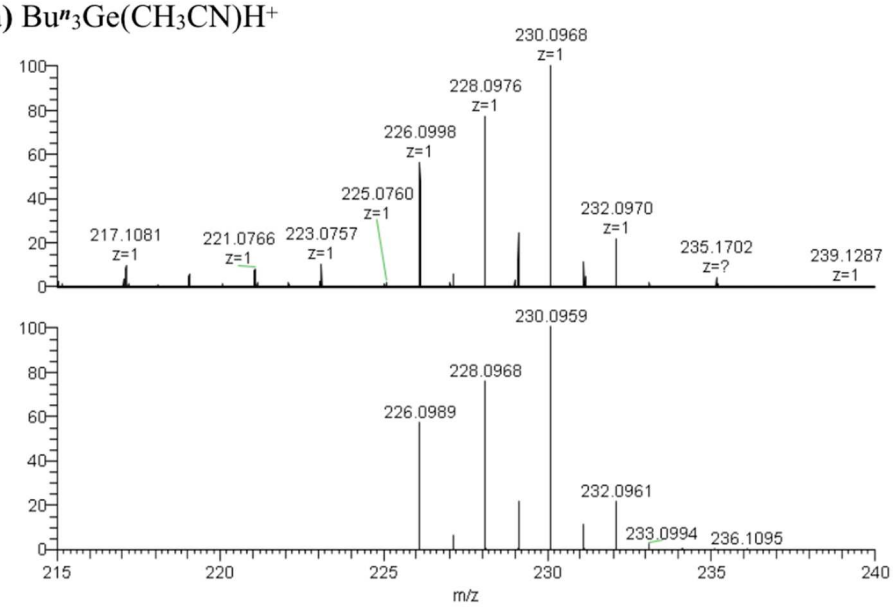


**b)** $Bu^n_3Ge^+$

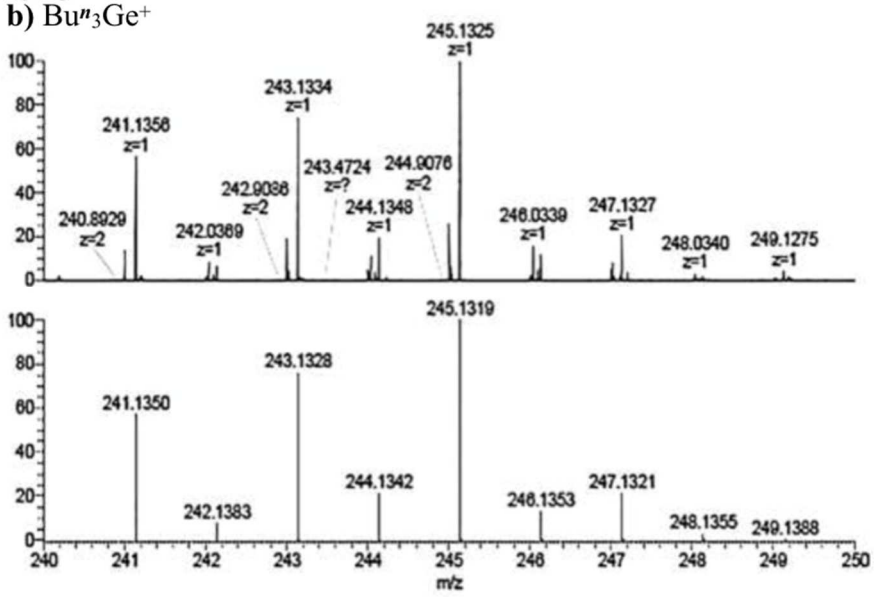

**c**) $Ph_2Ge(CH_3CN)H^+$

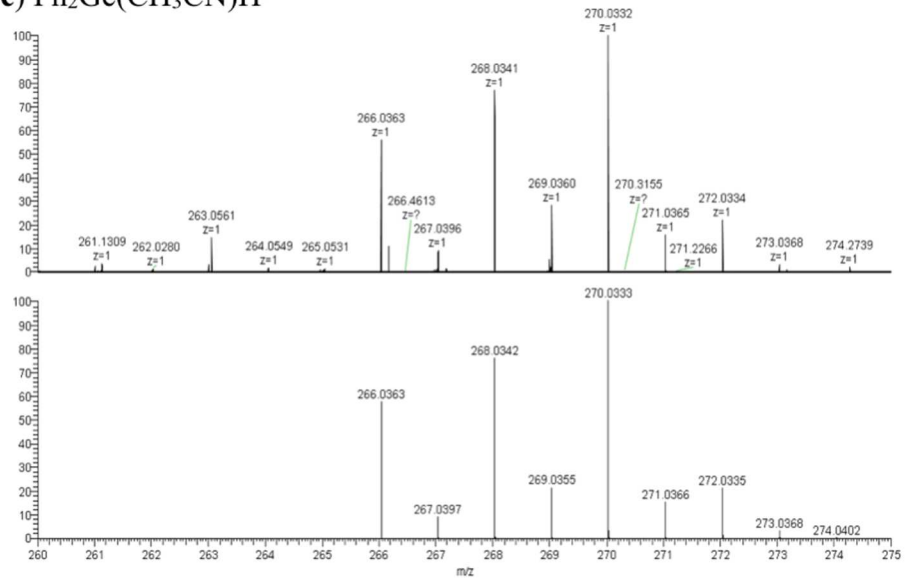


**d)** $Bu^n_3Ge(CH_3CN)H^+$

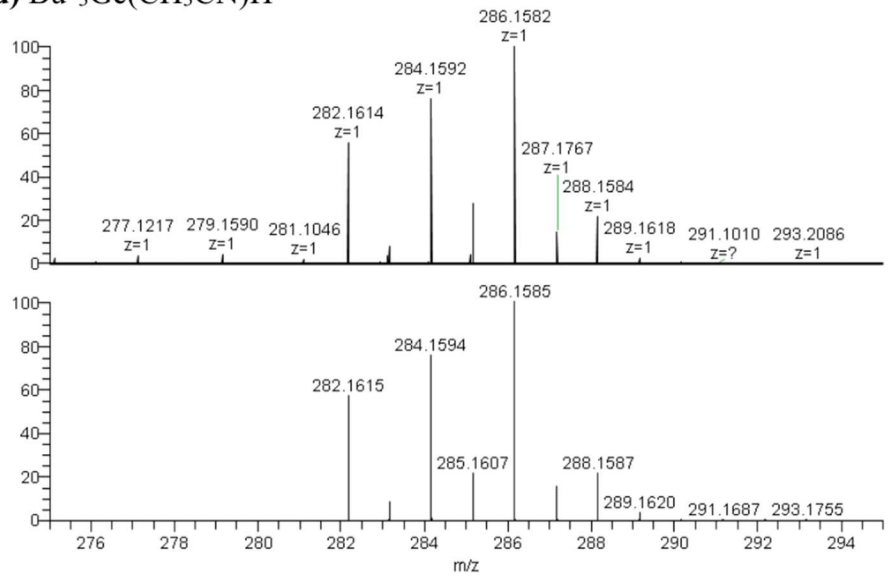

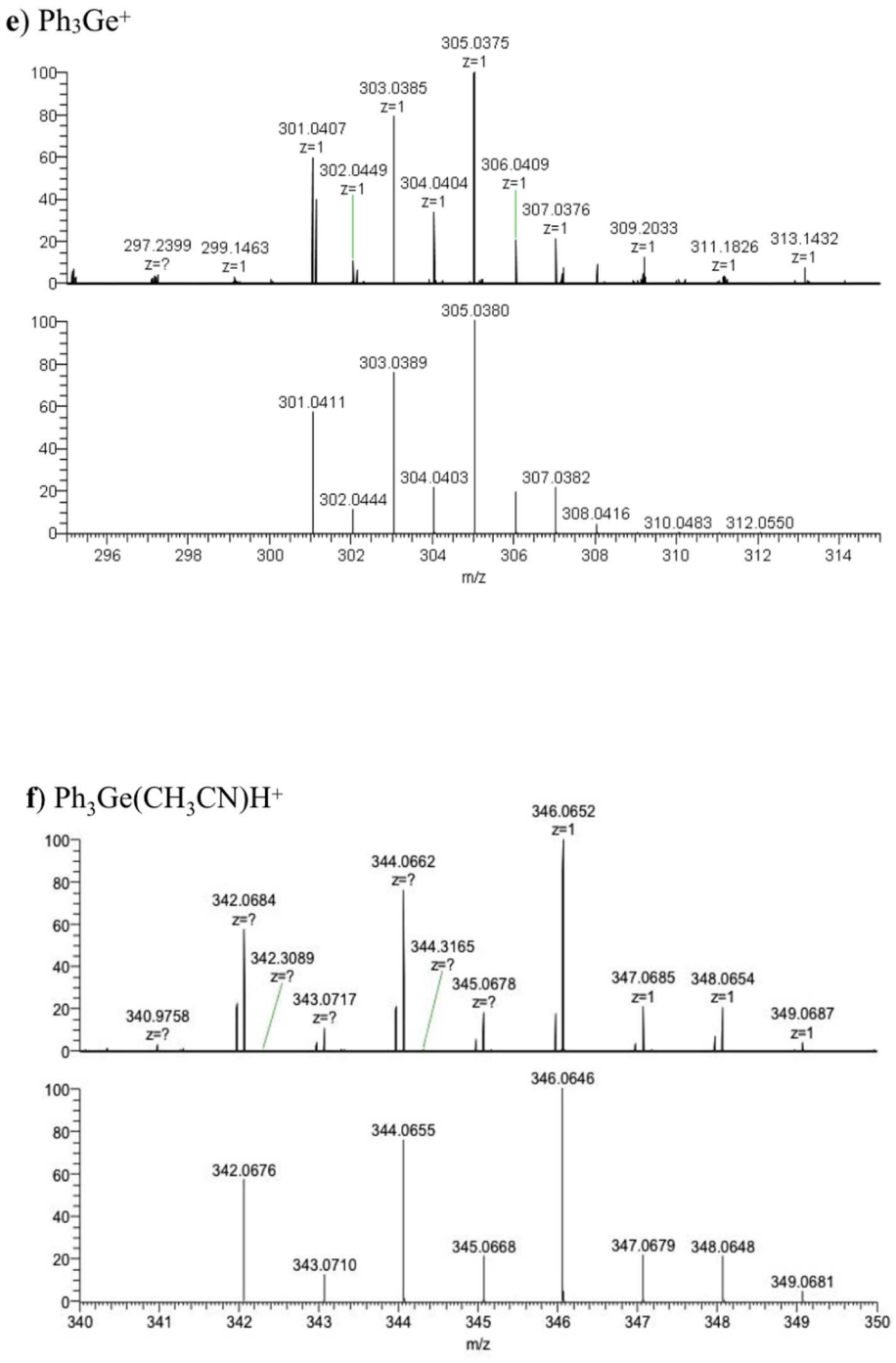


**Figure 3.4:** HRAM-MS data of six photoproducts of product mixture $Bu^n_3GeGePh_2GeBu^n_3$ (**1**): $Bu^n_2GeH(CH_3CN)^+$ (**a**), $Bu^n_3Ge^+$ (**b**), $Ph_2GeH(CH_3CN)^+$ (**c**), $Bu^n_3Ge(CH_3CN)^+$ (**d**), $Ph_3Ge^+$ (**e**), and $Ph_3Ge(CH_3CN)^+$ (**f**).

A sample of unphotolyzed trigermane (**1**) was also analyzed using HRAM-MS as a control for comparison. The sample had a signal at *m/z* = 368.2119 amu matching to $Bu^n_3Ge(CH_3CN)_3^+$ and a weaker peak at *m/z* = 594.2128 amu corresponding to $Bu^n_3GeGePh_2(CH_3CN)_3^+$ ion (**Table 3.2** and **Figure 3.4)**. These results showed that the linear oligomers themselves do not remain intact under the experimental conditions. Yet, irrespective of trigermane **1** being photolyzed or not, the $Bu^n_3Ge^+$ ion was observed. This means that this species could be produced from multiple sources: **1**, $Bu^n_3GeOAc$ (**5**), and/or $Bu^n_3GeH$ (**6**). These two compounds, **5** and **6,** were also examined *via* HRAM-MS. The photoproduct **5** was synthetically prepared, and had the most intense peak at *m/z* = 327.1342 amu assigned to $Bu^n_3Ge(CH_3CN)_2^+$ ion, and another weaker signal at *m/z* = 428.2320 amu relates to the $Bu^n_3GeOAc(CH_3CN)_3H^+$ ion. The MS/MS of the latter ion shows two signals at *m/z* = 368.2113 and 327.1847 amu which result from the subsequent fragmentation into the $Bu^n_3Ge(CH_3CN)_3^+$ and $Bu^n_3Ge(CH_3CN)_2^+$ ions, respectively. These solvated ions of $Bu^n_3GeOAc$ were not observed in the HRAM-MS photoproduct mixture of trigermane **1**. However, the non-solvated and $Bu^n_3Ge(CH_3CN)^+$ mono-solvated $Bu^n_3Ge^+$ ions, which did appear, could have also been generated directly form **5**. The sample of commercially produced **6** had a signal with *m/z* = 286.1582 and 505.2684 amu that match to the $Bu^n_3Ge(CH_3CN)^+$ and $Bu^n_3GeOGeBu^n_3H^+$ ions, respectively, again indicating that these species detected in the photolysis product mixture of **1** could also potentially arise from **6** being generated.

The HRAM-MS of $Ph_2Ge(H)OAc$ (**3**), a signal at *m/z* = 270.0239 matching the $Ph_2Ge(CH_3CN)H^+$ ion that is identical to the observed peaks in the HRAM-MS of the photoproduct mixture of **1**. The most intense peak in the HRAM-MS of **3** at *m/z* = 473.0180 is assigned to the $Ph_3Ge_2(CH_3CN)(H_2O)_3^+$ ion, that is generated under experimental MS conditions. The MS/MS analysis of this ion results in fragmentation into $Ph_3Ge^+$, and daughter ions $Ph_2Ge(OH)^+$ and $Ph_2GeH^+$ at *m/z* = 305.0374, 245.0012, and 270.0239, respectively. From the

data discussed, it can be concluded that the ion observed in the photolytic product mixture of **1**, at *m/z* = 305.0385, is probably generated from the experimental conditions of the mass spectrometer rather than due to the presence of an actual photoproduct. Therefore, the $Ph_3Ge^+$ ion is observed due to $Ph_2Ge(H)OAc$ (**3**) being present in the photolytic product mixture.

In addition to **3** the HRAM-MS of independently synthesized $Bu^n_2Ge(H)OAc$ (**4**), the other potential germylene trapping product, was also analyzed. The most intense signals from **4** were observed at *m/z* = 230.0968 and 393.1447 amu corresponding to the $Bu^n_2Ge(CH_3CN)H^+$ and $Bu^n_4Ge_2(H_2O)H^+$ ions. However, only the first of the two ion signals was seen in the HRAM-MS of the photolyzed product mixture of **1**. In the case of the $Bu^n_2Ge(CH_3CN)H^+$ ion, the species was likely generated from the fragmentation of the free and solvated $Bu^n_2Ge^+$ present. Looking at the MS/MS of the $Bu^n_3Ge(CH_3CN)_3^+$ ion, the fragmentation reveals both free $Bu^n_3Ge^+$ and $Bu^n_2Ge(CH_3CN)H^+$ even under the lowest energy MS/MS conditions. Based on the above results and the absence of the expected resonance in the $^1H$ NMR spectrum of the photolysis mixture, corresponding to the hydrogen atom in $Bu^n_2Ge(H)OAc$ (**4**) in the photolyzed product mixture of **1**, it can be postulated that the generation of $Bu^n_2Ge$: did not occur.

The digermane $Bu^n_3GeGePh_3$ (**2**) was photolyzed under similar experimental conditions to the trigermane **1**. The oligomer **2** was dissolved in a solution of THF and irradiated for 18 hours with ten equivalents of AcOH as the trapping agent. The photolysis product was worked up in the same manner as **1** before its $^1H$ NMR was taken in benzene-$d_6$. The spectrum showed multiple overlapping peaks in both aryl and alkyl regions. However, distinct resonances were observed at δ 5.85 (s), 4.02 (sept, $J$ = 3.0 Hz), 1.90 (s), and 1.81 (s) ppm. These peaks are indicative of the presence of $Ph_3GeH$, $Bu^n_3GeH$ (**6**), and $Bu^n_3GeOAc$ (**5**), and $Ph_3GeOAc$. The last peak of δ 1.81 ppm matches identically to a commercial sample of $Ph_3GeOAc$.

Once photolyzed, the photoproduct mixture from **2** was also analyzed by electron impact

GC-MS. The GC traces contains six main signals for the product mixture, with retention times at 10.9, 16.4, 23.7, 29.9, 40.2, and 42.7 minutes (**Table 3.3**). The first four compounds eluted at $t_r$ = 10.9, 16.4, 23.7, and 29.9 minutes indicate the presence of $Bu^n_3GeH$ (**6**), $Bu^n_3GeOGeBu^n_3$, $Bu^n_3GeOAc$ (**5**), and $Bu^n_6Ge_2$ (**7**) respectively. These species have identical retention times and mass spectra found for the photoproduct mixtures of trigermane **1**. The three most abundant components in the GC trace of **2** are $Bu^n_3GeH$ (**6**), $Bu^n_3GeOGeBu^n_3$, and $Bu^n_3GeOAc$ (**5**). These species are being formed by the generation of germyl radicals.

| | Area % | *m/z* | Assignment |
|---|---|---|---|
| $Bu^n_3GeH$ (**6**) | 70.1 | 189 | $Bu^n_2GeH^+$ |
| ($t_r$ = 10.9 min) | | 133 | $Bu^n_3GeH_2^+$ |
| | | 75 | $GeH^+$ |
| $Bu^n_3GeOGeBu^n_3$ | 11.3 | 223 | $Bu^n_2GeO(H_3O)^+$ |
| ($t_r$ = 16.4 min) | | 167 | $Bu^nHGeO(H_3O)^+$ |
| | | 131 | $Bu^nGe^+$ |
| $Bu^n_3GeOAc$ (**5**) | 11.7 | 265 | $Bu^n_2Ge(C_2H_3O_2)(H_2O)^+$ |
| | | 209 | $Bu^nGe(C_2H_3O_2)(H_2O)H^+$ |
| | | 153 | $Ge(C_2H_3O_2)(H_2O)H_2^+$ |
| $Bu^n_3GeGeBu^n_3Ge$ (**7**) | 1.7 | 431 | $Bu^n_5Ge_2^+$ |
| | | 375 | $Bu^n_4Ge_2H^+$ |
| | | 319 | $Bu^n_3Ge_2H_3^+$ |
| | | 263 | $Bu^n_2Ge_2H_3^+$ |
| | | 207 | $Bu^nGe_2H_4^+$ |
| $Ph_6Ge_2$ | 0.9 | 305 | $Ph_3Ge^+$ |
| ($t_r$ = 40.2 min) | | 228 | $Ph_2Ge^+$ |

| | | | |
|---|---|---|---|
| | | 151 | $PhGe^+$ |
| $Bu^n_3GeGePh_3$ (**2**) | 0.5 | 379 | $Ph_3Ge_2H_2^+$ |
| | | 305 | $Ph_3Ge^+$ |
| | | 189 | $Bu^n_2GeH^+$ |
| | | 151 | $PhGe^+$ |
| | | 133 | $Bu^nGeH_2^+$ |

**Table 3.3:** Electron impact GC-MS data for photolyzed $Bu^n_3GeGePh_3$ (**2**).

The last two peaks eluted had longer retention times at $t_r$ = 40.2 and 42.7 minutes and were observed only for the digermane **2**. The MS of the first species ($t_r$ = 40.2 mins) has peaks at *m/z* = 305, 228, and 151 amu that correspond to the $Ph_3Ge^+$, $Ph_2Ge^+$, and $PhGe^+$ ions, which are the daughter ions from $Ph_3Ge^+$ formed by fragmentation of successive phenyl groups. This species comes from the hexaphenyl digermane $Ph_6Ge_2$ that forms by the combination of two $Ph_3Ge$· radicals coupling in the product mixture. These findings were also confirmed by comparison of the GC-MS to a commercial sample of $Ph_6Ge_2$ that showed an identical retention time and mass spectrum.[90] The last compound to elute off the column at $t_r$ = 42.7 mins contained signals *m/z* = 379, 305, 198, 151, and 133 amu, which matched the ions $Ph_3Ge_2H_2^+$, $Ph_3Ge^+$, $Bu^n_2GeH^+$, $PhGe^+$, and $Bu^n_3GeH_2^+$. This fragmentation pattern indicates the presence of unreacted digermane **2** in the photolyzed mixture, which was also confirmed by the GC-MS analysis of a pure sample of **2** for comparison.

The HRAM-MS of the photolysis product mixture of digermane **2** were also obtained and had signals of *m/z* = 305.0383, 286.1588, and 452.9151 amu. These mass values correspond to the $Ph_3Ge^+$, $Bu^n_3Ge(CH_3CN)^+$, and $Bu^nPh_3Ge_2(H_3O)^+$ ions respectively. The $Ph_3Ge^+$ ion was generated from $Ph_3GeH$, $Ph_6Ge_2$, $Ph_3GeOAc$, while the other ion of $Bu^n_3Ge(CH_3CN)^+$ resulted from the presence of $Bu^n_3GeOAc$ (**5**), $Bu^n_3GeH$ (**6**), $Bu^n_3GeGeBu^n_3$ (**7**). These two ions, including

the third signal (*m/z* = 452.29151) assigned to the ion to $Bu^{n}Ph_3Ge_2(H_3O)^+$, can also all be attributed to the presence of unreacted **2** in the product mixture.

### 3.3 Conclusion

The oligogermanes **1** and **2** have been photolyzed using UV-C light in the presence of AcOH as a germylene trapping agent. The $^1$H NMR and the GC-MS data showed the decomposition process of **1** occurred by homolytic scission of both single Ge – Ge bonds to form a germylene $Ph_2Ge$: and two $Bu^{n}_3Ge\cdot$ radicals (**Figure 3.6**). The generated radicals then undergo various transformations providing different photoproducts. The tributylgermyl radicals were trapped by acetic acid to form $Bu^{n}_3GeH$ (**6**) and $Bu^{n}_3GeOAc$ (**5**), and some $Bu^{n}_3Ge\cdot$ radicals also recombined in a chain contraction to produce the digermane $Bu^{n}_6Ge_2$ (**7**). The diphenylgermylene ($Ph_2Ge$:) was also trapped to generate $Ph_2Ge(H)OAc$ (**3**) *via* insertion into the O – H bond of acetic acid. The formation of germylene $Bu^{n}_2Ge$: was not observed, as the related trapping product $Bu^{n}_2Ge(H)OAc$ (**4**) was absent as shown by spectroscopic and spectrometric data.

The digermane **2** also underwent a similar decomposition pathway to the analogous trigermane, through homolytic scission of the Ge – Ge bond resulting in radical formation. The generated radicals, $Bu^{n}_3Ge\cdot$ and $Ph_3Ge\cdot$, reacted with the trapping reagent HOAc to form $Bu^{n}_3GeH$ (**6**), $Ph_3GeH$, and the acetate species $Bu^{n}_3GeOAc$ (**5**) and $Ph_3GeOAc$, respectively. Lastly, these radicals were observed to recombine to yield the two digermanes $Bu^{n}_6Ge_2$ (**7**) and $Ph_6Ge_2$ by the coupling of either two $Bu^{n}_3Ge\cdot$ or two $Ph_3Ge\cdot$ radicals, respectively.

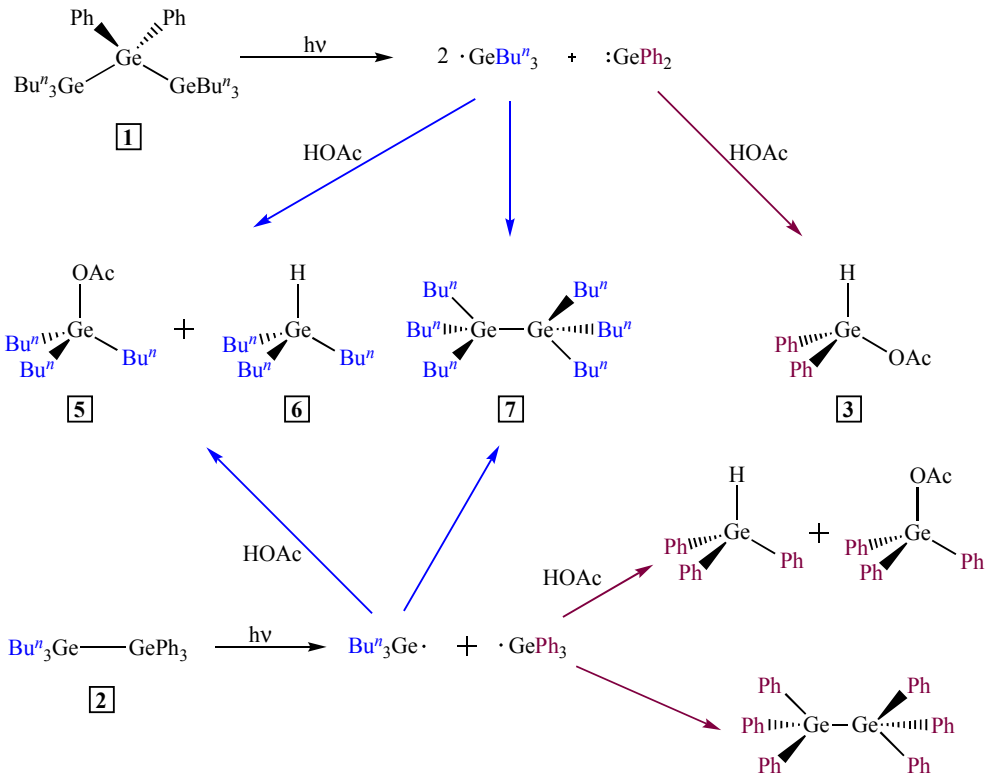


**Scheme 3.6:** Photodecomposition of oligogermanes (**1**) and (**2**) either by germylene (red) or germyl radical (blue) formation.

### 3.4 Experimental

*General Considerations*

All reagents were handled under an inert atmosphere of $N_2$ using standard Schlenk, syringe, and glovebox techniques. Solvents were dried using a Glass Contour solvent purification system. Both $Bu^n_3GeNMe_2$ and $Bu^n_3GeGePh_3$ were prepared based on previous literature procedure, with $Bu^n_3GeGeBu^n_3$ (**7**) prepared *in situ*.[91] All other germanium compounds including $Ph_2GeH_2$, $Bu^n_2GeH_2$, $Ph_6Ge_2$, $Bu^n_3GeCl$, and $Bu^n_3GeH$ (**6**) were obtained from Gelest Inc. Glacial acetic acid was purchased from Aldrich. All materials were used as received. $^1H$ and $^{13}C$ NMR spectra were recorded on the 400 and 100 MHz, respectively, using a Varian UNITY INOVA 400

spectrometer. A Luzchem photolysis panel with five UV- C lamps was used to conduct the photolysis experiments. GC-MS data was obtained on a Shimadzu QP2010 GC-MS, while a Thermo Fischer Q Exactive™ Hybrid Quadruple-Orbitrap™ Mass Spectrometer was used to collect HRAM-MS data. Elemental analyse were performed by Galbraith Laboratories.

*Methods*

In each of the initial studies 300 mg of the corresponding germane was dissolved in THF (15 mL) in a 100 mL quartz flask and the flask was closed with a septum and copper wire under an inert atmosphere of nitrogen. The flask was removed and connected to a Schlenk line under blowing nitrogen, and glacial acetic acid (30 mol equivalents) was directly injected into the THF solution. The solution was then irradiated with UV-C light for 18 hs. The THF was then removed *in vacuo* and the remaining thick liquid was dissolved in benzene (10 mL) and the excess acetic acid was extracted using water (3 x 5 mL). The volatiles from the benzene layer were then removed *in vacuo* to yield the trapping product (approximately 150 mg) as a colorless oil. The timed $^1$H NMR experiment was performed using 0.05 M of **1** and 0.1 M AcOH in 0.5 mL of cyclohexane-$d_{12}$ in a quartz NMR tube.

*Synthesis of $Bu^n_3Ge(GePh_2)GeBu^n_3$ (**1**)*

To a solution of $Bu^n_3GeNMe_2$ (1.385 g, 4.810 mmol) in acetonitrile (15 mL) was added a solution of $Ph_2GeH_2$ (0.500 g, 2.18 mmol) in acetonitrile (10 mL) under an atmosphere of nitrogen. The reaction mixture was sealed in a Schlenk tube under nitrogen and stirred for 48 hs at 85 °C. The acetonitrile was removed *in vacuo* and the resulting oil was vacuum distilled in a Kugelrohr oven (125 °C, 0.10 torr) to yield 0.992 g of **1** (64%) as a colorless oil. $^1$H NMR ($C_6D_6$, 25 °C): δ 7.73 (d, $J$ = 8.4 Hz, 6H, *o*-H), 7.22 (m, 6H, *m*-H), 7.14 (d, $J$ = 7.8 Hz, 3H, *p*-H), 1.49 (m, 6H, -$CH_2CH_2CH_2CH_3$), 1.34 (q, $J$ = 7.8 Hz, 6H, -$CH_2CH_2CH_2CH_3$), 1.19 (m, 6H, -

$CH_2CH_2CH_2CH_3$), 0.90 (t, $J$ = 7.2 Hz, 9H, -$CH_2CH_2CH_2CH_3$) ppm. $^{13}$C NMR ($C_6D_6$, 25 °C): δ 140.7 (*ipso*- $C_6H_5$), 136.1 (*ortho*- $C_6H_5$), 128.3 (*para*- $C_6H_5$), 128.1 (*meta*- $C_6H_5$), 28.8 (-$CH_2CH_2CH_2CH_3$), 27.1 (-$CH_2CH_2CH_2CH_3$), 15.0 (-$CH_2CH_2CH_2CH_3$), 13.9 (-$CH_2CH_2CH_2CH_3$) ppm. *Anal.* Calcd. for $C_{36}H_{64}Ge_3$: C, 60.47; H, 9.03. Found: C, 60.35; H, 9.11.

Synthesis of *$Bu^n_3GeGePh_3$ (**2**)*

Compound **2** was prepared in a similar fashion to literature.[73] A solution of $Bu^n_3GeNMe_2$ (0.300 g, 1.04 mmol) in $CH_3CN$ (10 mL) was added to a solution of $Ph_3GeH$ (0.318 g, 1.04 mmol) in $CH_3CN$ (10 mL) in a Schlenk tube. The reaction mixture was heated at 85 °C for 48 hs. The volatiles were removed *in vacuo* to yield 0.474 g of **2** (83%) as a white solid. $^1$H NMR ($C_6D_6$, 25 °C): δ 7.72-7.64 (m, 6H, *meta*- $C_6H_5$), 7.24-7.16 (m, 9H, *ortho*- $C_6H_5$ and *para*- $C_6H_5$), 1.52-1.39 (m, 6H, $GeCH_2$), 1.27 (sext, $J$ = 7.8 Hz, 6H, $GeCH_2CH_2CH_2CH_3$), 1.21-1.15 (m, 6H, $GeCH_2CH_2CH_2CH_3$), 0.81 (t, $J$ = 6.9 Hz, 9H, $GeCH_2CH_2CH_2CH_3$) ppm. $^{13}$C NMR ($C_6D_6$, 25 °C): δ 139.7 (*ipso*- $C_6H_5$), 135.7 (*ortho*- $C_6H_5$), 128.7 (*para*- $C_6H_5$), 128.6 (*meta*- $C_6H_5$), 28.8, 26.8, 14.5, 13.8 (butyl carbons) ppm. *Anal.* Calcd for $C_{30}H_{42}Ge_2$:C, 65.77; H, 7.73. Found: C, 65.74; H, 7.80.

*Synthesis of $Ph_2Ge(H)OAc$ (**3**)*

The reaction Schlenk, charged with $Ph_2GeHCl$[47photo] (0.27 g, 1.0 mmol) was covered with aluminum foil as reaction was light sensitive. Reagent was dissolved in 5 mL of benzene before solution of AgOAc (0.22 g, 1.3 mmol) in 10 mL of benzene was added in the dark as a suspension. Reaction was left to stir in the dark for 12 hours, filtered through Celite, and solvent was evaporated from filtrate producing the 0.25 g of **3** (85%) as a colorless oil. $^1$H NMR ($C_6D_6$, 25 °C): δ 7.65 (t, $J$ = 7.9 Hz, 4H, *o*-$C_6H_5$), 7.16-7.11 (m, 6H, *m*-$C_6H_5$ and *p*-$C_6H_5$), 6.72 (s, 1H, Ge – *H*), 1.86 (s, 3H, -OC(O)$CH_3$) ppm. $^{13}$C NMR ($C_6D_6$, 25 °C): δ 173.3 (-O*C*(O)$CH_3$), 135.0

(*ipso*-$C_6H_5$), 134.6 (*ortho*-$C_6H_5$), 130.3 (*meta*-$C_6H_5$), 128.3 (*para*-$C_6H_5$), 21.1 (-OC(O)$CH_3$ ppm. *Anal.* Calcd. for $C_{14}H_{14}GeO_2$ (286.85 g/mol): C, 58.61; H, 4.92. Found: C, 58.39; H, 4.85.

*Synthesis of $Bu^n_2Ge(H)OAc$ (**4**)*

A Schlenk flask was wrapped with aluminum foil, with $Bu^n_2GeHCl$[47photo] (0.40 g, 1.8 mmol) dissolved in 10 mL of benzene. A suspension of AgOAc (0.36 g, 2.2 mmol) was added to the solution in the dark and the reaction left stirring for 48 hs. The reaction mixture was then filtered through Celite and solvent was removed *in vacuo* from the filtrate to yield 0.38 g of **4** (86%) as a colorless oil. $^1$H NMR ($C_6D_6$, 25 °C): δ 5.71 (pent, $J$ = 3.9 Hz, 1H, Ge – *H*), 1.86 (s, 3H, -OC(O)C*H*$_3$), 1.44-1.38 (m, 4H, -$CH_2$C*H*$_2$$CH_2CH_3$), 1.24 (sext, $J$ = 8.0 Hz, 4H, -$CH_2CH_2$C*H*$_2$$CH_3$), 0.81 (t, $J$ = 7.8 Hz, 4H, -C*H*$_2$$CH_2CH_2CH_3$), 0.78 (t, $J$ = 7.8 Hz, 6H, $CH_2CH_2CH_2$C*H*$_3$) ppm. $^{13}$C NMR ($C_6D_6$, 25 °C): δ 173.2 (-O*C*(O)$CH_3$), 26.5 (-OC(O)*C*$H_3$), 24.9 (-$CH_2$*C*$H_2CH_2CH_3$), 15.8 (-$CH_2CH_2$*C*$H_2CH_3$), 13.5 (-$CH_2CH_2CH_2$*C*$H_3$), 1.0 (-*C*$H_2CH_2CH_2CH_3$) ppm. *Anal.* Calcd. for $C_{10}H_{22}GeO_2$ (246.87 g/mol): C, 48.63; H, 8.98. Found: C, 48.55; H, 8.87.

*Synthesis of $Bu^n_3GeOAc$ (**5**)*

A Schlenk flask, covered with aluminum foil, is charged with $Bu^n_3GeCl$ (0.40 g, 1.4 mmol) in 5 mL of benzene. The suspension of AgOAc (0.29 g, 1.7 mmol) in 10 mL benzene was added to the solution and left to stir for 12 hours in the dark. Solution was filtered through the Celite and dried *in vacuo* to yield 0.41 g of **5** (94%) as a colorless oil. $^1$H NMR ($C_6D_6$, 25 °C): δ 1.90 (s, 3H, -OC(O)C*H*$_3$), 1.49-1.43 (m, 6H, -$CH_2$C*H*$_2$$CH_2CH_3$), 1.30 (sext, $J$ = 8.0 Hz, 6H, -$CH_2CH_2$C*H*$_2$$CH_3$), 1.14 (t, $J$ = 8.0 Hz, 6H, -C*H*$_2$$CH_2CH_2CH_3$), 0.88 (t, $J$ = 8.0 Hz, 9H, -$CH_2CH_2CH_2$C*H*$_3$) ppm. $^{13}$C NMR ($C_6D_6$, 25 °C): δ 173.0 (-O*C*(O)$CH_3$), 26.1 (-OC(O)*C*$H_3$), 21.7 (-$CH_2$*C*$H_2CH_2CH_3$), 16.0 (-$CH_2CH_2$*C*$H_2CH_3$), 13.5 (-$CH_2CH_2CH_2$*C*$H_3$), 1.0 (-*C*$H_2CH_2CH_2CH_3$) ppm. *Anal.* Calcd. for $C_{14}H_{30}GeO_2$ (302.98 g/mol): C, 55.49; H, 9.98. Found: C, 55.31; H, 9.86.

*Commercially obtained - $Bu^n_3GeH$ (**6**)*

*Previously prepared - $Bu^n_3GeGeBu^n_3$ (**7**)*

*Synthesis of $Bu^n_3GeNMe_2$ (**8**)*

To a solution of $Bu^n_3GeCl$ (1.000 g, 3.58 mmol) in benzene (10 mL) was added $LiNMe_2$ (0.219 g, 4.29 mmol) in benzene (5 mL) in a 100 mL Schlenk flask. The reaction was allowed to stir at room temperature for 18 hours. The solution was then filtered through Celite and the volatiles were removed *in vacuo* to yield 0.961 g of $Bu^n_3GeNMe_2$ (93 %) as a colorless liquid. $^1H$ NMR ($C_6D_6$, 25 °C): δ 2.62 (s, 6H, GeN-($CH_3$)$_2$), 1.52-1.30 (m, 12H, $GeCH_2CH_2CH_2CH_3$), 0.93 (t, $J$ = 7.2 Hz, 9H, -$GeCH_2CH_2CH_2CH_3$), 0.89 (m, 6H, $GeCH_2$) ppm. $^{13}C$ NMR ($C_6D_6$, 25 °C): δ 41.5 (-N($CH_3$)$_2$), 27.4, 26.9, 14.1 (butyl carbons), 13.2 (-$CH_2CH_2CH_2CH_3$) ppm. *Anal.* Calcd for $C_{14}H_{33}GeN$: C, 58.38; H, 11.55. Found: C, 58.28; H, 11.79.

*Photolysis of $Bu^n_3Ge(GePh_2)GeBu^n_3$ (**1**) in THF*

The reaction was complete in a 100 mL quartz flask charged with a solution of **1** (0.300 mg, 0.420 mmol) in THF (15 mL). Glacial acetic acid (0.75 mL, 0.79 g, 13.1 mmol) was syringed into the reaction mixture under an atmosphere of $N_2$ atmosphere. Sample was left stirring and irradiated with UV-C light for 18 hs, after which volatiles were removed *in vacuo*. The colorless oil was dissolved in benzene (15 mL) and washed with water (2 x 10 mL) to remove excess acetic acid. Organic layer was dried over anhydrous $MgSO_4$, filtered over Celite, and dried to yield a thick oil.

*Photolysis of $Bu^n_3Ge(GePh_2)GeBu^n_3$ (**1**) in $C_6D_{12}$*

Within a quartz NMR tube, **1** (0.035 g, 0.049 mmol) was dissolved in cyclohexane-$d_{12}$ (0.5 mL) and glacial acetic acid (5.6 μL, 0.0059 g, 0.098 mmol) was added. The reaction was

irradiated with UV-C light for 1 minute and the $^{1}H$ NMR spectrum taken immediately afterwards for 10 minutes. The sample was then exposed to UV-C light for 2 minute intervals, until a total of 30 minutes of exposure time was reached, afterwards exposed for 15 minute intervals.

*Photolysis of $Bu^{n}_{3}GeGePh_{3}$ (**2**) in THF*

A quartz flask was charged with **2** (0.375 g, 0.684 mmol) and dissolved in THF (20 mL). To the reaction mixture, glacial acetic acid (0.59 mL, 0.615 g, 6.55 mmol) was added via syringe under an $N_2$ atmosphere. The mixture was irradiated with UV - C light for 18 hours and the product was dried under vacuum yielding a colorless oil. Product was dissolved in benzene (15 mL) and solution was washed with water (2 x 10 mL) to remove excess acetic acid. The top benzene layer was separated, dried over anhydrous $MgSO_4$, and filtered. The remaining solvent was removed and resulting in a thick oil (0.351 g).

# CHAPTER IV

## SYNTHESIS AND INVESTIGATION OF THE PHYSICAL PROPERTY AND STRUCTURE RELATIONSHIP OF BRANCHED OLIGOGERMANES $(Me_3Ge)_3GePh$, $(Me_2Bu^tGe)_3GePh$, AND $(Me_2PhGe)_3GePh$.

### 4.1 Introduction

Similar to hydrocarbons, linear, cyclic, and branched structures are also known for their heavier group 14 analogues. One difference between carbon and its heavier counterparts is the weakness of the bonds for silicon, germanium, or tin element bonds, which need to be stabilized by organic substituents (ie. methyl, phenyl, *n*-butyl, etc.). Long-chain hydrocarbons, highly branched structures, and polycyclic species are common for carbon based molecules. However, these same materials are less known for heavier group 14 elements. This chapter focuses on the synthesis of a series of branched germanium compounds via the hydrogermolysis reaction, and an investigation of their physical properties.

The preparation and synthesis of branched oligomers were difficult and relatively rare before the mid-2000s, with very few examples reported throughout literature. Such compounds include $(Ph_3Ge)_3GeR$ (R= H, $CH_3$),[92] $(Cl_2PhGe)_3GePh$,[93] $(Me_2PhGe)_3GePh$,[93] $(PhX_2Ge)_3GePh$ (X = OMe, SMe, $Me_2N$, $Et_2P$),[94] $(Me_3Ge)_3GeCl$,[95] and $(Me_3Ge)_4Ge$.[96-97] In 2008 the first structurally

characterized branched oligogermanes was reported $(Ph_3Ge)_3GePh$.[98] This laid the ground work for the preparation of other branched oligomers including $(Ph_3Ge)_3GeX$ (X = H, Cl, Br, I),[99] **(**$Ph_3Ge)_4Ge$,[100] $(Me_3Ge)_3Ge(GePr^i_3)$,[101] $(Me_3Ge)_3GeSiPr^i_3$,[102] and mixed linear/branched species $(Me_3Ge)_3GeGe(GeMe_3)$[95] and $(Me_3Ge)_3GeGeMe_2Ge(GeMe_3)$.[102]

### 4.2 Results & Discussion

A series of branched oligogermanes $(Me_3Ge)_3GePh$ (**1**), $(Me_2Bu^tGe)_3GePh$ (**2**), and $(Me_2PhGe)_3GePh$ (**3**) were synthesized and characterized by NMR spectroscopy ($^1H$, $^{13}C$, and $^{73}Ge$), UV-visible spectroscopy, and electrochemical methods (CV, DPV). These three compounds, as well as $(Bu^n_3Ge)_3GePh$ (**4**), were all analyzed using high resolution accurate mass mass spectrometry (HRAM-MS), representing the first HRAM-MS investigation of branched oligogermanes.

The three oligogermanes **1-3** were prepared by the hydrogermolysis reaction shown in **Scheme 4.1**, however, compounds **2-4** will be of primary focus throughout the chapter as compound **1** was primarily investigated by co-authors Shumaker, F. A, and Knight, C. J. The amides $R_3GeNMe_2$ ($R_3$ = $Me_3$, $Me_2Bu^t$, or $Me_2Ph$) were prepared from the corresponding chlorides $R_3GeCl$ by reaction with $LiNMe_2$ in either THF or $Et_2O$. All three branched compounds were pale yellow liquids at room temperature. Crystallization of these compounds were attempted, but X-ray quality crystals could not be obtained. A previous synthetic route was reported to prepare compound **3,** involving the insertion of a germylene (PhGeCl) into the Ge – Cl bonds of $PhGeCl_3$ to yield $(Cl_2PhGe)_3GePh$. This branched species was subsequently reacted with MeMgI to produce **3** that was isolated as a liquid.[93] The previously synthesized $(Bu^n_3Ge)_3GePh$ also was obtained as a liquid.

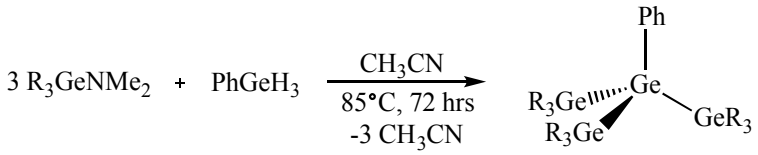


$R_3Ge$ = $Me_3Ge$ (**1**), $Me_2Bu^tGe$ (**2**), and $Me_2PhGe$ (**3**)

**Scheme 4.1**: Synthetic preparation of branched compounds **1-3**.

All the aforementioned branched compounds were characterized *via* $^1H$ and $^{13}C$ NMR spectroscopy while their electronic and optical properties were probed by CV/DPV and UV-visible, respectively. The aryl region of the $^1H$ and $^{13}C$ NMR spectra of **1-3** appeared nearly identical, with **3** having additional peaks due to the three phenyl groups on the peripheral $Me_2$*Ph*Ge- groups. The $^1H$ NMR spectrum of **2** had a peak at δ 0.98 ppm which corresponds to the methyl protons of the *tert*-butyl groups. Each of the branched compounds, $(R_3Ge)_3GePh$ [R = $Me_3$ (**1**), $Me_2Bu^t$ (**2**), $Me_2Ph$ (**3**)], exhibit a singlet resonance for the peripheral methyl groups, observed at δ 0.37, 0.74, and 0.27 ppm respectively. The $^{13}C$ NMR spectra for these branched species also are very similar in the aryl region, with different patterns appearing in the alkyl region. The $^{13}C$ NMR of compound **3** has four additional peaks for the phenyl groups of the peripheral ligands at δ 138.8 (*ipso*), 134.0 (*ortho*), 127.8 (*para*), and 123.3 (*meta*) ppm. The $^{13}C$ NMR spectrum of compound **2** had resonances at δ 28.3 (-C(*C*$H_3$)) and 26.9 (-*C*($CH_3$) ppm corresponding to the methyl and central carbons in the *tert*-butyl substituent, respectively. Resonances for the methyl carbons of all branched species (**1-3**) appear at δ 0.2, -3.4, and -0.2 ppm, respectively. An upfield shift was observed due to the increased shielding as the peripheral methyl groups in **1** are replaced by a *tert*-butyl or phenyl group in **2** and **3**. The *tert*-butyl group is the most electron donating substituent, and results in the most upfield resonance of -3.4 ppm for the methyl groups of $(Me_2Bu^tGe)_3GePh$ (**2**).

The electrochemical properties of branched species **1-4** were examined using cyclic and differential pulse voltammetry. The CV and DPV voltammograms are overlaid in the plots below

(**Figures 4.1** and **4.2**) and the oxidation potential values are shown in **Table 4.1**. The experiments were conducted in dichloromethane using 0.1 M [Bu$^n_4$N][$PF_6$] as the supporting electrolyte with a Ag/AgCl reference electrode and a glassy carbon working electrode. The observed oxidation potentials indicated the ease of oxidation of the branched oligomers as **4** < **2** < **3** < **1** from harder to easiest to oxidize. Compounds **1-3** all exhibited a single oxidation wave, while **4** showed two distinct oxidation waves.

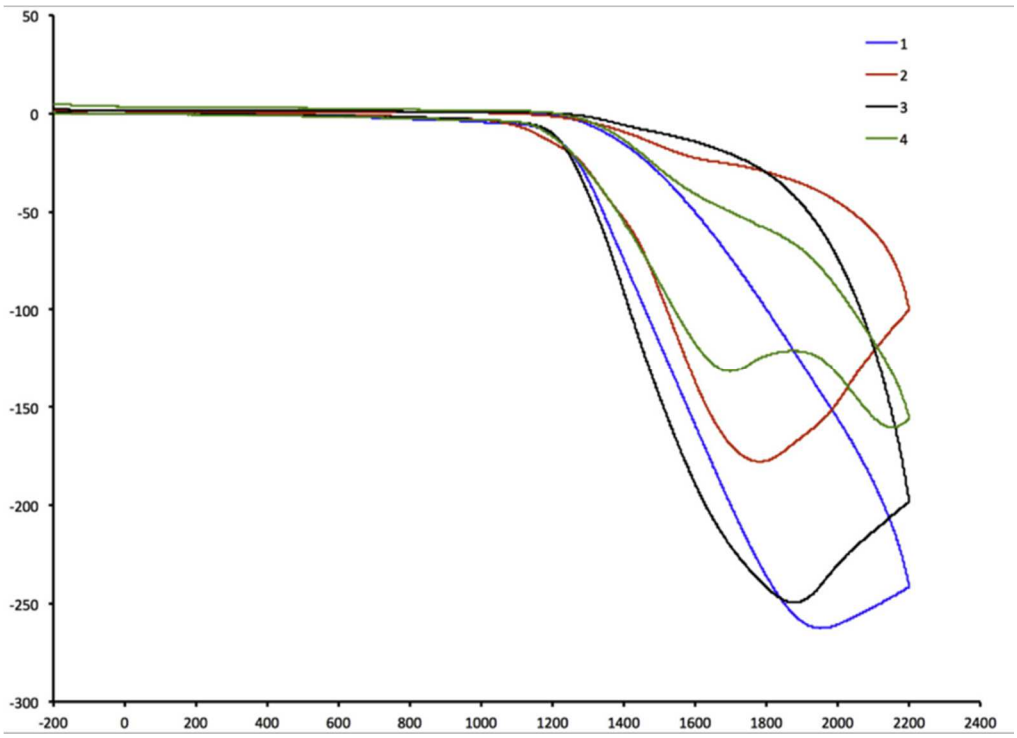


**Figure 4.1:** Overlaid CV plots of **1-4** solution with 0.1 M [Bu$^n_4$N][$PF_6$] in $CH_2Cl_2$.

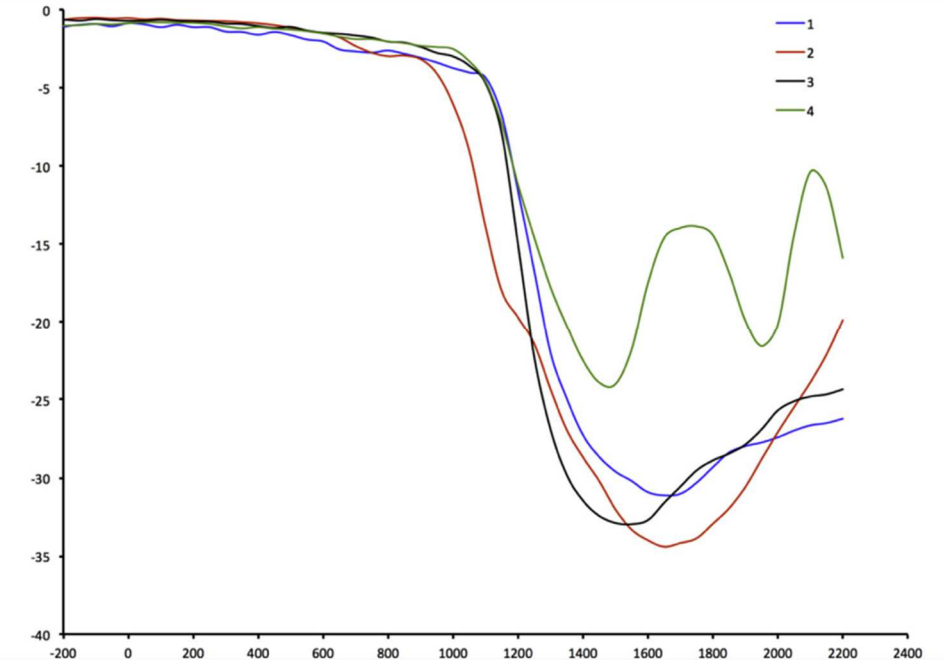


**Figure 4.2:** Overlaid DPV plot of **1-4** solution with 0.1 M $[Bu^{n}_{4}N][PF_6]$ in $CH_2Cl_2$.

The oxidation potentials observed for these systems can be correlated to the electron donor or acceptor properties of the organic substituents on the peripheral germanium atoms. Compound **1** has the most positive oxidation potential at 1951 and 1650 mV for CV and DPV repsectively, with $Me_3Ge$- ligands having minimal inductive electron donating effects. The branched compound $(Me_2Bu^{t}Ge)_3GePh$ (**2**), has an added *tert*-butyl substituent, that in comparison to **1**, is more electron donating. The oxidation potential of **2** is less positive than **1**, observed at 1782 mV and 1575 mV in the CV and DPV respectively. This indicates that **2** is easier to oxidize than **1,** which is consistent with previous findings, as more highly donating substituents destabilize the energy of the HOMO in these systems, and as the energy of the HOMO is destabilized the molecule becomes easier to oxidize.[103]

| Compound | $E_{ox}$ (CV, mV) | $E_{ox}$ (DPV, mV) |
|---|---|---|
| $(Me_3Ge)_3GePh$ **(1)** | 1951 | 1650 |
| $(Me_2Bu^tGe)_3GePh$ **(2)** | 1782 | 1575 |
| $(Me_2PhGe)_3GePh$ **(3)** | 1877 | 1600 |
| $(Bu^n_3Ge)_3GePh$ **(4)** | 1691, 2153 | 1500, 1950 |
| $(Ph_3Ge)_3GePh$ **(5)** | 1435 | 1295 |

**Table 4.1:** Oxidation potential values for branched oligogermanes **1-5**.

The branched germane **3** exhibited an oxidation potential of 1877 mV in its CV and 1600 mV in its DPV. These potentials are intermediate between the corresponding values for **1** and **2**. As compound $(Me_2PhGe)_3GePh$ (**3**) introduces a phenyl substituent, replacing the $-Bu^t$ and –Me alkyl groups, the possibility of $\pi$-type interactions arises. This occurs when the σ-bonding framework of the $Ge_4$ backbone overlaps with the $\pi^*$-orbitals of the phenyl ring. Previous studies have reported several linear and branched oligogermanes, that have the phenyl rings behave as both σ-donor and $\pi$-acceptor ligands. This dual effect destabilizes the HOMO by inductive σ-donation while it also simultaneously stabilizes it by the $\pi$-acceptor interaction.[103-104] The σ-donation interaction renders **3** easier to oxidize than **1**, but the $\pi$-acceptor interaction makes it more difficult to oxidize that **2**.

The branched oligomer $(Bu^n_3Ge)_3GePh$ (**4**) showed two oxidation waves at 1691 (CV) and 1500 mV (DPV), making it the easiest to oxidize of all the four branched oligogermanes. It was expected that oxidation potential of **4** would be the least positive due to the electron donating ability of the three *n*-butyl substituents, which results in the $Ge_4$ framework being the most electron rich within the series. A second irreversible oxidation wave for **4** was also observed at 2153 (CV) and 1950 (DPV) mV, suggesting the species generated after the first oxidation event is stable enough to undergo further oxidation. These types of multiple oxidation waves are

commonly seen in aryl substituted linear oligogermanium systems, but is the first example of this pattern seen in branched species.[105-106]

The second oxidation wave can be explained by the *n*-butyl substituents stabilizing the species produced from **4** after the first oxidation, by means of its inductive electron donating ability. It is plausible that both linear and branched oligogermanes break apart by homolytic scission of the Ge – Ge bonds after the oxidation event, which was observed with the photolytic experiments conducted. Attempts were made to isolate the products generated after oxidation by using acetic acid or $CCl_4$ as trapping agents, in order to observe the presence of any germanium-based radicals or germylenes that were produced after the oxidation event. Bulk electrolysis experiments were conducted on **1-4** with acetic acid as the trapping agent but after workup an intractable product mixture resulted which produced no identifiable products by $^1$H NMR spectroscopy. The same process was attempted using $CCl_4$ as the trapping agent for the branched compounds **1-4**, and **4** produced $Bu^n_3GeCl$, that was isolated by distillation. The $^1$H and $^{13}$C NMR spectra of the distillate was compared with a commercial sample of $Bu^n_3GeCl$ to confirm its identity, and was further confirmed by elemental analysis. If homolytic bond cleavage of the Ge – Ge bond occurred after the first oxidation, the formation of a neutral or cationic $Bu^n_3Ge\cdot$ radical would result and this would subsequently convert to $Bu^n_3GeCl$ after abstraction of a chlorine from $CCl_4$. The remaining neutral or cationic trigermane fragment $(Bu^n_3Ge)_2GePh\cdot$ would also be converted to a chloride $(Bu^n_3Ge)_2GePhCl$ which would be oxidized in the second oxidation event and undergo decomposition to generate two more equivalents of $Bu^n_3GeCl$. It was thought that compounds **1-3** could also show similar decomposition pathways but these were not observed, likely due to polymerization or further rapid decomposition after oxidation.

UV-visible spectroscopy was used to study the absorbance properties of the branched compounds **1-4**, and an overlaid plot of their spectra shown in **Figure 4.3**, while their absorbance data collected in **Table 4.2**. The extinction coefficients of oligogermanes with $\sigma \longrightarrow \sigma^*$ electronic

transitions are usually on the order of $10^4$ $M^{-1}$ $cm^{-1}$. As seen with other oligogermanes, the HOMO/LUMO gap is affected by the electronic and steric nature of the organic substituents on the germanium atoms, thus having a direct effect on the position of the $\lambda_{max}$ for the branched compounds.[103,107] Both oligogermanes **2** and **4** exhibit absorbance maxima with the highest energies at 223 and 224 nm, respectively, indicating that they have the largest gap between the HOMO and LUMO. Compound **1** $(Me_3Ge)_3GePh$ has a red-shifted $\lambda_{max}$ = 237 nm, which indicates a slightly smaller HOMO/LUMO gap in comparison to compounds **2** and **4**. Lastly, the $\lambda_{max}$ for $(Me_2PhGe)_3GePh$ (**3**) is further red shifted with a $\lambda_{max}$ at 245 nm, indicating a further decrease in the HOMO/LUMO gap of the molecule. This is due to the phenyl substituents on the peripheral germanium atoms as there is conjugation between the $\pi^*$-orbitals on the phenyl groups and the σ-bonding system of the $Ge_4$ backbone.

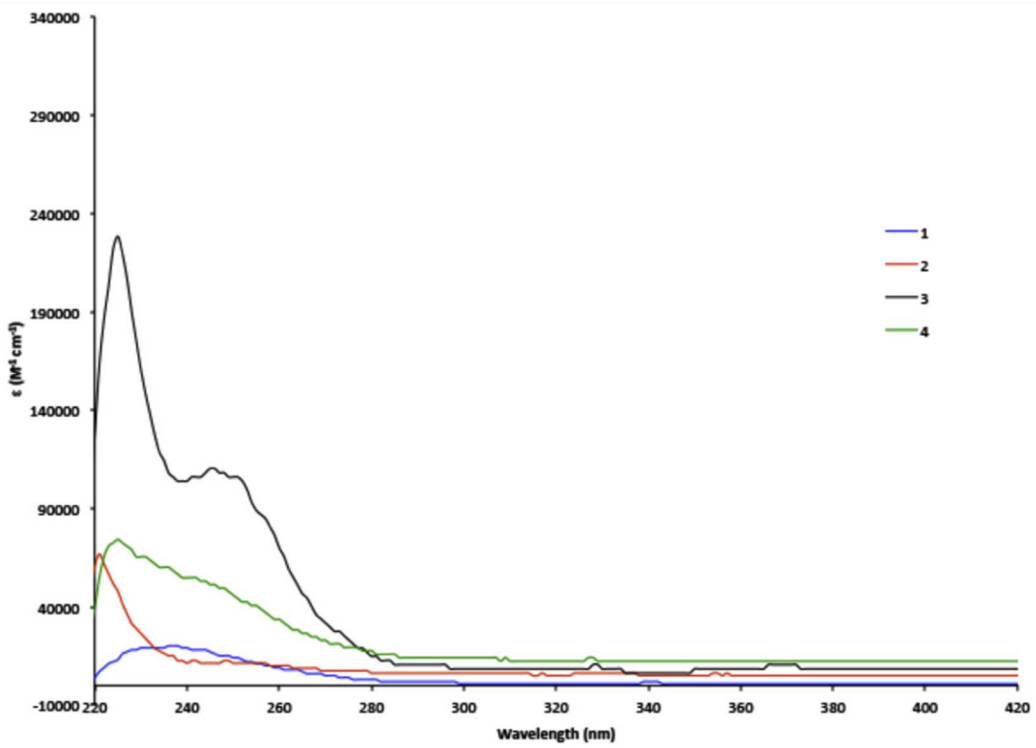


**Figure 4.3:** Overlaid UV-visible plot for the oligogermanes **1-4** in $CH_2Cl_2$ solution.

| Compound | $\lambda_{max}$ (nm) | $\varepsilon$ ($M^{-1}$ $cm^{-1}$) |
|---|---|---|
| $(Me_2Bu^tGe)_3GePh$ **(1)** | 237 | $2.0 \times 10^4$ |
| $(Me_2Bu^tGe)_3GePh$ **(2)** | 223 | $5.2 \times 10^4$ |
| $(Me_2PhGe)_3GePh$ **(3)** | 245 | $5.5 \times 10^4$ |
| $(Bu^n{}_3Ge)_3GePh$ **(4)** | 224 | $7.4 \times 10^4$ |

**Table 4.2**: UV-visible data for branched oligogermanes **1-4** in $CH_2Cl_2$.

The branched compounds **1-4** were also characterized by $^{73}$Ge NMR spectroscopy with the data collected in **Table 4.3**. The $^{73}$Ge nucleus is difficult to observe as it has a spin of 9/2, a high quadrupole moment, and a low observation frequency. This low resonance frequency causes acoustic ringing in the probe during acquisition, and as a consequence a large number of scans are needed to obtain meaningful spectral data.[108-111] These complications cause the germanium NMR to be difficult to probe. Previous spectroscopic data on numerous oligogermanes has shown that the chemical shifts for germanium atoms are dependent on the substituent pattern present and number of attached germanium atoms. Resonances for trisubstituted germanium atoms $R_3Ge$-, disubstituted germanium atoms $–R_2Ge–$, and monosubstituted germanium range between δ -30 to -75 ppm, -110 to -140 ppm, and -185 to -235 ppm respectively.

The resonance for the central germanium atom ($(R_3Ge)_3$*Ge*Ph) in **1-4** had chemical shifts ranging from δ -188 to -207 ppm. Trialkyl-substituted oligogermane **4** has a peak furthest downfield at δ – 196 ppm, while the resonances for the central germanium of **2** and **3** appear upfield in comparison at δ -207 and -204 ppm. This trend in upfield shifts of the $^{73}$Ge NMR resonances is also seen in the presence of aryl and branched alkyl substituents on linear oligogermanes.[112] The resonances for the peripheral germanium atoms were only seen for **1** and **4**, due to the need for a symmetric environment about germanium to have a $^{73}$Ge NMR resonance sharp enough to observe. Broadening of the resonances into the baseline is typically observed

with asymmetric environments about a germanium atom, which is seen for the peripheral germanium atoms of both **2** and **3** due to their substituent pattern. The resonance for $(Bu^{n}_{3}Ge)_3GePh$ (**4**) is found within the range of trialkyl-substituted germanium atoms of similar composition, with $Ge_{peripheral}$ chemical shifts from -30 to -60 ppm and $G_{central}$ chemical shifts varying from -100 to -200 ppm.[112]

| Compound | $\delta$ –$Ge_{peripheral}$ (ppm) | $\Delta_{1/2}$ –$Ge_{peripheral}$ (Hz) | $\delta$ –$Ge_{central}$ (ppm) | $\Delta_{1/2}$ –$Ge_{central}$ (ppm) |
|---|---|---|---|---|
| $(Me_2Bu^{t}Ge)_3GePh$ **(1)** | -45 | 296 | -188 | 157 |
| $(Me_2Bu^{t}Ge)_3GePh$ **(2)** | n/o | n/o | -207 | 296 |
| $(Me_2PhGe)_3GePh$ **(3)** | n/o | n/o | -204 | 104 |
| $(Bu^{n}_{3}Ge)_3GePh$ **(4)** | -33 | 240 | -195 | 100 |

[a] n/o = not observed

**Table 4.3:** $^{73}$Ge NMR data for branched oligogermanes **1-4**.

The HRAM-MS spectra for these compounds were also obtained, and are the first such studies done on branched oligogermanes. The spectral data are collected in **Table 4.3**. Previous work using this methodology has shown that the parent compounds appear as adducts with $CH_3CN$ and also adducts with $H_2O$.[113] This is due to $CH_3CN$ used in sample preparation and water being present in trace amounts within the solvent. This also generates germoxanes as oxygen insertion into the Ge – Ge bonds can occur due to the presence of water.

| Compound | *m/z* | Assignment | Calcd. *m/z* |
|---|---|---|---|
| **2** | 670.0970 | $(Me_2Bu^{t}Ge)_3GePh(CH_3CN)H^{+}$ | 670.1138 |
| | 551.0922 | $(Me_2Bu^{t}Ge)_2GePh(CH_3CN)_2^{+}$ | 551.0918 |
| | 510.0656 | $(Me_2Bu^{t}Ge)_2GePh(CH_3CN)^{+}$ | 510.0652 |

| | | | |
|---|---|---|---|
| | 352.0331 | $(Me_2Bu^tGe)GePh(CH_3CN)H^+$ | 352.0036 |
| | 243.0907 | $(Me_2Bu^tGe)(CH_3CN)_2^+$ | 243.0911 |
| | 202.0641 | $(Me_2Bu^tGe)(CH_3CN)^+$ | 202.0646 |
| | 161.0377 | $(Me_2Bu^tGe)^+$ | 161.0380 |
| **3** | 782.0344 | $(Me_2PhGe)_2(Me_2PhGeO)GePh(CH_3CN)(H_2O)_2OH$ | 782.0359 |
| | 377.0171 | $(Me_2PhGe)_2OH^+$ | 377.0176 |
| | 222.0328 | $(Me_2PhGe)_2$ | 222.0333 |
| | 181.0063 | $Me_2PhGe^+$ | 181.0067 |
| **4** | 922.3793 | $(Bu^n_3Ge)_3GePh(CH_3CN)H^+$ | 922.3955 |
| | 678.2539 | $(Bu^n_3Ge)_2GePh(CH_3CN)^+$ | 678.2530 |
| | 528.2840 | $(Bu^n_3Ge)_3(CH_3CN)^+$ | 528.2840 |
| | 286.1579 | $Bu^n_3Ge(CH_3CN)^+$ | 286.1585 |
| | 245.1315 | $Bu^n_3Ge^+$ | 245.1319 |

**Table 4.4:** HRAM-MS data for oligogermanes **2-4**.

The spectral data of $(Me_2Bu^tGe)_3GePh$ (**2**) indicates that it does not undergo oxygen insertion into any of the germanium bonds, and the parent ion is found as the protonated $CH_3CN$ adduct $(Me_2Bu^tGe)_3GePh(CH_3CN)H^+$. The fragmentation pattern also shows the successive loss of one peripheral $Me_2Bu^tGe$- group which generated the $(Me_2Bu^tGe)_2GePh(CH_3CN)_n^+$ (n = 1 or 2), $(Me_2Bu^tGe)GePh(CH_3CN)H^+$, and $(Me_2Bu^tGe)(CH_3CN)_n^+$ (n = 1-3) ions.

Compound $(Me_2PhGe)_3GePh$ (**3**) has its molecular ion found as a protonated germoxane in the form of $(Me_2PhGe)_2(Me_2PhGeO)GePh(CH_3CN)(H_2O)_2OH^+$. This species fragments into the protonated digermoxane $(Me_2PhGe)_2OH^+$, $Me_2PhGe(CH_3CN)^+$, and $Me_2PhGe^+$ ions. The molecular ion for $(Bu^n_3Ge)_3GePh$ (**4**) is observed as the protonated acetonitrile solvate $(Bu^n_3Ge)_3GePh(CH_3CN)H^+$. The fragmentation pattern is generated by the loss of $Bu^n_3Ge$- groups to yield the $(Bu^n_3Ge)_2GePh(CH_3CN)H^+$ ion. Solvated digermane ion is also formed $(Bu^n_3Ge)_2(CH_3CN)^+$, with the peripheral $Bu^n_3Ge$- group resulting in the $(Bu^n_3Ge)(CH_3CN)^+$ and $Bu^n_3Ge^+$ ions.

## 4.3 Conclusion

Three branched oligogermanes $(Me_3Ge)_3GePh$ (**1**), $(Me_2Bu^tGe)_3GePh$ (**2**), and $(Me_2PhGe)_3GePh$ (**3**) were synthesized by the hydrogermolysis reaction, and along with **4** were characterized *via* NMR, CV/DPV, and UV-visible spectroscopy. These studies have shown that subtle changes of the substituent composition on the peripheral germanium atoms can result in measureable changes in both oxidation potential and absorbance maxima. Amongst these oligogermanes, only compound **4** was found to possess two irreversible oxidation waves in both its CV and DPV. Bulk electrolysis of **4** also underwent bulk electrolysis in the presence of $CCl_4$ to yielded $Bu^n_3GeCl$. The chloride was isolated and **4** was determined to decompose via homolytic scission of the Ge – Ge bonds to generate radical species.

The aforementioned oligogermanes were further characterized by $^{73}Ge$ NMR spectroscopy, with the resonances of some of the peripheral and all of the central germaniums observed. HRAM-MS were also obtained for compounds **1-4**, with the corresponding parent ions seen as adducts with either acetonitrile solvent or as a germoxanes resulting from oxygen insertion into the Ge – Ge bonds. These parent ions fragment into several daughter ions, and these studies represent the first use of HRAM-MS studies on branched oligogermanes.

## 4.4 Experimental

*General Considerations*

Preparations and further manipulations were done under nitrogen atmosphere using standard Schlenk, syringe, and glovebox techniques. All solvents were dried using a Glass Contour solvent purification system. Literature procedures were used to prepare $Me_3GeNMe_2$, $Me_2Bu^tGeNMe_2$, and $Me_2PhGeNMe_2$. Commercial $PhGeH_3$ was purchased from Gelest and used without further purification. A Bruker Inova spectrometer was used to obtain NMR spectra using

a 400 MHz ($^{1}$H) or 100 MHz ($^{13}$C). The UV-visible spectra were taken on an Ocean Optics Red Tide USB650UV spectrometer. The DigiIvy DY2312 potentiostat recorded the electrochemical data, including CV, DPV, and BE. The working electrode is glassy carbon, a platinum wire counter electrode, and a Ag/AgCl as a reference electrode using 0.1 M [Bu$^{n}_{4}$N][$PF_6$] in $CH_2Cl_2$ solution as the supporting electrolyte. A Thermo Fischer Q Exactive™ Hybride Quadrupole-Orbitrap™ Mass Spectrometer was used to collect the HRAM-MS data. Elemental analyses were conducted at Galbraith Laboratories.

*Synthesis of $(Me_3Ge)_3GePh$ (**1**)*

A Schlenk tube was charged with $PhGeH_3$ (0.255 g, 1.67 mmol) and a solution of $Me_3GeNMe_2$ (0.810 g, 5.01 mmol) in $CH_3CN$ was added to the pot. The reaction mixture was heated in an oil bath at 85 °C for 72 h and then cannulated to another flask. Volatiles were removed *in vacuo* to produce **1** (0.60 g, 72%) as a pale yellow oil. $^{1}$H NMR ($C_6D_6$, 25 °C): δ 7.52 (d, $J$ = 7.6 Hz, 2H, *o*-$C_6H_5$), 7.19-7.05 (m, 3H, *m*-$C_6H_5$ and *p*-$C_6H_5$), 0.37 (s, 27H, -$CH_3$) ppm. $^{13}$C NMR ($C_6D_6$, 25 °C): δ 137.2 (*ipso*-$C_6H_5$), 135.8 (*ortho*-$C_6H_5$), 128.5 (*meta*-$C_6H_5$), 127.8 (*para*-$C_6H_5$), 0.2 (-$CH_3$) ppm. *Anal.* Calcd. for $C_{15}H_{32}Ge_4$: C, 35.80; H, 6.41. Found: C, 35.91; H, 6.38.

*Synthesis of $(Me_2Bu^tGe)_3GePh$ (**2**)*

In a Schlenk tube, a solution of $Me_2Bu^tGeNMe_2$ (1.60 g, 7.85 mmol) in 11 mL of $CH_3CN$ was added to $PhGeH_3$ (0.390 g, 2.55 mmol). The reaction mixture was heated in an oil bath at 95 °C for 72 hours. The sample was cannulated to a fresh Schlenk flask before the solvent was evaporated to yield **2** (1.38 g, 86%) a pale yellow oil. Crude product was purified by distillation in a Kugelrohr oven (120 °C, 0.03 torr). $^{1}$H NMR ($C_6D_6$, 25 °C): δ 7.51 (d, $J$ = 8.0 Hz, 2H, *o*-$C_6H_5$), 7.17-7.03 (m, 3H, *m*-$C_6H_5$ and *p*-$C_6H_5$), 0.98 (s, 27H, -C($CH_3$)$_3$), 0.74 (s, 9H, -$CH_3$) ppm. $^{13}$C NMR ($C_6D_6$, 25 °C): δ 138.8 (*ipso*-$C_6H_5$), 136.0 (*ortho*-$C_6H_5$), 128.4 (*meta*-$C_6H_5$), 127.8

(*para*- $C_6H_5$), 28.3 (-C($CH_3$)), 26.9 (-$C$($CH_3$)), -3.4 (s, -$CH_3$) ppm. *Anal.* Calcd. for $C_{24}H_{50}Ge_4$: C, 45.79; H, 8.01. Found: C, 45.66; H, 8.06.

*Synthesis of $(Me_2PhGe)_3GePh$ (**3**)*

A solution of $Me_2PhGeNMe_2$ (1.37 g, 6.12 mmol) in 12 mL of $CH_3CN$ was added to $PhGeH_3$ (0.30 g, 1.97 mmol) in a Schlenk tube. The reaction was sealed and heated in an oil bath at 95 °C for 72 h. Crude sample was cannulated to a fresh Schlenk flask and volatiles were removed *in vacuo*. The byproducts were removed from the product by distillation in a Kugelrohr oven (130 °C, 0.02 torr) to yield **3** (1.11 g, 82%) as a pale yellow oil. $^1$H NMR ($C_6D_6$, 25 °C): δ 7.31-7.25 (m, 8H, *o*-$C_6H_5$Ge and *o*-$C_6H_5Me_2$Ge), 7.12-7.05 (m, 4H, *p*-$C_6H_5$Ge and *p*-$C_6H_5Me_2$Ge), 6.92-6.80 (m, 8H, *m*-$C_6H_5$Ge and *m*-$C_6H_5Me_2$Ge), 0.27 (s, 18H, -$CH_3$) ppm. $^{13}$C NMR ($C_6D_6$, 25 °C): δ 141.7 (*ipso*-$C_6H_5$Ge), 138.8 (*ipso*-$C_6H_5Me_2$Ge), 136.6 (*ortho*-$C_6H_5$Ge), 134.0 (*ortho*- $C_6H_5Me_2$Ge), 128.4 (*meta*-$C_6H_5$Ge), 123.3 (*meta*-$C_6H_5Me_2$Ge), 127.9 (*para*-$C_6H_5$Ge), 127.8 (*para*-$C_6H_5Me_2$Ge), -0.2 (s, -$CH_3$) ppm. *Anal.* Calcd. for $C_{30}H_{38}Ge_4$: C, 52.26; H, 5.56. Found: C, 52.15; H, 5.49.

# CHAPTER V

## SYNTHESIS OF A SERIES OF TRIISOPROPYL TERMINATED OLIGOGERMANES $Pr^{i}_{3}Ge(GePh_2)_nGePr^{i}_{3}$ ($n$ = 0-3) HIGHLIGHTING A LUMINESCENT AND DICHROIC PENTAGERMANE

### 5.1 Introduction

Polymers with extended backbones of heavier group 14 elements exhibit unique electronic and optical properties not normally associated with saturated carbon-containing polymers, a result of inherent $\sigma$ – delocalization. These properties include a red shift of $\lambda_{max}$ with increasing chain length, emissive behavior, and semiconducting behavior.[114] Polygermanes and germanium nanomaterials are two important classes of materials of interest due to their possible implementation in photoconductors, photoresists, and other nonlinear optical materials.[115-117] As the limitations of silicon based materials are being reached, polygermanes and germanium nanomaterials could serve as substitutes for various silicon based devices. Although many polymeric catenates have been prepared their exact composition remains largely unknown. It has been suggested that polymeric systems have random regions of order and disorder. This can be attributed to corresponding to areas with trans-coplanar chains terminated with out-of-plane twists which are scattered throughout the structure.[12] On the other hand, smaller oligogermane systems are finite molecules, having both structures and compositions that can be precisely

determined, and these molecules can be used as small-molecule models for their larger polymeric counterparts.

Several long-chain oligogermanes have been reported in the literature, including $Ge_{10}Me_{22}$, $Ge_nMe_{2n}(SMe)_2$ ($n$ = 1-10), $Ge_{11}Me_{22}Ph_2$, $Ge_5Ph_{12}$, and the previously synthesized hexagermane $Pr^i_3Ge(GePh_2)_4GePr^i_3$.[59,100,105,118-119] The hexagermane was originally assumed to be the first discrete oligogermane, to exhibit both an absorbance and an emission maxima comparable to that of known polygermanes. In addition to these unique properties, the hexagermane also showed dichroism in the solid state. Based on these observations it was predicted that oligogermanes need to have a minimum of six germanium atoms in order for them to behave similarly to the larger polymericmaterials. However, with the crystallization of the pentagermane $Pr^i_3Ge(GePh_2)_3GePr^i_3$ this was proven false as the pentagermane also exhibited optical properties which are typically seen for larger systems. The complete series of isopropyl terminated oligogermanes $Pr^i_3Ge(GePh_2)_nGePr^i_3$ ($n$ = 0-3) were prepared for comparison, and no such properties similar to the polymer were observed. This could be attributed to the fact that polygermanes themselves have portions of five to six germanium atoms, arranged in an ordered fashion.

**5.2 Results and Discussion**

The series of isopropyl terminated oligogermanes, ranging from a di- to a pentagermane, were all prepared using the hydrogermolysis method. Initially the amide was prepared by transforming $Pr^i_3GeCl$ (**1**) to its corresponding amide $Pr^i_3GeNMe_2$. However, during the time of preparation an industrial shortage of the starting chloride required the development of a new synthetic pathway. A previously reported preparatory synthesis used a Grignard reagent $Pr^iMgCl$ with $GeCl_4$, but this resulted in low yields and a mixture of $Pr^i_2GeCl_2$ and $Pr^i_3GeCl$ in a 5:1 ratio. A few other methods were previously reported but also yielded a mixture of products and low

yields.[120-122] It was thought that $Pr^{i}_{3}GeCl$ could be prepared using a similar methodology which was used to make $ClPh_2GeGePh_2Cl$ and $ClPh_2GeGePh_3$ using $Cl_3CC(O)OH$. $PhGePr^{i}_{3}$ was synthesized by reacting $PhGeCl_3$ with excess $Pr^{i}MgCl$ in THF and stirring overnight. The reaction was quenched with 10% HCl, and the organic layer was dried over $MgSO_4$, filtered and finally dried to yield $PhGePr^{i}_{3}$. Triflic acid (1.2 equivalents) was then added to a stirring solution of $PhGePr^{i}_{3}$ in dichloromethane. The product was dried and varying reagents, including $NH_4Cl$ and ethereal HCl, were used to attempt to chlorinate, and then the product was distilled to further purify. However, this methodology still produced low yields and clean separations of the product mixture were difficult.

Another route was investigated using $Ge(OEt)_4$ as the starting material and provided subsequently higher yields and purity of $Pr^{i}_{3}GeCl$. It is important to note that two critical points must be observed to ensure preparation of pure $Pr^{i}_{3}GeCl$ shown in **Scheme 5.1**. The critical steps in the reaction are order of addition, where $Ge(OEt)_4$ needs to be added to $Pr^{i}Li$, and only two equivalents of $Pr^{i}Li$ instead of the anticipated use of three equivalents must be used. If either requirement is neglected, the product results in an intractable mixture of polymeric material. This method was used to reproducibly prepare $Pr^{i}_{3}GeCl$ (**1**), with overall yields of ca. 50% based on starting $Ge(OEt)_4$. The chloride was subsequently converted to either $Pr^{i}_{3}GeNMe_2$ or $Pr^{i}_{3}GeH$ (**2**) which was used to prepare the series of $Pr^{i}_{3}Ge(GePh_2)_nGePr^{i}_{3}$ ($n$ = 0-3) (**Scheme 5.1**). Using the hydrogermolysis reaction, one or two equivalents of amide was combined with either a germanium monohydride or dihydride to result in the series of isopropyl terminated oligogermanes (**Scheme 5.2**). The products were worked up after their optimized reaction times and purified using Kugelrohr distillation. Several of these reactions were observed to be more sluggish than usual and were typically run for 4-6 days for complete reaction.

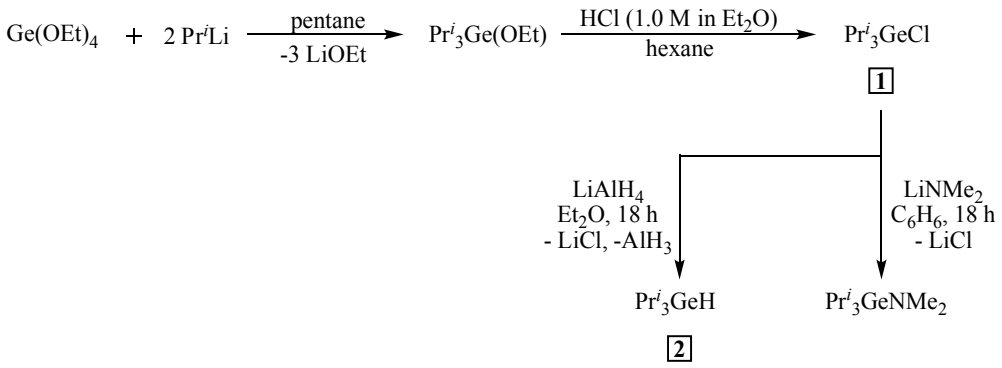


**Scheme 5.1:** Synthetic route for starting -$Pr^i_3$ substituted amide and hydride.

This work will focus on compounds **3**, **6-7** of the isopropyl substituted series, as co-authors Shumaker, A. F. and Roewe, K. D. had prepared **4** and **5** separately. The chlorogermane was converted to $Pr^i_3GeH$ using lithium aluminum hydride, and subsequently reacted with $Pr^i_3GeNMe_2$ to synthesize the digermane $Pr^i_6Ge_2$. The corresponding trigermane $Pr^i_3Ge(GePh_2)GePr^i_3$ (**5**) was prepared using two equivalents of $Pr^i_3GeNMe_2$ combined with $Ph_2GeH_2$ in 45% yield. Both yields of the di- and trigermanes are low, however this was also observed in other reported work for the di and trigermanes using $SmI_2$ as a reducing agent. The tetragermane $Pr^i_3Ge(GePh_2)_2GePr^i_3$ (**6**) was synthesized by reacting $HPh_2GeGePh_2H$ with two equivalents $Pr^i_3GeNMe_2$ resulting in a yield of 44%.[22] Finally, the corresponding pentagermane $Pr^i_3Ge(GePh_2)_3GePr^i_3$ (**7**) was prepared using $HPh_2Ge(GePh_2)GePh_2H$ (**3**) and two equivalents of $Pr^i_3GeNMe_2$ in 52% yield with a reaction time 7 days at 85 °C.

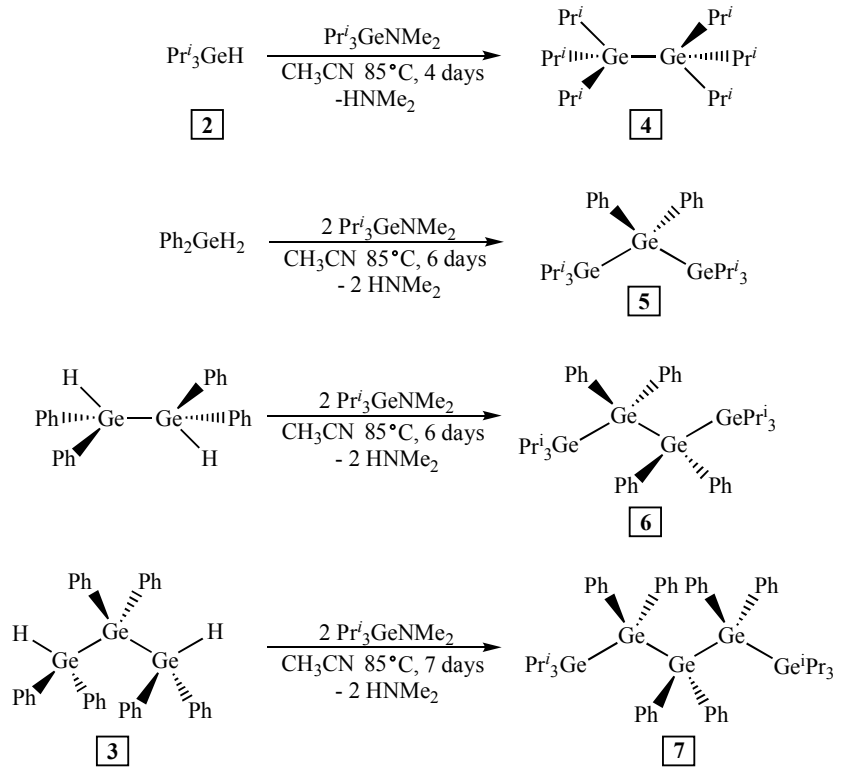


**Scheme 5.2:** Hydrogermolysis reaction -$Pr^i_3$ terminated oligomers **4-7**.

Preparation of any tetragermane (**6**) uses the 1,2-dihydro-1,1,2,2-tetraphenyldigermane $HPh_2GeGePh_2H$, the synthesis of which was discussed in the previous chapter. The 1,3-dihydro-1,1,2,2,3,3-hexaphenyltrigermane $HPh_2Ge(GePh_2)GePh_2H$ (**3**), used to synthesize the pentagermane, was prepared by a previous literature procedure using the (diarylgermyl)lithium $Ph_2GeHLi$ (**Figure 5.3**). Formation of this compound is accomplished by reacting a slight excess of *tert*-butyllithium $^t$BuLi with a stirred solution of $Ph_2GeH_2$; at -80 °C to avoid competitive alkylation reactions.[123] The (diarylgermyl)lithium species $Ph_2GeHLi$ slowly decomposes in THF at -40 °C within a span of 24 hours, which is promoted by the presence of an amine $NEt_3$. Depending on the length of reaction times, the respective di-, tri-, and tetragermyllithium species will form and can be isolated. This enables control over the product formation merely by varying the reaction time in the presence of an amine, and selectively yields the desired product without the production of unwanted side products. The (diarylgermyl)lithium species undergoes repeated

nucleophilic attack of itself, until water is added to result in the desired oligogermane $H(Ph_2Ge)_nH$ ($n$ = 2, 3, or 4). In order to obtain $H(Ph_2Ge)_3H$ (**3**), the reaction is left stirring for 9.5 hours before quenching. The product is filtered, volatiles removed *in vacuo*, and washed several times with hexane to remove impurities. If the product is very pure, a clear, viscous solution is oxidized.

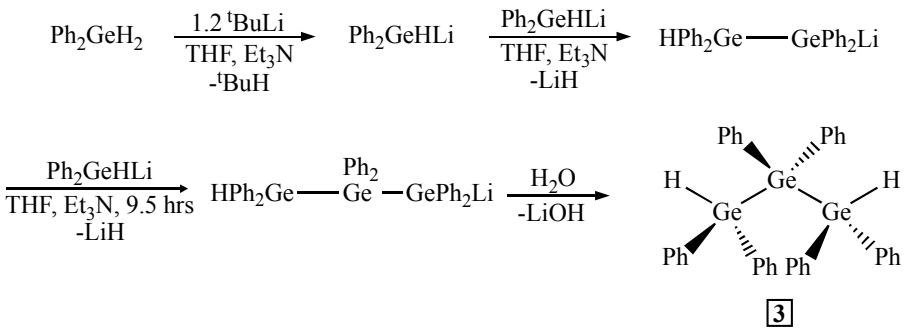


**Scheme 5.3:** Reaction route for the preparation of $H(GePh_2)_3H$ (**3**).[123]

The $^1H$ NMR spectrum of $H(Ph_2Ge)_3H$ (**3**) taken in benzene-$d_6$ contains multiplets in the aromatic region. Within the germanium hydride region a singlet at δ 5.68 ppm for the two magnetically equivalent germanium bound hydrogens at either end of the oligomer is observed. However, if the sample is impure several, hydride peaks at δ 5.72 ppm and 5.12 ppm are observed, and these signals correspond to $H(Ph_2Ge)_4H$ and the $Ph_2GeH_2$, respectively. The X-ray crystal structure of $H(Ph_2Ge)_3H$ was obtained **(Figure 5.3)** and is depicted in the ORTEP diagram shown below, and selected bond distances and bond angles are collected in **Table 5.1**, with full atomic coordinates listed in the appendix. The two Ge-Ge bond lengths of $H(Ph_2Ge)_3H$ measure 2.433(8) and 2.4308(3) Å, which averages to 2.4323(3) Å. These values are similar in distance to typical aryl-substituted trigermanes $Ge_3Ph_8$ (2.4348(2) and 2.441(2) Å) $Ge_3Tol_8$ (Tol = *p*-$CH_3(C_6H_4)$; 2.4450(4) and 2.4359(5) Å), $Tol_3GeGePh_2GeTol_3$ (2.4318(5) and 2.4338(4) Å), and $Ph_3GeGePh_2GePh_3$ (2.429(1) and 2.429(1) Å. The 1,3-dihydride $H(Ph_2Ge)_3H$ has a Ge-Ge-Ge

bond angle measuring 118.94(1)°, which is also similar in magnitude to the trigermanes $Ge_3Ph_8$ (121.3(1)°), $Ge_3Tol_8$ (117.54(1)°), $Tol_3GeGePh_2GeTol_3$ (114.80(2)°), and $Ph_3GeGePh_2GePh_3$ (120.3(1)°).[23,44,61] Due to the similarity of structural metrics between varying trigermanes, it can be concluded that the terminal hydrogen atoms along the $Ge_3$ chain has little effect on the metric parameters of the molecule.

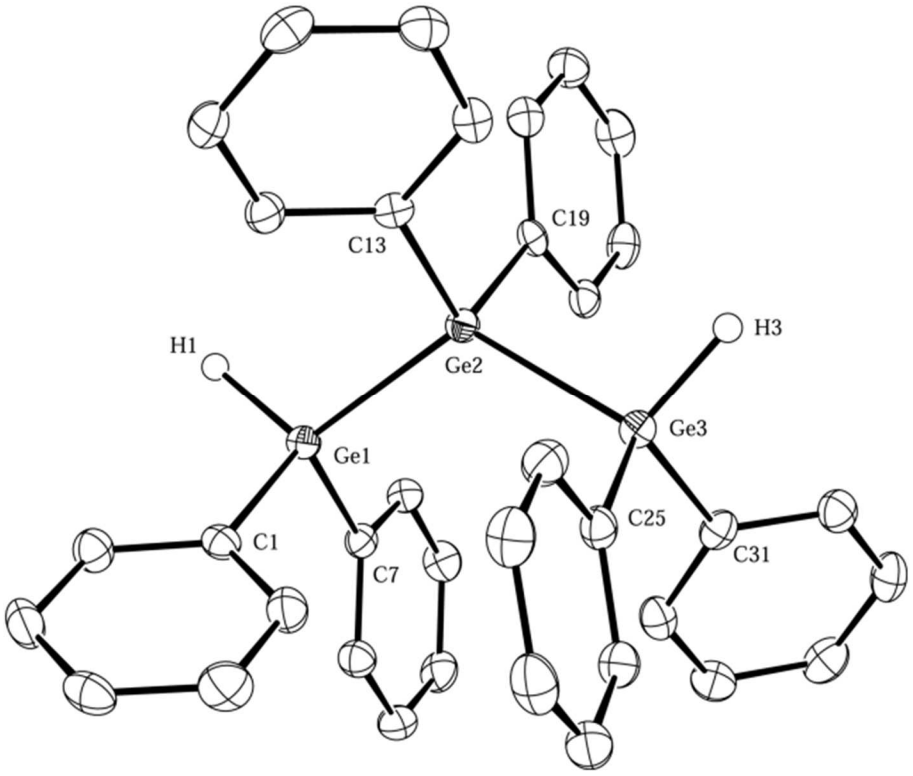


**Figure 5.1:** ORTEP diagram of $H(Ph_2Ge)_3H$ (**3**). Thermal ellipsoids are drawn at 50% probability.

| Bond Length | Å | Bond Angle | Degrees (°) |
|---|---|---|---|
| Ge(1) – Ge(2) | 2.4338(3) | C(13) – Ge(2) – C(19) | 110.29(9) |
| Ge(2) – Ge(3) | 2.4308(3) | C(24) – Ge(3) – C(31) | 111.12(9) |
| Ge(1) – C(1) | 1.951(2) | C(1) – Ge(1) – Ge(2) | 109.63(7) |
| Ge(1) – C(7) | 1.962(2) | C(7) – Ge(1) – Ge(2) | 112.15(6) |

| | | | |
|---|---|---|---|
| Ge(2) – C(13) | 1.960(2) | C(13) – Ge(2) – Ge(1) | 108.54(6) |
| Ge(2) – C(19) | 1.958(2) | C(19) – Ge(2) – Ge(1) | 108.78(6) |
| Ge(3) – C(25) | 1.951(2) | C(13) – Ge(2) – Ge(3) | 106.42(6) |
| Ge(3) – C(31) | 1.947(2) | C(19) – Ge(2) – Ge(3) | 103.66(6) |
| Ge(1) – Ge(2) – Ge(3) | 118.94(1) | C(25) – Ge(3) – Ge(2) | 112.64(7) |
| C(1) – Ge(1) – C(7) | 109.33(9) | C(31) – Ge(3) – Ge(2) | 113.77(7) |

**Table 5.1:** Selected bond distances (Å) and angles (◦) for **3**.

The pentagermane $Pr^{i}_{3}Ge(GePh_2)_3GePr^{i}_{3}$ (**7**) is shown as an ORTEP diagram in **Figure 5.5**, with selected bond distances and angles listed in **Table 5.3**. A significant distortion from idealized tetrahedral geometry is observed at the terminal germanium atoms of the $Ge_5$ backbone, which was also observed in the tetragermane as well. The average C-Ge-C bond angle measures 111.2(2)° at Ge(1) and 111.0(2)° at Ge(5). The average Ge-Ge bond distance of (**7**) is 2.4710(8) Å, and the average Ge-Ge-Ge bond angle is 117.01(3)°. The structural parameters of (**7**) are also comparable to that of the previously prepared $Ge_5Ph_{12}$ at both 295 K and 100 K.[59,96] The average Ge-Ge bond length in $Ge_5Ph_{12}$ measures 2.460(4) Å and the average Ge-Ge-Ge bond angle is 115.6(2)° at 295 K, with the same parameters of the structure observed as 2.4502(6) Å and 115.52(2)° when analyzed at 100 K. The pentagermane (**7**) has terminal Ge-Ge bonds which on average are 0.03 Å longer than those in both structures of $Ge_5Ph_{12.}$ Again this elongation is contributed to having three isopropyl groups, rather than three phenyl groups, at the terminal germanium atoms. However, the most significant structural difference between these two oligomeric species is $Ge_5Ph_{12}$ has four of the five germanium atoms located in the same plane. In (**7**), only the central three germanium atoms are coplanar. One terminal germanium atom is canted above the $Ge_3$ plane while the other is canted below this plane. This structural motif was first observed in the previously synthesized hexagermane $Pr^{i}_{3}Ge(GePh_2)_4GePr^{i}_{3}$. The

hexagermane has four central germanium atoms arranged in a coplanar fashion, with one terminal germanium atom canted above the $Ge_4$ plane and the other canted below the plane.

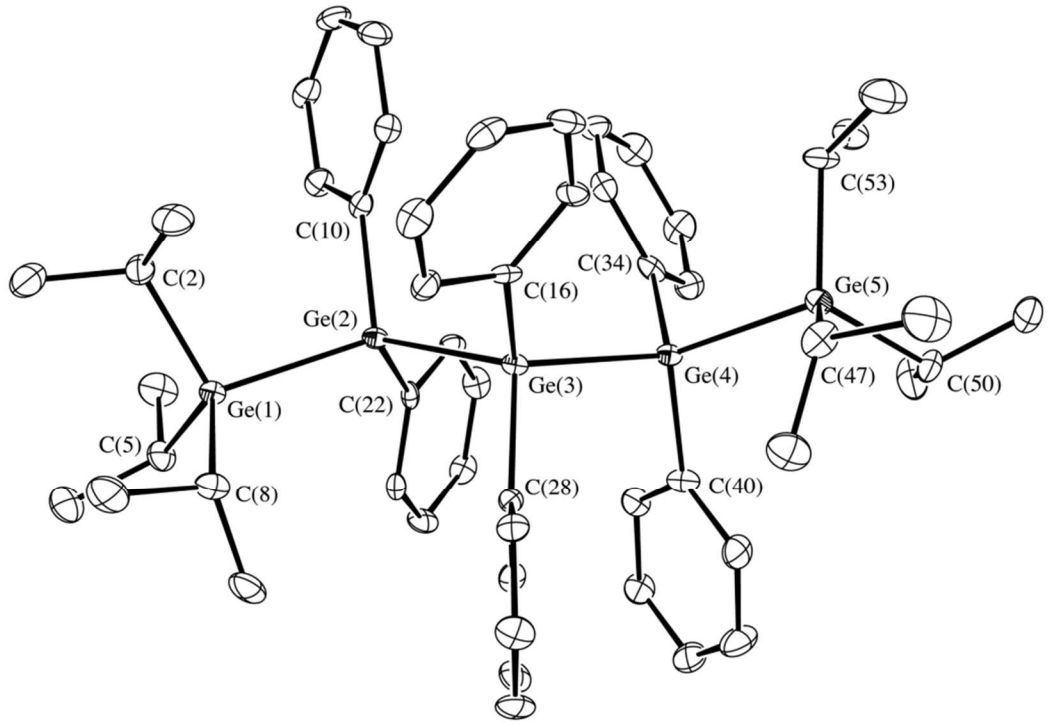


**Figure 5.2:** ORETP diagram of $Pr^{i}_{3}Ge(GePh_2)_3GePr^{i}_{3}$ (**7**). Thermal ellipsoids are drawn at 50% probability.

| Bond Length | Å | Bond Angle | Degrees (°) |
|---|---|---|---|
| Ge(1) – Ge(2) | 2.4775(8) | C(16) – Ge(3) – C(28) | 106.02(2) |
| Ge(2) – Ge(3) | 2.4654(8) | C(34) – Ge(4) – C(40) | 108.0(2) |
| Ge(3) – Ge(4) | 2.4769(8) | C(47) – Ge(5) – C(50) | 109.2(2) |
| Ge(4) – Ge(5) | 2.4641(8) | C(47) – Ge(5) – C(53) | 111.9(2) |
| Ge(1) – C(2) | 1.990(5) | C(50) – Ge(5) – C(53) | 111.9(2) |
| Ge(1) – C(5) | 1.988(5) | C(2) – Ge(1) – Ge(2) | 103.8(2) |
| Ge(1) – C(8) | 1.986(5) | C(5) – Ge(1) – Ge(2) | 107.4(2) |
| Ge(2) – C(10) | 1.974(5) | C(8) – Ge(1) – Ge(2) | 111.9(2) |
| Ge(2) – C(22) | 1.972(5) | C(10) – Ge(2) – Ge(1) | 105.3(2) |

| | | | |
|---|---|---|---|
| Ge(3) – C(16) | 1.969(5) | C(22) – Ge(2) – Ge(1) | 110.5(2) |
| Ge(3) – C(28) | 1.964(5) | C(10) – Ge(2) – Ge(3) | 110.8(2) |
| Ge(4) – C(34) | 1.955(5) | C(22) – Ge(2) – Ge(3) | 105.8(2) |
| Ge(4) – C(40) | 1.968(5) | C(16) – Ge(3) – Ge(2) | 108.7(2) |
| Ge(5) – C(47) | 1.999(5) | C(28) – Ge(3) – Ge(2) | 109.0(2) |
| Ge(5) – C(50) | 1.990(5) | C(16) – Ge(3) – Ge(4) | 114.0(2) |
| Ge(5) – C(53) | 1.990(5) | C(28) – Ge(3) – Ge(4) | 104.3(2) |
| Ge(1) – Ge(2) – Ge(3) | 118.92(3) | C(34) – Ge(4) – Ge(3) | 108.8(2) |
| Ge(2) – Ge(3) – Ge(4) | 114.35(3) | C(40) – Ge(4) – Ge(3) | 104.3(2) |
| Ge(3) – Ge(4) – Ge(5) | 117.76(3) | C(34) – Ge(4) – Ge(5) | 106.0(2) |
| C(2) – Ge(1) – C(5) | 111.1(2) | C(40) – Ge(4) – Ge(5) | 111.7(2) |
| C(2) – Ge(1) – C(8) | 112.6(2) | C(47) – Ge(5) – Ge(4) | 110.3(2) |
| C(5) – Ge(1) – C(8) | 109.9(2) | C(50) – Ge(5) – Ge(4) | 108.9(2) |
| C(10) – Ge(2) – C(22) | 104.8(2) | C(53) – Ge(5) – Ge(4) | 104.8(2) |

**Table 5.2:** Selected bond distances (Å) and angles (◦) for $Pr^{i}_{3}Ge(GePh_2)_3GePr^{i}_{3}$ (**7**).

### 5.3 Physical Properties of $Pr^{i}_{3}Ge(GePh_2)_3GePr^{i}_{3}$

With the pentagermane in hand, the physical properties of the series of isopropyl capped oligomers **4-7** were examined. The optical and electronic properties of oligogermanes can be tuned by altering the chain length of the backbone or by altering the organic substituents bound to the germanium atoms. In order to observe the trend in their physical properties with increasing chain length, UV-visible spectroscopy was used to monitor absorbance maxima and cyclic voltammetry (CV) and differential pulse voltammetry (DPV) were used to observe oxidation potentials of these systems. The observed maxima in the UV-visible spectra of oligogermanes is a result of an electronic transition promoting an electron from the highest occupied molecular orbital (HOMO) to the lowest unoccupied molecular orbital (LUMO), which is a $\sigma$-$\sigma^*$ electronic transition. Previous studies have reported that by increasing the number of Ge-Ge catentates within an oligomer a red shift of the $\lambda_{max}$ is observed in the UV-visible spectra. The degree of

electron donating ability of the organic substituents on the Ge atoms leads to a decrease in the oxidation potential of these compounds. This lowering of the potential indicates that the gap between the HOMO and LUMO decreases with an increase in both the degree of catenation and the electron donating ability of the organic substituents.

The absorbance maxima of the oligogermanes in their UV-visible spectra and can be altered by both substituent effects and changes in the germanium chain length. A previous study was done on the digermanes $R_3GeGePh_3$ (R = H, Me, $Bu^s$, $C_{18}H_{37}$, $Hex^n$, $Bu^n$, and $Bu^i$) using UV-vis, electrochemistry, and DFT calculations to observe inductive effects of the alkyl substituents. It was concluded that increased inductive electron donation of substituents bound to the germanium resulted in overall destabilization of the HOMO because of greater electron density is placed into the germanium backbone. Simultaneously, the energy of the LUMO is destabilized, but to a lesser extent in comparison to the effects on the HOMO. Therefore, as inductive effects are increased there is a decrease in the HOMO/LUMO energy gap and a reduction in the energy on of the $\sigma$-$\sigma$* electronic transition. Due to this lowering of energy a bathochromic or red shift is seen in the UV absorbance maxima. Therefore, as more inductively donating substituents are added, the absorption maximum will be shifted to longer wavelengths.

A bathochromic shift of the $\lambda_{max}$ was also viewed with an increase in chain length but to a larger degree than observed for with a change in substituents. When increasing the number of catenated germanium atoms along the backbone of the chain there is a stabilization *via* conjugation of the LUMO. The other contributing factor is the ratio of electron-rich $R_2Ge^{II}$ centers to end capping $R_3Ge^{III}$ centers. As this ratio increases so does the energy of the HOMO, causing it to become destabilized. Collectively, as the LUMO is stabilized and the HOMO is destabilized the energy gap between the frontier molecular orbitals is decreased resulting in a red shift of the absorbance maximum.

The UV-visible spectra of the oligomer series **4-7** were recorded in dichloromethane, and as expected, successive red shift of the absorbance maxima were observed as the Ge – Ge chain

length increased. The digermane **4** exhibited a $\lambda_{max}$ at 231 nm as a shoulder, while the trigermane **5** and tetragermane **6** show distinct $\lambda_{max}$ peaks at 242 and 273, respectively. Lastly the pentagermane **7** exhibits a $\lambda_{max}$ at 300 nm which is blue-shifted by 10 nm from that of the previously reported hexagermane $Pr^{i}_{3}Ge(GePh_2)_4GePr^{i}_{3}$.

Both cyclic voltammetry (CV) and differential pulse voltammetry (DPV) were used to observe the trends of the electronic properties of oligomers. These electrochemical techniques are able to reveal information on the nature of the oxidation processes of these molecules. Unlike CV, which needs a more concentrated sample to provide distinct peaks, DPV is highly sensitive and this is due to the charging current being minimized or suppressed. CV and DPV both produce two forms of current when voltage is applied, where one is the charging current and the other is the faradaic current that is generated by the oxidation of the sample. This faradaic current can be better observed when the charging current is suppressed. In CV, a continuous charging potential is applied while simultaneously measuring the current without minimizing the charging current, but on the other hand, DPV applies a rectangular pulse potential where the current is measured during the last part of the pulse. This enables that the charging current to decay leaving only the faradaic current to be observed.[124]

Along with the discussed optical properties, the synthesized oligomeric series **4-7** also possess interesting electronic properties. Based on previously conducted studies of oligomeric germanium compounds, several trends on their electrochemical behaviors were established.[125-128] Oligomeric germanium compounds become easier to oxidize as the degree of catenation is increased and it is also seen that the oxidation potential of oligogermanes decreases when highly electron donating groups are introduced. Lastly, linear oligogermanes with aryl substituents on a minimum of one formally divalent germanium atom will exhibit a ($n$-1) successive irreversible oxidation waves where $n$ is the number of catenated germanium atoms within the chain.[129-130]

The series of isopropyl oligogermanes $Pr^{i}_{3}Ge(GePh_2)_nGePr^{i}_{3}$ ($n$ = 0-3) were characterized using cyclic voltammetry (CV) and differential pulse voltammetry (DPV) in dichloromethane

using 0.1 $[Bu^n_4N][PF_6]$ as the supporting electrolyte. The distinct oxidation potentials for both the CV and DPV studies of compounds **4-7** are listed in **Table 5**. The digermane $Ge_2Pr^i_6$ (**4**) showed no discernible oxidation wave under these experimental conditions, how **2** showed one oxidation wave. The (*n*-1) oxidation trend was seen for the trigermane **5**, with a single irreversible oxidation wave at 1555 mV in the CV and 1480 mV in the DPV. These values are comparable to the trigermane $Bu^n_3GePh_2GeBu^n_3$, with a single oxidation wave at 1540 mV in the CV and 1490 mV in the DPV. This is explained by the similarity of the inductively donating effects of both *n*-butyl and isopropyl groups. Other alkyl-substituted oligogermanes, such as a series of permethylated oligogermanes $Me(GeMe_2)_nMe$ ($n$ = 2-6)[25,85], only exhibit one irreversible oxidation wave in the CV regardless of chain length. The trigermane **5** and $Bu^n_3GePh_2GeBu^n_3$ also differ in their voltammograms from other perphenylated trigermanes which show two successive oxidation waves rather than one.[23] It is postulated that the presence of aryl substituents provides stabilization to the species that are generated after the oxidation event takes place. This is done in such a manner that the electrochemically generated species can also be oxidized as the sweep continues to a more positive potential. This oxidation pattern for the perphenylated $H(GePh_2)_3H$ (**3**) exhibited two oxidation waves in the CV at 1545 and 1865 mV and in the DPV at 1530 and 1890 mV. Both homo- and heterolytic cleavage of the single germanium-germanium bonds can presumably occur to generate various radicals and germylene products. However, these electrically generated products species have yet to be trapped from perphenylated **3** or higher oligomers.

| Compound | **3** | **6** | **7** |
|---|---|---|---|
| $E_{ox}$ (CV, mV) | 1545 | 1525 | 1560 |
| | 1865 | 1860 | 1695 (sh) |
| | | 2055 | 1875 |
| | | | 2095 |
| $E_{ox}$ (DPV, mV) | 1530 | 1400 | 1380 |

| | | | |
|---|---|---|---|
| | 1890 | 1820 | 1500 |
| | | 2030 | 1650 (sh) |
| | | | 1800 |
| | | | 2020 |
| $\lambda_{max}$ (nm) | 240 | 273 | 300 |
| $\varepsilon$ ($M^{-1}$ $cm^{-1}$) | 3.0 x $10^4$ | 4.6 x $10^4$ | 5.7 x $10^4$ |

**Table 5.3:** Average oxidation potential for oligomers **3**, **6-7**.

The tetragermane **6** has a voltammogram containing three irreversible oxidation waves at 1525, 1860, and 2055 mV in the CV and 1400, 1820, 2030 mV in the DPV. However, the pentagermane **7** showed four irreversible oxidation waves shown in **Figure 5.6** with values observed at 1380, 1500, 1800, and 2020 mV in the DPV. As for the shoulder which is present at 1650 mV, this can be attributed to a minor species being produced electrochemically. The pentagermane **7** has two unresolved peaks in the first two oxidation waves in its CV voltammogram. This results in the three features at 1560, 1875, and 2095 mV plus a shoulder at 1695 mV. As predicted, when comparing the DPV data of the oligomers (**3**, **6-7**) the ease of oxidation is correlated to the increase in chain length going from two germanium atoms to five along the backbone. This trend has also been observed in other series of oligogermanes. This effect can be attributed to the destabilization of the HOMO, as the chain length is increased. Thus, the pentagermane **7** is the easier to oxidize than its corresponding tetra- **6**, tri- **5**, and digermane **4**.

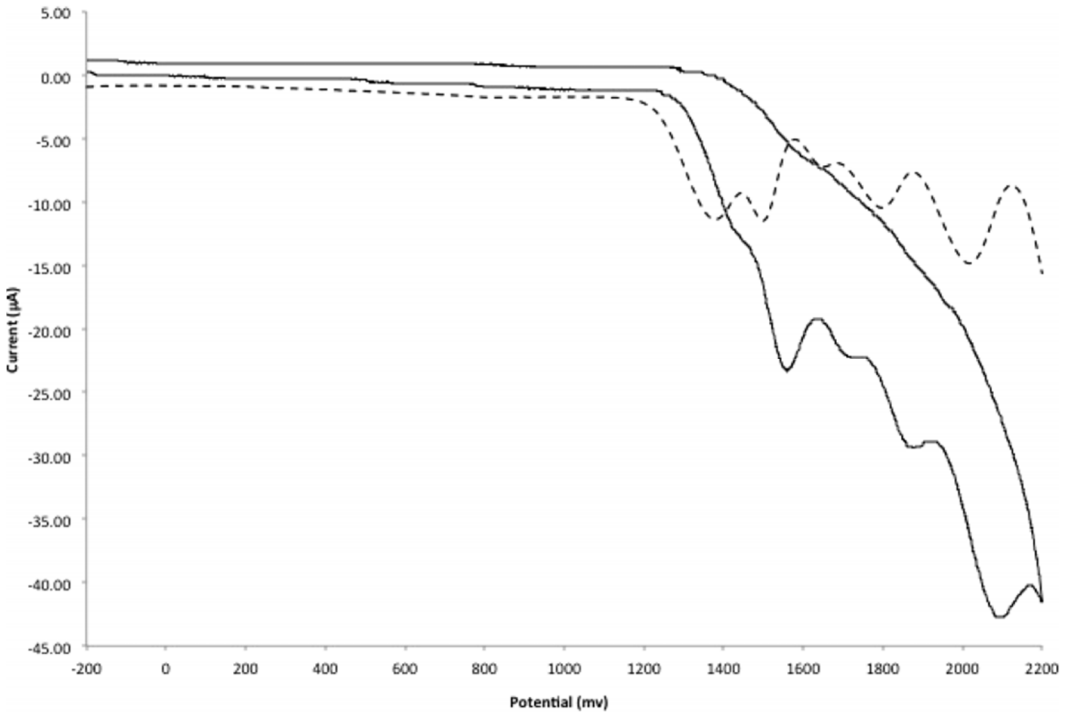


**Figure 5.3:** CV and DPV of **7** in $CH_2Cl_2$ and $[Bu^n_4N][PF_6]$ as the supporting electrolyte.

### 5.4 Luminescent and Dichroic Behavior of $Pr^i_3Ge(GePh_2)_3GePr^i_3$

As previously stated, polymeric group 14 compounds display physical properties which are not typically observed in shorter oligomeric species. Several polymeric germanium species have been reported to exhibit luminescent behavior but this was not observed in discrete germanium molecules until it was reported for the hexagermane $Pr^i_3Ge(GePh_2)_4GePr^i_3$.[116, 125,133] Therefore, it was assumed that oligomers must contain a minimum of six germanium atoms within the Ge – Ge backbone in order to exhibit similar emission properties to their larger polymeric analogs. With the successful crystallization and full characterization of the pentagermane (**7**), this was proven incorrect. The pentagermane was also luminescent in dichloromethane and exhibited a broad emission at 380 nm when the sample was excited at 302 nm. In **Figure 5.7**. the absorption spectrum is overlaid on the emission spectrum where both

spectra were recorded in $CH_2Cl_2$. In comparison to the hexagermane, the emission from **7** is red-shifted by 10 nm. This shows that as the number of catenated germanium atoms decreases that emission maximum shifts to lower energy. The absorbance and emission spectra of both the penta- **7** and the hexagermane are within the range reported for several polygermanes such as $(R_2Ge)_n$ (R = Et, $Pr^n$, $Bu^n$, Ph, *p*-Tol),[125,134] which have absorbance maxima ranging from 293 to 326 nm, while the polymer $((Me_3SiOC_6H_4)_2Ge)_n$ has an emission maximum at 369 nm. Due to the consistency in values, it is likely that within the polygermanes there are areas of order which consist of five or six germanium atoms in length. These regions of order would have the germanium atoms in a *trans*-coplanar arrangement to ensure that $\sigma$-delocalization can occur. Since there is a correlation between chain length and emission maxima this indicates that this attribute is also tunable, once again, by changing the number of germanium atoms along the backbone.

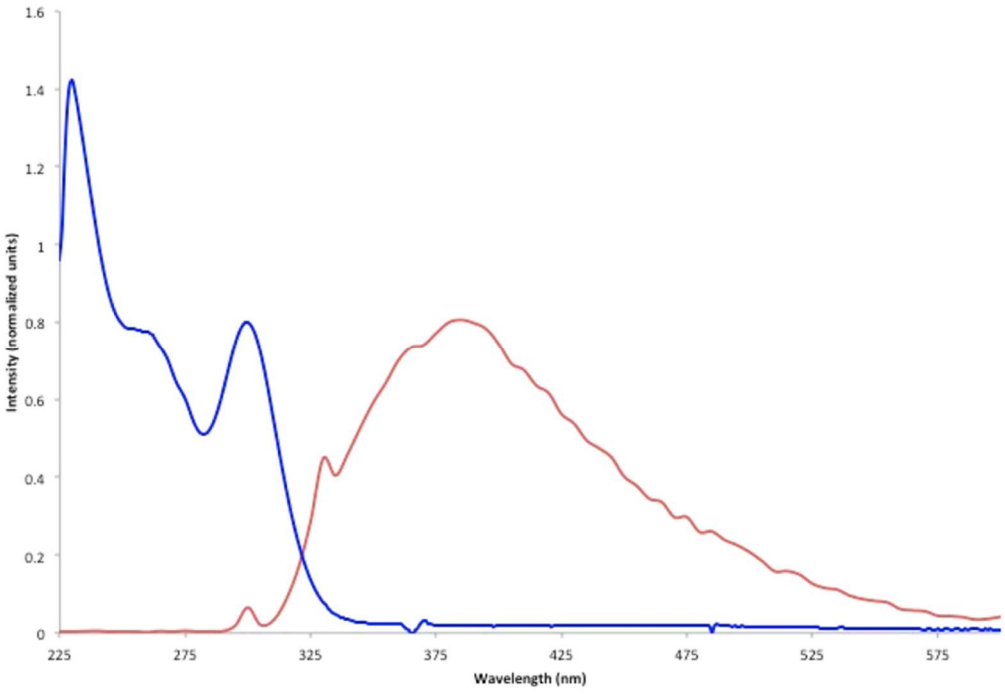


**Figure 5.4:** Overlaid UV-visible spectrum (blue) and emission spectrum (red) of **7** in $CH_2Cl_2$.

The crystal packing diagram of **7** is shown below in **Figure 5.8** along the crystallographic *b*-axis. The arrangement of the $Ge_5$ shows that individual molecules of **7** stacked in a repeating columnar fashion with the terminal germanium atoms canted above and below the central $Ge_3$ plane. This stacking pattern is seen along all three crystallographic axes, and resembles the packing seen for the hexagermane $Pr^{i}_{3}Ge(GePh_2)_4GePr^{i}_{3}$. The arrangement of the $Ge_5$ backbone imparts a long-range pseudo-chirality in the solid state, which explains why color changes are observed for different orientations under polarized light. This stacked columnar fashion packing within the crystal is responsible for its dichroic character.

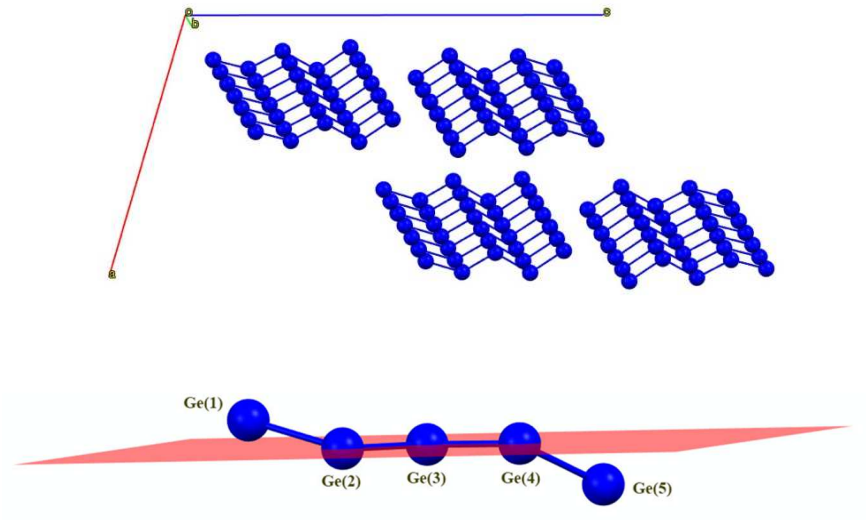


**Figure 5.5:** Structure of **7** in the solid state and packing diagram viewed along the *b*-axis (top). $Ge_3$ plane with canted terminal germanium atoms above and below (bottom).

A single crystal of the pentagermane (**7**), shown in **Figure 5.9**, appears colorless under ambient light and pale yellow under cross-polarized light in one orientation. However, when the crystal is rotated by 30° the crystal changes color to a brilliant purple/blue color.

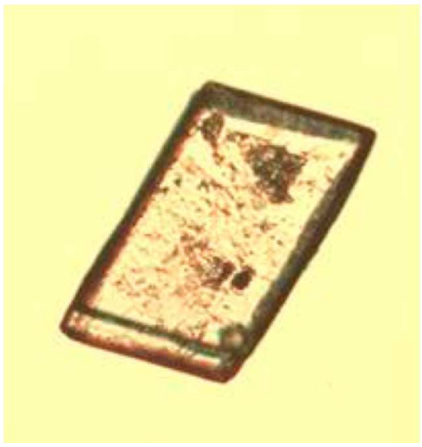

**Figure 5.6:** Single crystal of (**7**) viewed under ambient light.

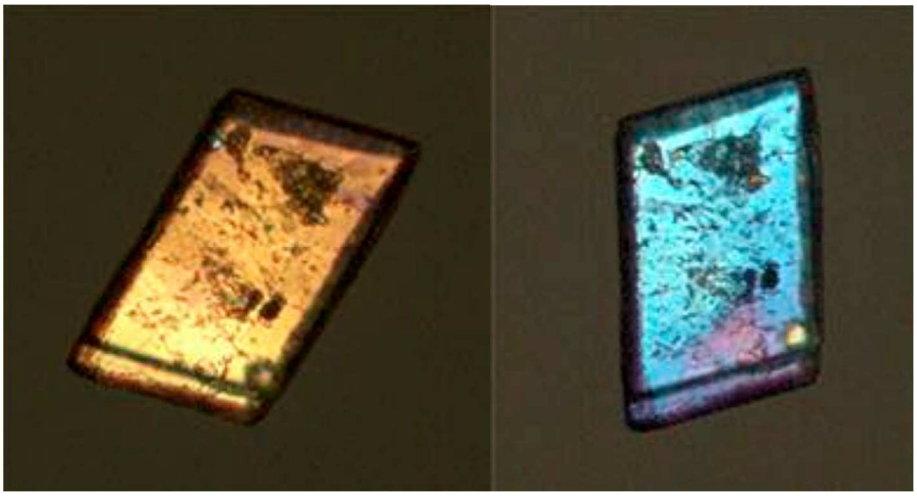

**Figure 5.7:** Single crystal of (**7**) rotated 30 ° under cross-polarized light.

## 5.5 Conclusion

A series of linear oligogermanes $Pr^{i}_{3}Ge(GePh_2)_nGePr^{i}_{3}$ ($n$ = 0-3) **4-7** were prepared using the hydrogermolysis reaction and were characterized by UV-visible spectroscopy and CV/DPV analysis, where the pentagermane is the focus of this work. As the backbone of the oligomers are incrementally lengthened by one germanium atom at a time, a successive red shift was observed in the absorbance maxima and the molecules also became easier to oxidize. X-ray quality crystals

of the pentagermane $Pr^{i}_{3}Ge(GePh_2)_3GePr^{i}_{3}$ were obtained. The pentagermane had its three central germanium atoms form a $Ge_3$ plane with one terminal $Pr^{i}_{3}Ge$- group canted above and the other canted below the $Ge_3$ plane. Crystals of the pentagermane were observed to be dichroic and they appear pale yellow or blue depending on its orientation under cross polarized light. This is attributed to the stacking of the individual molecules of $Pr^{i}_{3}Ge(GePh_2)_3GePr^{i}_{3}$ in the crystal, where they assemble in a columnar fashion along all three crystallographic axes. The pentagermane also exhibits luminescence with an emission maximum at 380 nm when excited near its absorbance maximum (300 nm). This emission was comparable to the previous synthesized hexagermane $Pr^{i}_{3}Ge(GePh_2)_4GePr^{i}_{3}$, but was red shifted by 10 nm. Although both hexa- and pentagermane mimic properties of their larger polymeric counterpart, the pentagermane was the smallest linear compound to do so. As the physical properties can all be tuned by substituent and chain length variation, these materials could prove useful in development of new luminescent materials.

## 5.6 Experimental

*General Considerations*

All manipulations were carried out under standard Schlenk, syringe, and glovebox techniques, with solvents being dried using a Glass Contour solvent purification system. NMR spectral data was taken on a 400 MHz ($^1$H) Bruker Inova spectrometer. Reagents and starting materials, such as $Ge(OEt_4)$, $Ph_2GeH_2$, HCl (1.0 M in $Et_2O$) and $Pr^{i}Li$ (0.70 M in pentane), were all obtained from Gelest or Sigma Aldrich.

*Synthesis of $Pr^{i}_{3}GeOEt$*

A Schlenk flask was charged with a stirring solution of 0.70 M $Pr^{i}Li$ in pentane (47.0 mL, 33 mmol), and $Ge(OEt)_4$ (4.16 g, 16.4 mmol) was added in pentane (10 mL) was added dropwise over a span of 20 minutes due to its exothermic nature. A gelatinous material formed immediately upon addition of $Ge(OEt)_4$. The reaction mixture was stirred for 18 hours with the volatiles removed *in vacuo*. The crude reaction mixture was dissolved in benzene (75 mL), filtered through Celite, and dried *in vacuo* to yield the product as a pale yellow oil (0.82 g, 60% based on $Pr^{i}Li$). $^{1}H$ NMR ($C_6D_6$, 25 °C): δ 3.72 (q, $J$ = 8.1 Hz, 2H, -OC$H_2$$CH_3$), 1.38 (sept, $J$ = 8.0 Hz, 3H, -C$H$$(CH_3)_2$), 1.26 (t, $J$ = 8.1 Hz, 3H, -$OCH_2CH_3$), 1.17 (d, $J$ = 8.0 Hz, 18H, -$CH(CH_3)_2$ ppm. $^{13}C$ NMR ($C_6D_6$, 25 °C): δ 59.5 (-O$C$$CH_2CH_3$), 18.8 (-$C$$H(CH_3)_2$), 18.1 (-$CH(CH_3)_2$), 15.3 (-$OCH_2CH_3$) ppm. Anal. Calcd for $C_{11}H_{26}GeO$: C, 53.50; H, 10.61. Found: C, 53.67; H, 10.69.

*Synthesis of $Pr^{i}_{3}GeCl$* ***(1)***

A Schlenk tube was charged with $Pr^{i}_{3}GeOEt$ (0.54 g, 2.19 mmol) in hexane (20 mL) and 1.0 M $HCl_{(ether)}$ (10.0 mL, 10 mmol) was added. The reaction mixture was left to stir for 1.5 hours and then dried *in vacuo* to yield the product **1** (0.43 g, 82%) as a colorless oil. $^{1}H$ NMR ($C_6D_6$, 25 °C): δ 1.40 (sept, $J$ = 8.1 Hz, 3H, -C$H$$(CH_3)_2$), 1.09 (d, $J$ = 8.1 Hz, 18H, -$CH(CH_3)_2$) ppm. $^{13}C$ NMR ($C_6D_6$, 25 °C): δ 19.1 (-$C$$H(CH_3)_2$), 18,9 (-$CH(CH_3)_2$) ppm. Anal. Calcd for $C_9H_{21}ClGe$: C, 45.54; H, 8.92. Found: C, 45.57; H, 8.89.

*Synthesis of $Pr^{i}_{3}GeH$* ***(2)***

A Schlenk flask with a solution of $Pr^{i}_{3}GeCl$ (0.36 g, 1.5 mmol) in $Et_2O$ (25 mL) was added to a suspension of $LiAlH_4$ (0.07 g, 2 mmol) in $Et_2O$ (20 mL). The reaction mixture was stirred overnight and then was quenched with degassed, deionized water at -78 °C. The mixture

was allowed to warm up to room temperature and was filtered through Celite. The organic layer was separated from the aqueous, and washed with $Et_2O$ (3 x 5 mL). The combined organic layers were dried over anhydrous $MgSO_4$. The mixture was filtered and volatiles were removed *in vacuo* to yield **2** (0.15 g, 49%) the product as a colorless oil. $^1H$ NMR ($C_6D_6$, 25 °C): δ 3.74 (s, 1H, Ge-H), 1.29 (sept, $J$ = 8.0 Hz, 3H, -C*H*$(CH_3)_2$), 1.15 (d, $J$ = 8.0 Hz, 18H, -CH(C*H*$_3)_2$) ppm. $^{13}C$ NMR ($C_6D_6$, 25 °C): δ 21.1 (-CH(*C*$H_3)_2$), 13.8 (-*C*H$(CH_3)_2$) ppm. Anal. Calcd for $C_9H_{22}Ge$: C, 53.27; H, 10.93. Found: C, 53.11; H, 10.98.

*Synthesis of $HPh_2Ge(GePh_2)GePh_2H$* ***(3)***

A Schlenk flask held a solution of $Ph_2GeH_2$ (1.44 g, 6.27 mmol) in 6 mL $Et_3N$ and was cooled to - 80 °C before 1.7 M $^t$BuLi (4.42 mL, 7.52 mmol) was cannulated to the reaction flask dropwise. The mixture was stirred slowly and allowed to warm to room temperature over 9.5 h. A white precipitate formed in solution within 45 min of combining the reagents. The reaction was quenched with deionized water and dried over $MgSO_4$ and stirred for 1 h. Product was subsequently filtered over Celite and washed with 30 mL hexane. Volatiles were removed *in vacuo* and crude product was also washed with 20 mL benzene to remove impurities. Resulting white solid was again dried to produce pure **3** (1.24 g, 29%).

*Synthesis of $Pr^i_3GeGePr^i_3$* ***(4)***

A Schlenk tube with a solution of $Pr^i_3GeH$ (0.15 g, 0.74 mmol) in $CH_3CN$ (10 mL) was added to a solution of $Pr^i_3GeNMe_2$ (0.15 g, 0.61 mmol) in $CH_3CN$ (10 mL). The mixture was sealed in a Schlenk tube and heated at 85 °C for 48 h. Volatiles were then removed *in vacuo* and the crude product mixture was distilled in a Kugelrohr oven (0.05 Torr, 125 °C). Product **4** (0.176 g, 72%) was a colorless oil. $^1H$ NMR ($C_6D_6$, 25 °C): δ 1.41 (sept, $J$ = 8.8 Hz, 6H, -C*H*$(CH_3)_2$),

1.08 (d, $J$ = 8.8 Hz, 36H, -CH(C$H_3$)) ppm. $^{13}$C NMR ($C_6D_6$, 25 °C): δ 20.1 (-CH(*C*$H_3$)$_2$), 19.5 (-*C*H(CH$_3$)$_2$) ppm. Anal. Calcd for $C_{18}H_{42}Ge_2$: C, 53.54; H, 10.48. Found: C, 53.41; H, 10.39.

*Synthesis of $Pr^i_3Ge(GePh_2)GePr^i_3$* ***(5)***

To a solution of $Ph_2GeH_2$ (0.145 g, 0.634 mmol) in $CH_3CN$ (15 mL) was added a solution of $Pr^iGeNMe_2$ (0.360 g, 1.46 mmol) also in $CH_3CN$ (15 mL). The reaction was heated in an oil bath at 85 °C for 48 h. The resulting solution was dried *in vacuo* and the crude product mixture was distilled via Kugelrohr oven (0.04 Torr, 135 °C). The remaining material was identified as product **5** (0.180 g, 45%) isolated as a colorless oil. $^1$H NMR ($C_6D_6$, 25 °C): δ 7.48 (d, $J$ = 6.4 Hz, 4H, *o*-$C_6H_5$), 6.99-6.90 (m, 6H, *m*-$C_6H_5$ and *p*-$C_6H_5$), 1.33 (sept, $J$ = 7.2 Hz, 6H, -C*H*(CH$_3$)$_2$), 0.96 (d, $J$ = 7.2 Hz, 36H, -CH(C$H_3$)$_2$) ppm. $^{13}$C NMR ($C_6D_6$, 25 °C): δ 138.5 (*ipso*-$C_6H_5$) 135.9 (*o*-$C_6H_5$), 128.6 (*m*-$C_6H_5$), 128.5 (*p*-$C_6H_5$), 21.3 (-CH(*C*H$_3$)$_2$), 16.8 (-*C*H(CH$_3$)$_2$) ppm. Anal. Calcd for $C_{30}H_{52}Ge_3$: C, 57.14; H, 8.31. Found: C, 57.07; H, 8.25.

*Synthesis of $Pr^i_3Ge(GePh_2)_2GePr^i_3$* ***(6)***

A solution of $Pr^i_3GeNMe_2$ (0.48 g, 1.94 mmol) in $CH_3CN$ (10 mL) was added to a solution of $HPh_2GeGePh_2H$ (0.42 g, 0.92 mmol) stirring in $CH_3CN$ (15 mL). The Schlenk tube was sealed and heated in an oil bath at 100 °C for 6 days. The reaction was pumped down and the resulting crude product mixture was distilled *via* Kugelrohr oven (170 °C, 0.005 Torr). The subsequent product **6** (0.35 g, 44%) was isolated as a yellow solid. $^1$H NMR ($C_6D_6$, 25 °C): δ 7.56 (d, $J$ = 6.8 Hz, 8H, *o*-$C_6H_5$), 6.97 (m, 8H, *m*-$C_6H_5$) 6.90 (t, $J$ = 7.2 Hz, 4H, *p*-$C_6H_5$) 1.53 (sept, $J$ = 7.6 Hz, 6H, -C*H*(CH$_3$)$_2$), 1.16 (d, $J$ = 7.6 Hz, 36H, -CH(C$H_3$)$_2$) ppm. $^{13}$C NMR ($C_6D_6$, 25 °C): δ 138.2 (*ipso*-$C_6H_5$), 137.1 (*o*-$C_6H_5$), 128.5 (*m*-$C_6H_5$), 128.3 (*p*-$C_6H_5$), 21.3 (-CH(*C*H$_3$)$_2$), 16.7 (-*C*H(CH$_3$)$_2$) ppm. Anal. Calcd for $C_{42}H_{62}Ge_4$: C, 58.85; H, 7.29. Found: C, 58.75; H, 7.32.

*Synthesis of $Pr^{i}_{3}Ge(GePh_2)_3GePr^{i}_{3}$* ***(7)***

A solution of $Pr^{i}_{3}GeNMe_2$ (0.29 g, 1.19 mmol) in $CH_3CN$ (5 mL) was added to $H(GePh_2)_3H$ (0.39 g, 0.57 mmol) in $CH_3CN$ (10 mL). The reaction was done in a sealed Schlenk tube and heated in an oil bath at 130 °C for 7 days. A white precipitate formed, and was separated from filtrate by filtration. The white solid was then washed multiple times with hexane (25 mL), isolated, and identified as **7** (0.32 g, 52%). $^{1}$H NMR ($C_6D_6$, 25 °C): δ 7.80 (d, $J$ = 8.1 Hz, 4H, *o*-$C_6H_5$), 7.44 (d, $J$ = 8.2 Hz, 8H, *o*-$C_6H_5$), 7.44 (d, $J$ = 8.2 Hz, 8H, *o*-$C_6H_5$), 7.20-7.08 (m, 14H, *p*-$C_6H_5$ and *m*-$C_6H_5$), 7.02 (t, $J$ = 8.0 Hz, 4H, *p*-$C_6H_5$), 1.54, (sept, $J$ = 8.3 Hz, 6H, -C*H*$(CH_3)_2$), 0.96 (d, $J$ = 8.3 Hz, 36H, -CH(C*H*$_3)_2$) ppm. $^{13}$C NMR ($C_6D_6$, 25 °C): δ 140.8 (*ipso*-$C_6H_5$), 140.4 (*ipso*-$C_6H_5$), 137.2 (*o*-$C_6H_5$), 136.9 (*o*-$C_6H_5$), 128.5 (*m*-$C_6H_5$), 128.2 (*m*-$C_6H_5$), 128.1 (*p*-$C_6H_5$), 127.9 (*p*-$C_6H_5$), 21.4 (-CH(*C*$H_3)_2$), 18.4 (-*C*H$(CH_3)_2$) ppm. Anal. Calcd for $C_{54}H_{72}Ge_5$: C, 59.81; H, 6.69. Found: C, 59.47; H, 6.60.

# CHAPTER VI

# ATTEMPTED PREPARTION OF CYCLIC PERARYLATED OLIGOGERMANES $(GeAr_2)_4$ AND $(GeAr_2)_5$ VIA COUPLING REACTION WITH $Ar_2GeCl_2$ AND ALKALI METAL

## 6.1 Introduction

Preparative chemistry and structural studies of a variety of arylgermanium halides $Ar_nGeX_{(4-n)}$ and hydrides $Ar_nGeH_{(4-n)}$ ($n$ = 1-3) have been slow in development due a lack of reliable synthetic pathways. However, these materials have become of interest recently for their potential as useful starting materials for the preparation of new oligomeric, cyclic, and polymeric germanium compounds.[135-136] The synthetic pathways typically used for silicon and tin derivatives are not viable for the preparation of organogermanium compounds, requiring extensive investigations into preparatory routes for these compounds.[135,137] Synthetic routes using organometallics compounds include organolitihum or organomagensium compounds (RLi, RMgX), comproportionation reactions, or halogenation reactions starting from organogermanes.[138-143] Although there are a multitude of methods known, a versatile and reliable pathway to prepare arylgermanium compounds had until recently been elusive.[24,44,145] The focus of this study was to prepare a series of 2,5-xylyl ($C_6H_3(CH_3)_2$-) substituted tri- $Ar_3GeCl$, di- $Ar_2GeCl_2$ and monoaryl $ArGeCl_3$ germanes with the intention of preparing perarylated cyclic oligogermanes ($Ar_8Ge$, $Ar_{10}Ge_5$) from them. These cyclic compounds could be ring-opened and

used as starting materials to ultimately synthesize a new series of discrete linear oligomers having extended Ge – Ge chains.

The first reported organogermanium compound tetra-ethylgermanium $Et_4Ge$ was first synthesized in 1887, and for years remained the only reported organic derivative of germanium.[31] It was not until tetraphenylgermanium $Ph_4Ge$ was synthesized by Drew and Morgan, and later tolyl derivatives, that quaternary organic species came into focus.[141] The classical methods for preparation of arylgermanes in literature are involved the treatment of germanium tetrachloride $GeCl_4$ with an aryl Grignard, a Wurtz-Fittig reaction, or arylithium reagents. However, these routes were not very selective, provided product mixtures, and resulted in low yields of arylgermanes.[98] Recently, work was done on a series of novel tetraarylgermanes $Ar_4Ge$ (aryl = tolyl, xylyl, naphthyl, and mesityl derivatives) and triarylgermanium halides $Ar_3GeX$ (X = Cl, Br).[144]

The aryl ligands were chosen for steric bulk bearing methyl groups in varying positions towards the germanium atoms. Grignard reagents were typically formed with an excess of magnesium in combination with an aryl halide. Once formed, the Grignard was further reacted with a metal halide to yield the desired product. This procedure was well known for other group 14 elements and smaller ligands.[146] However, this route proved synthetically challenging when preparing organogermanium compounds bearing larger substituents. Such drawbacks included the formation of mixtures, from which the product was either intractable or was difficult to separate out cleanly, long laborious work-up procedures, low yields, and subsequent high costs.[143]

The aryl substituted germanium compounds ArMg-Cl were prepared using the Grignard method shown in **Scheme 6.1**. A slight excess of magnesium was reacted with the desired arylhalide, and filtered off before further reaction with $GeCl_4$. Removal of any excess magnesium in the reaction is crucial in preventing hexa-aryldigermanes ($Ar_6Ge_2$) from forming. This side product will form *via* the generation of the germyl Grignard reagent $Ar_3Ge{\cdot}MgX$, created in the

presence of any free magnesium with $Ar_3GeX$.[147] A solution of $GeCl_4$ in $Et_2O$ was then added dropwise to the Grignard solution and refluxed for a minimum of 1 hour, and allowed to stir overnight at room temperature. Once the reaction was complete it was quenched under acidic conditions and the organic layer separated and worked up. However, the synthesis of the various substituted triarylgermanium halides ($Ar_3GeX$) required different stoichiometric ratios of Grignard reagent depending on the desired product. It was found by Wolf *et al*. that the patterning and orientation of the substituents play a more crucial role on the number of residues ($Ar_4Ge$ or $Ar_3GeX$) which can be accommodated around a single germanium metal, rather than the actual size of the ligand.[148] The study showed that sterically demanding substituents, in this case methyl groups, on at least one *ortho*- position, resulted in preferential formation of triarylgermanium halides $Ar_3GeX$. One complication in preparing pure triarylgermanium halides, also seen with other group 14 analogs, is the occurrence of halogen-metal exchange.[135-136,149] The resulting halide mixtures were ignored as the subsequent products could be separated and all utilized as starting materials for varying reactions.

$$\text{aryl-Br} + \text{Mg} \xrightarrow{Et_2O/THF} \text{aryl-Mg-Br} \xrightarrow[\text{toluene}]{GeX_4} \text{aryl}_n\text{GeX}_{4-n}$$

**Scheme 6.1:** Grignard reaction for the synthesis of $Ar_4Ge$ and $Ar_3GeCl$ (Ar = 2,5-xylyl).[144]

Much work has also been done on the preparation of homocyclic group 14 compounds, including cyclo tetra-, penta-, and hexamers. The synthesis of perphenylated cyclosilanes was achieved by the addition of dichlorodiphenylsilane $Ph_2SiCl_2$ with either sodium, lithium, or magnesium[150-151] and this preparation of phenylated cyclosilanes was first described by Kippng.[152] Three crystalline compounds, were isolated from their reaction and identified octaphenyltetrasilane, decaphenylcyclopentasilane, and dodecaphenylcyclohexasilane relating to $(Ph_2Si)_n$ where $n$ = 4, 5, and 6 respectively.[153-155] Homocyclic germanium compounds were

prepared using a similar route. Using dichlorodiphenylgermane $Ph_2GeCl_2$ and sodium metal the corresponding octaphenylcyclotetragermane $(GePh_2)_4$, decaphenylcyclopentaagermane $(GePh_2)_5$, and dodecaphenylcyclohexagermane $(GePh_2)_6$ were prepared in varying ratios.[49,57,156] It was the previous work of Ross and Dräger which reported the octaphenylcyclotetragermane $(Ge_2Ph_2)_4$ by a Wurtz-type coupling shown in **Scheme 6.2**.[49] This reaction uses $Ph_2GeCl_2$ that is refluxed for one hour over sodium metal in boiling toluene. The reaction was quenched, filtered, and crystalline solids were washed with pentane, producing a mixture with $(GePh_2)_4$ as the major product.

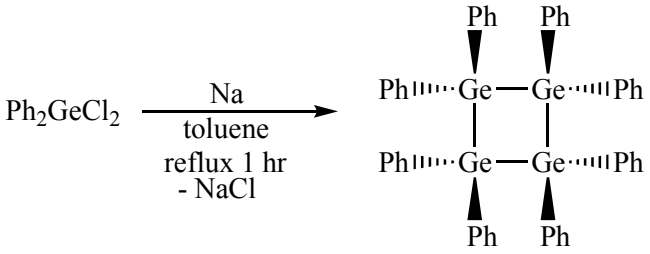


**Scheme 6.2:** Synthesis of octaphenylcyclotetragermane $(Ge_2Ph_2)_4$ *via* Wurtz-type coupling.[49]

Advantageously using the strain present in this species, Dräger reported a ring-opening reaction with cycloctetragermane using molecular iodine to yield $I(GePh_2)_4I$.[53] Similar chlorinated species $Cl(GePh_2)_nCl$ ($n$ = 2, 3, and 4) were prepared by germylene $Ph_2Ge$: insertion into $Ph_2GeHCl$ followed by chlorination using $CCl_4$. The Weinert group has been able ring open the aforementioned $(Ge_2Ph_2)_4$ with molecular bromine to yield the dibromide $Br(GePh_2)_4Br$.[60] This reaction was synthetically simple due to the alleviation of ring strain, which enables the process to occur favorably and quickly.[157] The reaction was visually ascertained to be complete by the persistence of a faint yellow color upon addition of $Br_2$ to the solution. Once ring opened and halogenated, the 1,4-dihalotetragermane was converted to the analogous hydride. However, only the successful conversion of the dibromine terminated tetragermane was achieved through

addition of $LiAlH_4$ in $Et_2O$ to yield octaphenyltetragermane $H(GePh_2)_4H$. The 1,4-dihydride material was used to prepare the longest, fully characterized, hexagermane using the hydrogermolysis with two equivalents of $Pr^i_3GeNMe_2$.[157]

Similar ring opening reactions were conducted on silicon analogs using lithium metal to produce $\alpha,\omega$-dilithiated oligosilanes $Li(SiPh_2)_nLi$ ($n$ = 4, 5, 6).[153-155] These studies inspired the pathway directed at preparing various perarylated cyclogermanes, converting them to linear oligomers *via* ring opening and thus used as subsequent precursors for preparing longer linear oliogogermanes. Initially decaphenylcyclopentagermane $(GePh_2)_5$ was prepared using a literature route by reacting dichlorodiphenylgermane $Ph_2GeCl_2$ with 10 equivalents of magnesium in refluxing tetrahydrofuran (THF).[41] The mixture was quenched under dilute acid and the organic layer was worked up. Once isolated, $(GePh_2)_5$ was reacted with various stoichiometric ratios of lithium metal under argon. The solution turned from a light yellow to dark red after stirring for minimum of 18 hours. As the lithiated species was not isolated, the reaction was assumed to be complete visually by examining the solution color. In order to confirm the preparation of 1,5-lithiodecaphenylpentagermane, the reaction was quenched with degassed $H_2O$ in order to form the corresponding hydride $H(GePh_2)_5H$. However, when spectroscopically probed by $^1H$ NMR, multiple hydride peaks appeared in the range of $\delta$ 5.0 – 7.0 ppm, corresponding to $Ph_2GeH_2$, the 1,2-dihydride $HPh_2GeGePh_2H$, the 1,3-dihydride $HPh_2GeGePh_2GePh_2H$, and other species present in the crude mixture. This indicates that the Ge – Ge bond cleavage by lithium is occurring in an uncontrolled fashion and subsequently breaking more than one bond. Therefore, even if 1,5-dilithiodecaphenylpentagermane is being produced it seems to be undergoing a secondary cleavage which would account for the many hydride resonances. In an attempt to control the reaction rate with the metal surface, the solubility of the cyclogermanes was examined using various aryl ligands. The focus of this chapter is the preparation of the $(2,5\text{-xylyl})_2GeCl_2$ and its subsequent use to synthesize the octaarylcyclotetragermane ($Ar_8Ge_4$) and decaarylcyclopentaagermane ($Ar_{10}Ge_5$).

## 6.2 Results and Discussion

The preparation of pure $(2,5\text{-xylyl})_2GeCl_2$ (**1**) was needed to synthesize the cyclic analogs, $(Ar_2Ge)_4$ (**4**) and $(Ar_2Ge)_5$ (**5**) (Ar = 2,5-xylyl or $(\text{-}C_6H_3(CH_3)_2)$), of the previously mentioned perphenylated species $(Ph_2Ge)_4$ and $(Ph_2Ge)_5$. The Grignard was prepared from the reaction of 1-bromo-2,5-xylene with a slight excess of magnesium turnings in a refluxing solution of $Et_2O$ and left to stir for 4 hours. The mixture was filtered and added dropwise to 0.6 equivalents of $GeCl_4$ and left stirring in an ice bath, resulting in a cloudy white mixture. The reaction was stirred for a minimum of 4 hours, after which the solution was quenched with 10% HCl until the solution turned clear. The organic layer was worked up to yield a light yellow solid which was further dried to remove any remaining *p*-xylene. The sample was analyzed by GC-MS with four main components in the product mixture with retention times at 11.42, 16.17, 23.49, and 27.39 minutes. The peak at $t_r$ = 11.42 minutes is a small peak of unreacted xylene as its MS has features at *m/z* = 184, 105, and 79 corresponding to $(C_6H_2(CH_3)_2Br)^+$, $(C_6H_3(CH_3)_2)^+$, and Br. The second compound eluted off the column with $t_r$ = 16.17 minutes is the trichloride $ArGeCl_3$ with a MS having peaks at *m/z* = 284, 248, 179, 104, and 77 amu, which correspond to the parent ion $(ArGeCl_3^+)$, and $(ArGeCl^+)$, $(ArGeH_2^+)$, $(C_6H_2(CH_3)_2^+)$, and $(C_6H_5^+)$, respectively. The main peak eluting third off the column is dichloride $Ar_2GeCl_2$ with $t_r$ = 23.49 minutes as its MS has peaks at *m/z* = 354, 248, 179, 104, and 77 amu, corresponding to the parent ion $(Ar_2GeCl_2H^+)$ and $(ArGeCl_2^+)$, $(ArGeH_2^+)$, $(C_6H_2(CH_3)_2^+)$, and $(C_6H_5^+)$, respectively. The final eluted compound with $t_r$ = 27.39 minutes matches the fragmentation of monochloride $Ar_3GeCl$, with MS features at *m/z* = 424, 387, 318, 283, 209, 177, 105, and 79 amu, indicating the presence of $(Ar_3GeClH^+)$, $(Ar_3Ge^+)$, $(Ar_2GeCl^+)$, $(Ar_2GeH^+)$, $(Ar_2^+)$, $(ArGe^+)$, $(Ar^+)$, and Br. This fragmentation shows removal of Cl ion followed by successive loss of the Ar- groups. However, in other various trials it was found that lowering the stoichiometry of the tetrahalide reagent to 0.6 equivalents strongly

favored the formation of dichloro- ($Ar_2GeCl_2$) over the trichloro- ($ArGeCl_3$) and monochloro- ($Ar_3GeCl$) compounds.

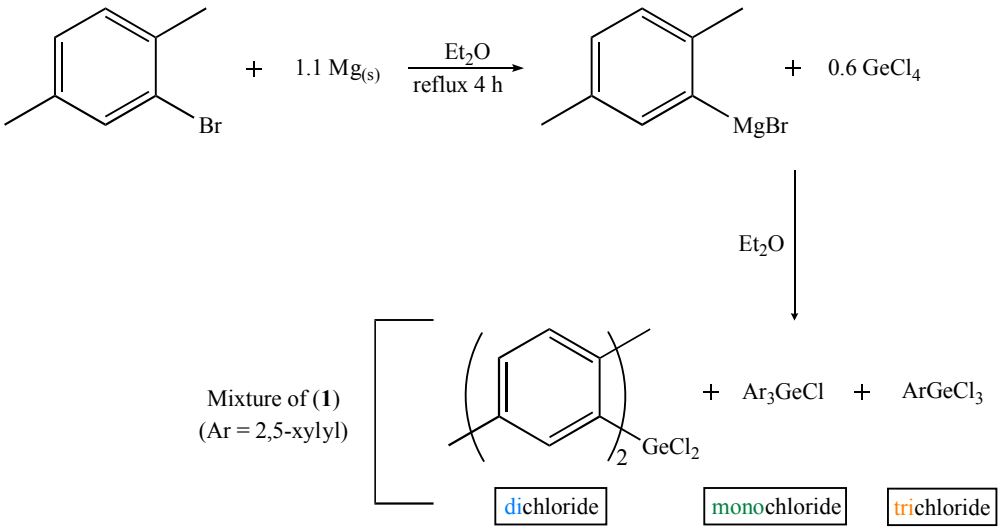


**Scheme 6.3:** Grignard synthesis for preparing chloride mixture $Ar_nGeCl_{(4-n)}$ ($n$ = 1-3) (**1**).

The mixture of chlorides, (*2,5*-xylyl)$_3$GeCl, (*2,5*-xylyl)$_2$GeCl$_2$, and (*2,5*-xylyl)GeCl$_3$ produced could not be separated without first converting them to the analogous hydrides in **Scheme 6.4**. This was done by reacting the product mixture with two equivalents of $LiAlH_4$ in solvent that was left to stir overnight. The reaction was quenched with dilute acid, filtered, and washed with potassium L(+)-tartrate hydrate. The organic phase was further washed with $Et_2O$, dried over $Na_2SO_4$, and dried at 0 °C in an ice bath. The resulting product mixture was analyzed by GC-MS to verify products, showing a chromatogram having three major compounds with retention times at 10.12, 20.31, and 25.29 minutes. The first eluted compound off the column was $ArGeH_3$ at $t_r$ = 10.12 minutes, with its MS fragmentation patterning *m/z* = 180, 165, 151, 107, 91, and 78 amu matching parent ion (($C_6H_3(CH_3)_2GeH_3^+$, then successive loss of methyl groups giving (($C_6H_3(CH_3)Ge^+$) and ($C_6H_3GeH^+$), ($C_6H_3(CH_3)_2)H_2^+$, ($C_6H_3(CH_3)$)$H^+$, and $PhH^+$, respectively. The second eluted compound at $t_r$ = 20.31 minutes was $Ar_2GeH_2$, and has the

following fragmentation: *m/z* = 284, 180, 165, 151, 105, and 77, these peaks correspond to $(C_6H_3(CH_3)_2)_2GeH_2^+$, $(C_6H_3(CH_3)_2)GeH_3^+$, $(C_6H_3(CH_3))GeH_3^+$, $(C_6H_3)GeH_4^+$, $(C_6H_3(CH_3)_2^+$, and $PhH^+$ respectively. The last compound eluted off is $Ar_3GeH$ at $t_r$ = 25.29 minutes, and its MS has leaks at *m/z* = 284, 269, 207, 192, and 178 amu. These peaks correspond to the ions of $(C_6H_3(CH_3)_2)_2GeH^+$, followed by the loss of one methyl group, $(C_6H_3(CH_3)_2)_2^+$ with another loss of a methyl group, and $ArGeH^+$, respectively.

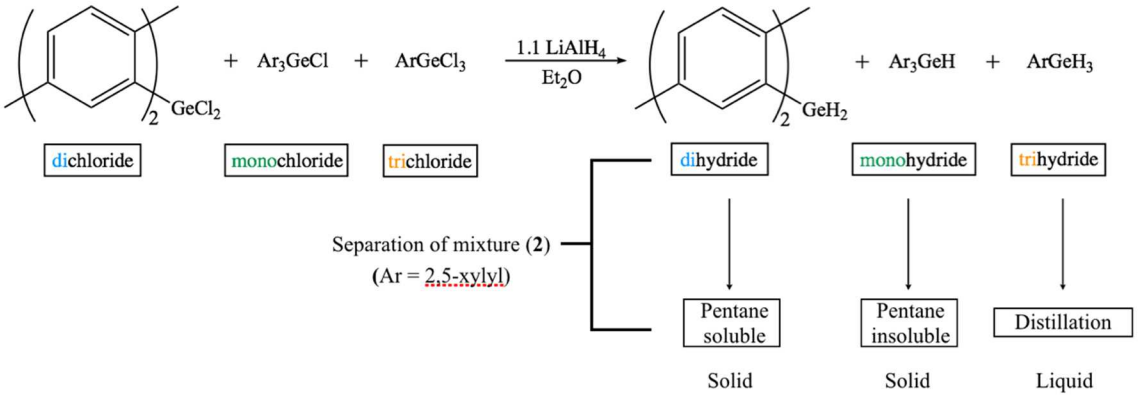


**Scheme 6.4:** Synthetic preparation of $Ar_nGeH_{(4-n)}$ (*n* = 1-3) (**2**) mixture and separation.

Separation and purification of the mixture of hydrides was carried out. A short path distillation was used to remove (2,5-xylyl)$GeH_3$, as a clear liquid while the remaining mixture of (2,5-xylyl)$_3$GeH and (2,5-xylyl)$_2GeH_2$ was separated by solubility. The remaining yellow solution was dried and washed with pentane, and (2,5-xylyl)$_2GeH_2$ is soluble while (2,5-xylyl)$_3$GeH is insoluble.

| | *m/z* | Assignment |
|---|---|---|
| 2,5-$(CH_3)_2(C_6H_3)$ | 184 | $(CH_3)_2C_6H_2Br^+$ |
| ($t_r$ = 11.42 min) | 105 | $(CH_3)_2C_6H_3^+$ |

| | | |
|---|---|---|
| | 79 | $Br^+$ |
| $ArGeCl_3$ | 284 | $((CH_3)_2C_6H_2)GeCl_3^+$ |
| ($t_r$ = 16.17 min) | 248 | $((CH_3)_2C_6H_2)GeCl^+$ |
| | 179 | $((CH_3)_2C_6H_2)GeH_2^+$ |
| | 104 | $((CH_3)_2C_6H_2)^+$ |
| | 77 | $(C_6H_5)^+$ |
| $Ar_2GeCl_2$ | 354 | $((CH_3)_2C_6H_2)_2GeCl_2H^+$ |
| ($t_r$ = 23.49 min) | 248 | $((CH_3)_2C_6H_2)_2GeCl_2^+$ |
| | 179 | $((CH_3)_2C_6H_2)_2GeH_2^+$ |
| | 104 | $((CH_3)_2C_6H_2)_2^+$ |
| | 77 | $(C_6H_5)^+$ |
| $Ar_3GeCl$ | 424 | $((CH_3)_2C_6H_2)_3GeClH^+$ |
| ($t_r$ = 27.39 min) | 387 | $((CH_3)_2C_6H_3)_3Ge^+$ |
| | 318 | $((CH_3)_2C_6H_3)_2GeCl^+$ |
| | 283 | $((CH_3)_2C_6H_3)_2GeH^+$ |
| | 209 | $((CH_3)_2C_6H_3)_2^+$ |
| | 177 | $((CH_3)_2C_6H_3)Ge^+$ |
| | 105 | $((CH_3)_2C_6H_2)^+$ |
| | 79 | $Br^+$ |

**Table 6.1:** GC-MS data for product mixture of the chlorides from (**1**).

The side products generated from the LAH reaction, $Ar_3GeH$ and $ArGeH_3$, and the major $Ar_2GeH_2$ species could all be used as starting materials a new series of linear oligomers, since these materials could be used in the hydrogermolysis reactions. Pure $Ar_2GeH_2$ was then dissolved

in $CCl_4$ and refluxed with a catalytic amount of Pd for 48 hours, replace the hydrogens with chlorine and yield $Ar_2GeCl_2$. The solution was filter cannulated, dried in a warm water bath, and washed with pentane to remove soluble impurities. The resulting insoluble white solid was identified by GC-MS as pure dichlordiarylgermane $Ar_2GeCl_2$ (**3**).

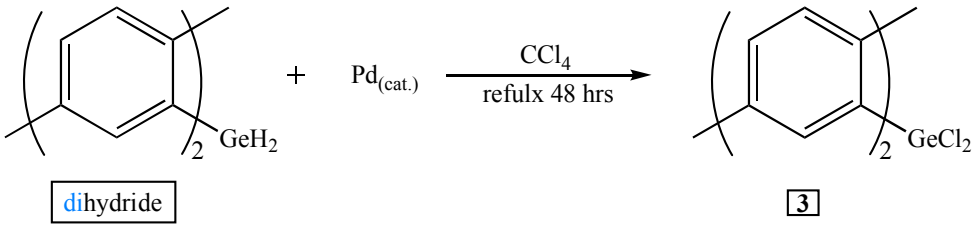


**Scheme 6.5:** Synthetic preparation of pure $(2,5\text{-xylyl})_2GeCl_2$ (**3**).

| | *m/z* | Assignment |
|---|---|---|
| $ArGeH_3$ | 180 | $((Me_2)(C_6H_3))GeH_3^+$ |
| ($t_r$ = 10.12 min) | 165 | $(Me(C_6H_3))Ge^+$ |
| | 151 | $(C_6H_3)GeH^+$ |
| | 107 | $((Me_2)(C_6H_3))H_2^+$ |
| | 91 | $(Me(C_6H_3))H^+$ |
| | 78 | $PhH^+$ |
| $Ar_2GeH_2$ | 284 | $((Me_2)(C_6H_3))_2GeH_2^+$ |
| ($t_r$ = 20.31 min) | 180 | $(Me_2(C_6H_3))GeH_3^+$ |
| | 165 | $(Me(C_6H_3))GeH_3^+$ |
| | 151 | $(C_6H_3)GeH_4^+$ |
| | 105 | $Me_2(C_6H_3)^+$ |
| | 77 | $PhH^+$ |
| $Ar_3GeH$ | 284 | $((Me_2)_2(C_6H_3))GeH^+$ |

| | | |
|---|---|---|
| ($t_r$ = 25.29 min) | 269 | $(Me_3(C_6H_3))Ge^+$ |
| | 207 | $(Me_2(C_6H_3))_2^+$ |
| | 192 | $Me_3(C_6H_3)_2^+$ |
| | 179 | $(Me_2(C_6H_3))GeH^+$ |

**Table 6.2:** GC-MS for the product mixture of hydrides (**2**).

Attempted synthesis of the cyclic compounds $(Ar_2Ge)_4$ (**4**) and $(Ar_2Ge)_5$ (**5**) were prepared by refluxing $Ar_2GeCl_2$ **3**. The cyclopentagermane **5** was synthesized using 10 equivalents of magnesium in THF, with a small amount of dibromoethane to activate the metal. A solution of $Ar_2GeCl_2$ in THF was added dropwise to the stirred flask of Mg metal, and refluxed for a total of 13 hours. The color of the solution turned from a light yellow to dark red in color to indicate the reaction had reached completion. This was also observed for the phenyl analog $(Ph_2Ge)_5$, with the reaction color changing from clear to dark brown.[41] After refluxing, the solution was also quenched with dilute acid, and the organic layer worked up. The resulting solid produced a brown solid, which appeared to still have impurities based on the numerous resonances in the aromatic region in both the $^1H$ and $^{13}C$ NMR spectra. The discoloration of the product was attributed to possible trapped impurities and the crude material was washed with toluene and dichloromethane (DCM) in an attempt to remove the impurities. Various other solvents were also used to test the solubility of the product, but it was only pentane which produced a whiter and purer solid. Although crystallization efforts were made, X-ray quality crystals have not been obtained thus far.

On the other hand, the cyclotetragermane (**4**) was prepared using three equivalents of sodium metal boiling in toluene. A solution of $Ar_2GeCl_2$ was slowly added dropwise to the reaction over a span of 2 hours. Slow addition of the dichloride solution was also essential in preparing $(GePh_2)_4$ to ensure formation of only the cyclotetragermane. If added too quickly, both

$(GePh_2)_5$ and $(GePh_2)_6$ would also start to form.[49] The solution was refluxed for a total of 8 hours, turning from clear to pink and finally a dark purple in color. Once the reaction color remained consistent the reaction was assumed to be completed. The solution was filtered while still hot and the resulting solution produced a yellow-white sticky solid upon removal of the volatiles. The product was washed with $Et_2O$ to remove the remaining NaCl salt, while the supernatant was separated and dried. The resulting solids were re-dissolved in toluene, syringe filtered, and superheated. The solution was allowed to cool slowly and X-ray quality crystals were produced. Upon analysis by X-ray diffraction, instead of seeing the expected octaarylcyclotetragermane $(Ar_2Ge)_4$ (**4**), a germyl-substituted cyclic oligogermane $ClGeAr_2(Ge_4Ar_7)$ (**6**) was found to be present (**Figure 6.3 and 6.4**), and this the first known species of its kind. The obtained xylene species shows a total of nine aromatic ligands around the molecule, with the four germanium atom ring having another single Ge – Cl moiety attached to the ring. The Ge(3) atom within the cyclic ring has only one (2,5-xylyl) group, and is directly bonded to the germyl-germanium Ge(5) having -$(2,5\text{-xylyl})_2$ and a chlorine atom as a substituents. The observed structure is postulated to be generated by an intramolecular aryl migration after the formation of $(GePh_2)_4$. However, more work must be done to confirm the progression of the reaction over time and to monitor product formation. As these are only preliminary results, further investigations must be conducted to optimize experimental conditions, elucidate the mechanistic pathway, and determine if **6** is the major product formed or if it is only a minor component.

Crystals of the germyl-substituted oligomer $ClGeAr_2(Ge_4Ar_7)$ (**6**) were of low quality but allowed for X-ray diffraction data to be obtained. Compound (**6**) crystallized in the monoclinic space group $P2_1/n$ and selected bond distances and angles are collected in **Table 6.1**. The germyl-substituted oligomer itself has average Ge – Ge, Ge – Cl and Ge – C bond lengths of 2.4817(5), 2.2060(12), and 1.9692(2) Å, respectively, while the observed average bond angles for the C – Ge – Ge and Ge – Ge – Ge are 113.1167 ° and 88.95 °. The puckering angles of **6** was measured to be 21.88 °, with a torsional angle of 15 ° along the planes of the Ge – Ge bond.

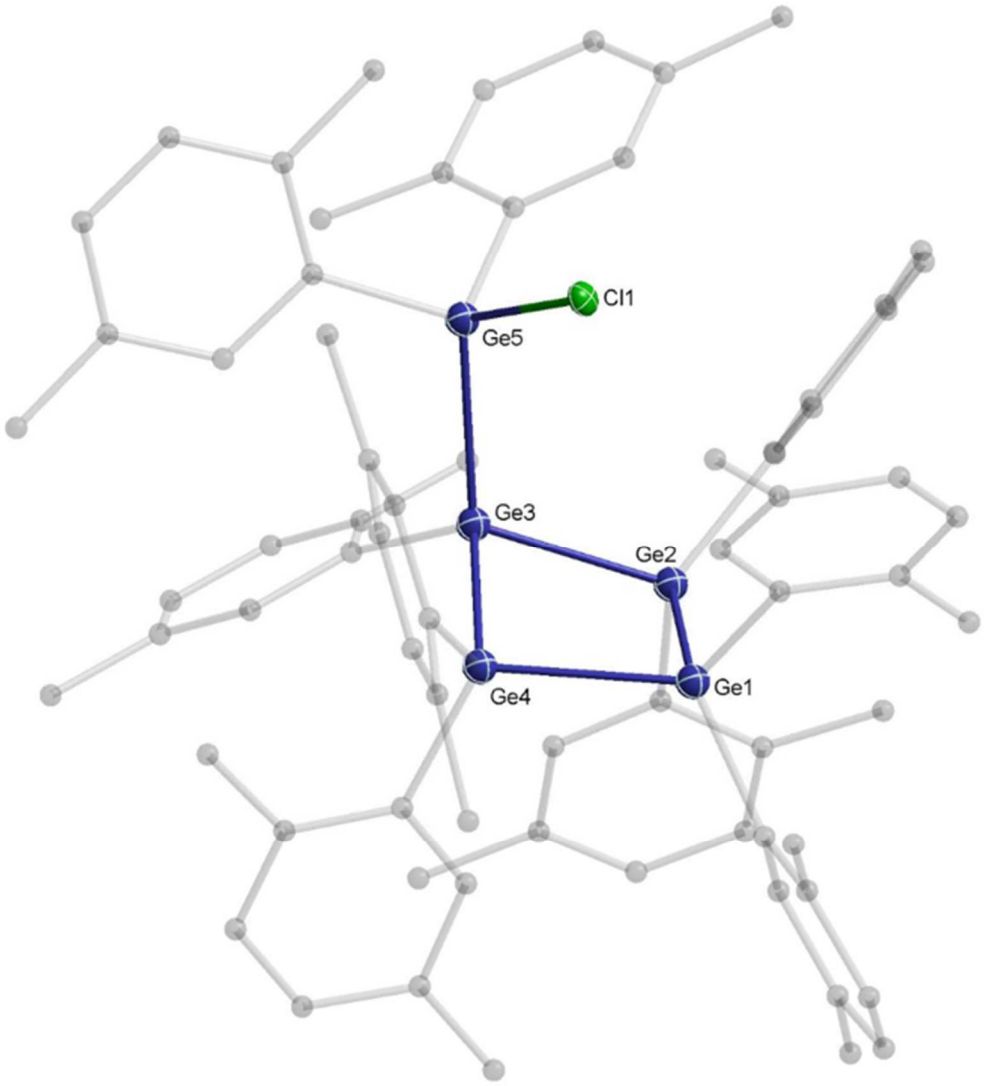


**Figure 6.1:** Side view of the crystal structure of the germyl-substituted cyclic oligogermane (**6**) with thermal ellipsoids drawn at 50% probability.

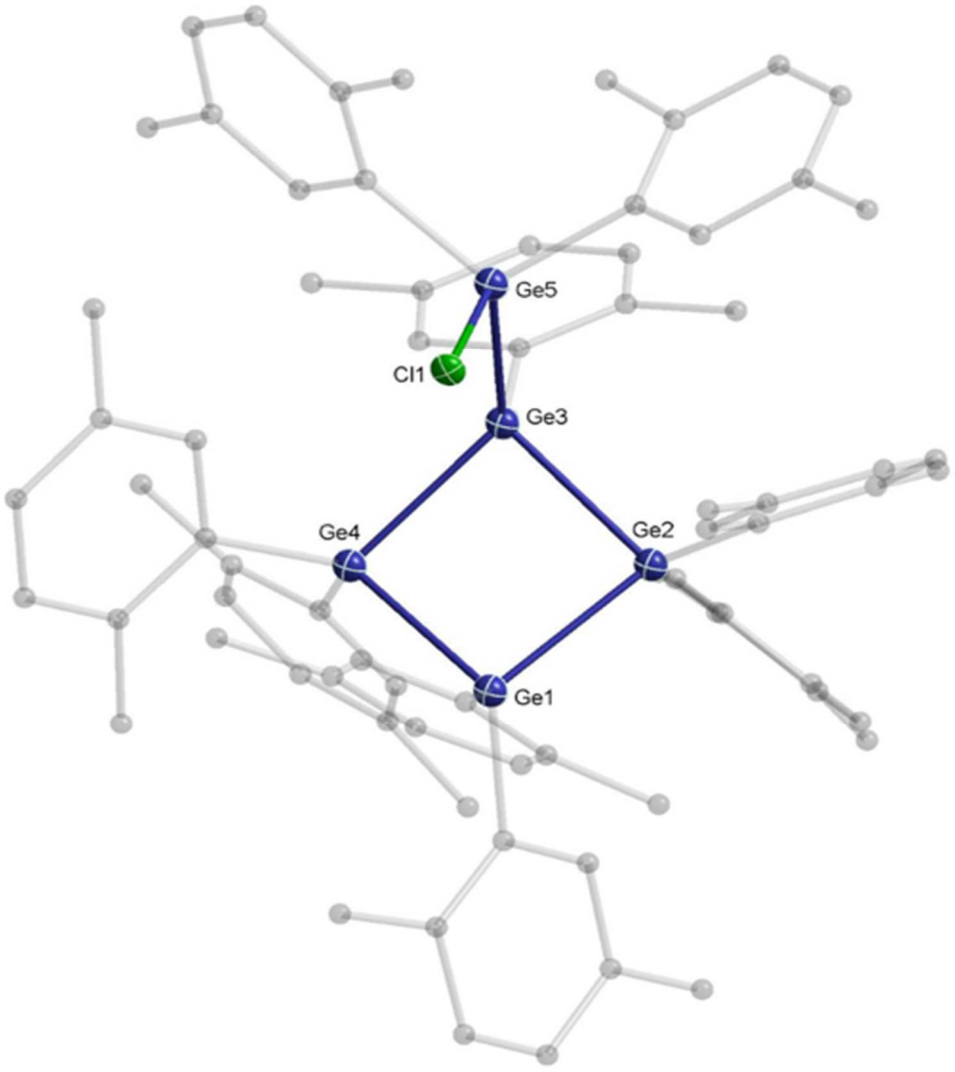


**Figure 13.2:** Top view of the crystal structure of the germyl-substituted cyclic oligogermane (**6**) with thermal ellipsoids drawn at 50% probability.

| Bond Length | Å | Bond Angle | Degrees (°) |
|---|---|---|---|
| Ge(1)—C(1) | 1.981 (4) | C(l) – Ge(1) – Ge(5) | 107.17(13) |
| Ge(1)—Ge(5) | 2.4584(7) | C(1) – Ge(1) – Ge(4) | 115.96(13) |
| Ge(1)—Ge(4) | 2.4809(7) | Ge(5) – Ge(1) – Ge(4) | 113.12(2) |
| Ge(1) – Ge(2) | 2.4818(7) | C(1) – Ge(1) – Ge(2) | 114.50(13) |
| Ge(2) – C(9) | 1.955(4) | Ge(5) – Ge(1) – Ge(2) | 116.61(2) |
| Ge(2) – C(17) | 1.967(4) | Ge(4) – Ge(1) – Ge(2) | 89.01(2) |
| Ge(2) – Ge(3) | 2.4883(7) | Ge(1) – Ge(2) – Ge(3) | 89.27(2) |
| Ge(3) – C(33) | 1.978(4) | Ge(2) – Ge(3) – Ge(4) | 88.46(2) |
| Ge(3) – C(25) | 1.979(5) | Ge(1) – Ge(4) – Ge(3) | 89.05.(2) |
| Ge(3) – Ge(4) | 2.4990(7) | C(65) – Ge(5) – Cl(1) | 104.62(14) |
| Ge(4) – C(41) | 1.970(5) | C(57) – Ge(5) – Cl(1) | 105.85.14 |
| Ge(4) – C(49) | 1.974(4) | C(65) – Ge(5) – Ge(1) | 116.70(14) |
| Ge(5) – C(65) | 1.957(5) | C(57) – Ge(5) – Ge(1) | 112.87(14) |
| Ge(5) – C(57) | 1.958(5) | Cl(1) – Ge(5) – Ge(1) | 105.80(4) |
| Ge(5) – Cl(1) | 2.2060(12) | C(9) – Ge(2) – C(17) | 112.61(18) |

**Table 6.3:** Selected bond distances and angles for germyl-substituted oligogermane (**6**).

Two X-ray structures of related cylcotetragermanes, such as $(GeTol_2)_4$ (Tol = *p*-$CH_3C_6H_4$) and $(GePh_2)_4$, show similar structural parameters in comparison to (**6**). Crystals of $(Ge_2Ph_2)_4$ were obtained from diffusion of hexane into benzene and crystallographic data obtained at 298 K.[136,158] Both the tolyl and the phenyl species possess $C_2$ symmetry. The $(GeTol_2)_4$ species has an average Ge – Ge bond distance of 2.461(0) Å, which is slightly shorter than the average corresponding Ge bond of $(GePh_2)_4$ at 2.464(2) Å. This shows the germanium bond distances are slightly shorter than those of $(GePh_2)_4$, and is also observed in other tolyl substituted oligogermanes.[23] However, **6** has longest average Ge – Ge bond distances out of all three compounds. The average Ge – Ge – Ge bond angles of 89.02(5) ° and 89.95(4) ° relate to $(GeTol_2)_4$ and $(GePh_2)_4$ respectively. Both of the aryl substituted species and **6**, have average Ge – Ge – Ge bond distances which are highly strained, as their values are more acute than the idealized angle of 109.5 ° for a tetrahedral germanium.

## 6.3 Conclusion

The germyl-substituted cycloctetragermane $ClGeAr_2(Ge_4Ar_7)$ (**6**) is the first known species of its type to be reported. Ring strain in cyclic oligogermanes was used as a means to prepare longer catenated oligogermanes, and although this structural attribute was used to easily convert $(GePh_2)_4$ cyclotetragermane into a dihalide $Br(GePh_2)_4Br$, it was not useful for the higher oligomer $(GePh_2)_5$. As an alternative, the preparation of a 1,5-dilithio species was attempted using lithium metal to cleave one Ge – Ge bond in the $(Ph_{10}Ge_5)$. However, in addition to the desired product secondary cleavage processes resulted in a product mixture of hydride species after quenching with $H_2O$. In order to control the solubility of the cyclic compounds the (2,5)-xylyl ligand was used to prepare perarylated cyclogermanes $(GeAr_2)_n$ ($n$ = 4 or 5). However, to date only **6**, which is a germyl-substituted cyclotetragermane, was obtained.

## 6.4 Experimental

*General Remarks*

All manipulations were carried out under inert atmosphere or nitrogen using standard Schlenk, syringe, and glovebox techniques. Solvents were dried using a solvent purification system. GC-MS analysis, X-ray Diffraction, and $^{1}H/^{13}C$ NMR were conducted at Graz University of Technology in Austria.

*Synthesis of (2,5-xylyl)$_2$GeCl$_2$/(2,5-xylyl)$_3$GeCl/(2,5-xylyl)GeCl$_3$ mixture (**1**)*

A 500 mL 3-neck flask was charged with magnesium turnings (3.50 g, 125.46 mmol) and heated out under inert atmosphere. Measured out 100 mL of $Et_2O$ into addition funnel and added 20 mL to turnings and began intermittently heating to initiate grignard. Once the solution turned

yellow, and was self-sustaining, the bromo-*p*-xylene (15.52 mL, 114.07 mmol) and $Et_2O$ solution was added drop-wise to the flask. The reaction was refluxed for a minimum of 4 hours after complete addition of xylene/$Et_2O$ solution. After refluxing, the prepared grignard was filter cannulated to another addition funnel. The prepared grignard was added drop-wise to 0.6 equivalents of $GeCl_4$ (7.80 mL 68.42 mmol) in 100 mL $Et_2O$ while stirring at 0°C. This resulted in a cloudy white mixture which was subsequently stirred for a minimum of 4 hours and then quenched with degassed 10% HCl (20 mL). The reaction mixture turned clear, and the top aqueous layer was cannulated to flask with $Na_2SO_4$. Organic phase was left stirring for 1 hour, filter cannulated to tared flask and dried *in vacuo* to yield a white yellow solid. Light yellow solid was dried further with a heat gun to drive off remaining p-xylene. GC-MS of sample was taken to confirm product mixtures of $(2,5\text{-xylyl})_3GeCl$, $(2,5\text{-xylyl})_2GeCl_2$, or $(2,5\text{-xylyl})GeCl_3$ produced.

*Synthesis of $(2,5\text{-xylyl})_2GeH_2$/$(2,5\text{-xylyl})_3GeH$/$(2,5\text{-xylyl})GeH_3$ mixture (**2**)*

The mixture of chlorides (16.76 g, 47.39 mmol) ***(1)*** was dissolved in 100 mL $Et_2O$ and stirred at 0°C. Pellets of $LiAlH_4$ (3.78 g, 99.51 mmol) were crushed and added portion-wise to the reaction and left stirring overnight. Reaction was quenched with 3% degassed $H_2SO_4$ (25 mL) in an ice bath. Solution was filter cannulated and stirred with potassium L(+)-tartrate hydrate (30 mL) for 30 minutes to balance pH and for anionic/cationic exchange of aluminum species. The organic phase was washed three times with $Et_2O$ and stirred over $Na_2SO_4$. The reaction was then filter cannulated to a tared flask and dried in an ice bath to prevent evaporation of volatile $(2,5\text{-xylyl})GeH_3$. Resulting product was analyzed by GC-MS to verify products, with majority $(2,5\text{-xylyl})_2GeH_2$. When mixtures of hydrides are observed, further separation and purification is done as follows. Short path distillation was done to condense a clear solution of $(2,5\text{-xylyl})GeH_3$ leaving a yellow solution of $(2,5\text{-xylyl})_2GeH_2$ and $(2,5\text{-xylyl})_3GeH$. Yellow solution was dried

and subsequently washed with pentane to separate soluble (2,5-xylyl)$_2$GeH$_2$ and insoluble (p-xylyl)$_3$GeH via cannulation. Dihydride was dried thoroughly before proceeding.

*Synthesis of pure (2,5-xylyl)$_2$GeCl$_2$ (**3**)*

A 3-neck flask was charged with pure (2,5-xylyl)$_2$GeCl$_2$ ***(2)*** and dissolved in 150 mL of $CCl_4$. Catalytic amount of Pd was added to the reaction and refluxed for 48 hours. Solution was filter cannulated to a Schlenk flask and dried in warm water bath. Solids were washed multiple times with pentane to remove soluble impurities. Insoluble white product was separated from soluble impurities and again dried under vacuum.

*Synthesis attempted of Octa-(2,5-xylyl) cyclotetragermane (**4**)*

The prepared (2,5-xylyl)$_2$GeCl$_2$ (1.51 g, 4.24 mmol) ***(3)*** was dissolved in 75 mL toluene and added drop-wise to a refluxing solution of sodium (0.30 g, 12.72 mmol) in 25 mL toluene. Once sodium was activated, addition was done slowly over a period of a few hours to favor cyclotetragermane formation. The reaction was refluxed for a total of 8 hours, turning from clear to pink, to purple, and finally to black in color. Solution was then hot filtered via filter cannula to another flask at 0°C. Product was dried resulting in a yellow-white solid. Product was washed with $Et_2O$ and white precipitate crashed out of solution. Solid was presumed to be salt after verifying high melting points. Yellow supernatant was cannulated away and dried. Aliquots of material were used for crystallization attempts using various solvents (ie. toluene, hexane, dioxane, pentane). This method produced no results, therefore all aliquots were recombined and dried. Solids were washed in toluene, syringe filtered to a vial, and dried again (solid appeared to be more white). Minimal solvent was used to re-dissolve the solids and was superheated. Vial was sealed with a septa and parafilm and then allowed to cool slowly. Crystals of x-ray quality were picked, but the product was instead germyl-substituted cyclic oligogermanes.

# REFERENCES


1. Winkler, C., *Chem. Ber.* **1886**, (19), 210-211.

2. Winkler, C. A.; *J. Prakt. Chem.* **1886**, 142, 177-229.

3. Haller, E. E., *Mater. Sci. Semicond. Process.* **2006**, 9, 408-422.

4. Aston, F.W., *Nature* **1923**, 111, 771.

5. Hitchcock, P. B.; Jasim, H. A.; Lappert, M. F.; Leung, W. P.; Rai, A. K.; Taylor, R. E., *Polyhedron* **1991**, 10 (11), 1203-1213.

6. Pillarisetty, R., *Nature* **2011**, 479 (7373), 324.

7. Glockling, F., *The chemistry of germanium*; Academic P.: New York, London, **1969**, 234.

8. Hayashi, T.; Uchimaru, Y., Reddy, N. P.; Tanaka, M.; *Chem. Lett*. **1992**, 647.

9. Lickiss, P. D., Science of Synthesis. *Organometallics, Compounds of Group 15 (Ge, Sn, Pb)*. Moloney, M.G. Eds. Thieme: New York, **2003**, 5, 12-45.

10. Thayer, J. S., *Appl. Organomet. Chem.* **1987**, 1, 227-234.

11. Foucher, D., Main Group Strategies towards Functional Hybrid Materials. *Catenated Germanium and Tin Oligomer and Polymers*. Baumgartner, T. Jäkle, F. Eds.; Wiley, New Jersey, **2018**, 209-233.

12. Miller, R.D.; Michl. J., *Chem. Rev.* **1989**, 89 (6), 1359-14. Miller, R.D., *Adv. Mater.* **1989**, 1, 433-440.

13. Zeigerler, J. M.; Fearon, F.W.G., *Silicon-based Polymer Science: A Comprehensive Resource*. American Chemical Society: Washington, D.C., **1989**.

14. Sita, L. R., *Acc. Chem. Res.* **1994**, 27, 191-197.

15. Sita, L. R., *Adv. Organomet. Chem.* **1995**, 38, 189-243.

16. Weinert, C. S., *Dalton Trans*. **2009**, 1691.

17. Balaji, V.; Michl, J., *Polyhedron*. **1991**, 10 (11), 1265-1284.

18. Abd-El-Aziz, A. S., *Half-century of Metal- and Metalloid-Containing Polymers*. Wiley-Interscience: Hoboken, N.J., **2003**.

19. Amadoruge, M. L.; Weinert, C.S., *Chem. Rev.* **2008**, 108 (10), 4253-4294.

20. Amadoruge, M. L.; Gardinier, J. R.; Weinert, C. S., *Organometallics* **2008**, 27 (15), 3753-3760.

21. Amadoruge, M. L.; DiPasquale, A. G.; Rheingold, A. L.; Weinert, C. S., *J. Organomet. Chem.* **2008**, 693 (10), 1771-1778.

22. Amadoruge, M. L.; Short, E. K.; Moore, C.; Rheingold, A. L.; Weinert, C. S., *J. Organomet. Chem.* **2010**, 695 (14), 1813-1823.

23. Schrick, E. K.; Forget, T. J.; Roewe, K. D.; Schrick, A. C.; Moore, C. E.; Golen, J. A.; Rheingold, A. L.; Materer, N. F.; Weinert, C. S., *Organometallics* **2013**, 32 (7), 2245-2256.

24. Okano, M.; Mochida, K., *Chem. Lett.* **1990**, 5, 701-704.

25. Mochida, K.; Hata, R.; Shimoda, M.; Matsumoto, F.; Kurosu, H.; Kojima, A.; Yoshikawa, M.; Masuda, S.; Harada, Y., *Polyhedron* **1996**, 15 (18), 3027-3032.

26. Mochida, K.; Hodota, C.; Hata, R.; Fukuzumi, S., *Organometallics* **1993**, 12 (2), 586-588.

27. Weinert, C. S., *Comments on Inorganic Chemistry* **2011**, 32, 55.

28. Dräger, M., *Silicon Germanium Tin Lead Cmpds.* **1983**, 7, 299.

29. Weinert, C. S. *In Comprehensive Organometallic Chemistry III*; Crabtree, R. H., Mingos, D. M. P., Eds.; Elsevier: London, **2006**, 3, 699.

30. Winkler, C. A.; *J. Prakt. Chem.* **1887**, 36 (1), 177-209.

31. Morgan, G. T.; Dugland, H.; Drew, K., *J. Chem. Soc., Trans*. **1925**, 127, 1760.

32. Shankar, R.; Saxena, A.; Brar, A. S., *J. Organomet. Chem.* **2002**, 650 (1-2), 223-230.

33. Miller, R. D.; Jenkner, P. K., *Macromolecules* **1994**, *27* (20), 5921-5923.

34. Sita, L. R., *Organometallics* **1992**, *11* (4), 1442-1444.

35. Sita, L. R., *Acc. Chem. Res.* **1994**, *27* (7), 191-197.

36. Baumgartner, J.; Fischer, R.; Fischer, J.; Wallner, A.; Marschner, C.; Florke, U., *Organometallics* **2005**, 24 (26), 6450-6457.

37. Chaubon, M. A.; Ranaivonjatovo, H.; Escudie, J.; Satge, J., *Main Group Metal Chemistry* **1996**, 19 (3), 145-160.

38. Power, P. P., *Chem. Rev.* **1999**, 99 (12), 3463-3503.

39. Triplett, K.; Curtis, M. D., *J. Organomet. Chem.* **1976**, 107 (1), 23-32.

40. Neumann, W. P.; Kuhlein, K., *Liebigs Ann. Chem.* **1965**, 683 (1), 1-11.

41. Castel, A.; Riviere, P.; Saintroch, B.; Satge, J.; Malrieu, J. P., *J. Organomet. Chem.* **1983**, 247 (2), 149-160.

42. Satgé, J.; Massol, M.; Rivière, P., *J. Organomet. Chem.* **1973**, 56, 1-39.

43. Roller, S.; Simon, D.; Drager, M., *J. Organomet. Chem.* **1986**, 301 (1), 27-40.

44. Gilman, H.; Gerow, C. W., *J. Am. Chem. Soc.* **1956**, 78 (20), 5435-5438.

45. Drager, M.; Ross, L., *Z. Anorg. Allg. Chem.* **1980**, 460 (1), 207-216.

46. Drager, M.; Ross, L.; Simon, D., *Z. Anorg. Allg. Chem.* **1980**, 466 (7), 145-156.

47. Drager, M.; Ross, L., *Z. Anorg. Allg. Chem.* **1980**, 469 (10), 115-122.

48. Ross, L.; Drager, M., *J. Organomet. Chem.* **1980**, 194 (1), 23-32.

49. Ross, L.; Drager, M., *J. Organomet. Chem.* **1980**, 199 (2), 195-204.

50. Ross, L.; Drager, M., *Z. Anorg. Allg. Chem.* **1981**, 472 (1), 109-119.

51. Drager, M.; Ross, L., *Z. Anorg. Allg. Chem.* **1981**, 476 (5), 95-104.

52. Drager, M.; Simon, D., *Z. Anorg. Allg. Chem.* **1981**, 472 (1), 120-128.

53. Ross, L.; Drager, M., *Z. Naturforsch B.* **1983**, 38 (6), 665-673.

54. Ross, L.; Drager, M., *Z. Anorg. Allg. Chem.* **1984**, 515 (8), 141-146.

55. Simon, D.; Haberle, K.; Drager, M., *J. Organomet. Chem.* **1984**, 267 (2), 133-142.

56. Ross, L.; Drager, M., *Z. Anorg. Allg. Chem.* **1984**, 519 (12), 225-232.

57. Drager, M.; Haberle, K., *J. Organomet. Chem.* **1985**, 280 (2), 183-196.

58. Roller, S.; Drager, M., *J. Organomet. Chem.* **1986**, 316 (1-2), 57-65.

59. Haberle, K.; Drager, M., *J. Organomet. Chem.* **1986**, 312 (2), 155-165.

60. Drager, M.; Simon, D., *J. Organomet. Chem.* **1986**, 306 (2), 183-192.

61. Haberle, K.; Drager, M., *Z. Anorg. Allg. Chem.* **1987**, 551 (8), 116-122.

62. Haberle, K.; Drager, M., *Z. Naturforsch B.* **1987**, 42 (3), 323-329.

63. Yokoyama, Y.; Hayakawa, M.; Azemi, T.; Mochida, K., *J. Chem. Soc. Chem. Comm.* **1995,** (22), 2275-2275.

64. Azemi, T.; Yokoyama, Y.; Mochida, K., *J. Organomet. Chem*. **2005**, 690, 1588.

65. Bochkarev, M. N.; Vyazankin, N. S.; Bochkarev, L. N.; Razuvaev, G. A., *J. Organomet. Chem.* **1976**, 110 (2), 149-157.

66. Subashi, E.; Rheingold, A. L.; Weinert, C. S., *Organometallics* **2006**, 25, 3211.

67. Bochkarev, M. N.; Vyazankin, N. S.; Bochkarev, L. N.; Razuvaev, G. A., *J. Organomet. Chem.* **1976**, 110, 149.

68. Chorley, R. W.; Hitchcock, P. B.; Lappert, M. F.; Leung, W. P.; Power, P. P.; Olmstead, M. M., *Inorg. Chim. Acta.* **1992**, 198, 203-209.

69. Cotton, J. D.; Davidson, P.J.; Lappert, M.F., *Dalton Trans.* **1976**, 21, 2275-2286.

70. Neumann, W. P., *Chem. Rev.* **1991**, 91 (3), 311-334.

71. Weinert, C. S.; Fenwick, A. E.; Fanwick, P. E.; Rothwell, I. P., *Dalton Trans.* **2003**, 4, 532-539.

72. Simon, D.; Häberle, K.; Dräger, M., *J. Organomet Chem.* **1984**, 267, 133-142.

73. Häberle, K.; Dräger, M., *Z Naturforsch* **1987**, 323-329.

74. Zaitsev, K.; Kapranov, A. A.; Oprunenko, Y. F.; Churakov, A.V.; Howard, J. A. K.; Tarasevich, B. N.; Karlov, S. S.; Zaitseva, G. S., *J. Organomet Chem.* **2012**, 700, 207-213.

75. Zaitsev, K.; Oprunenko, Y. F.; Churakov, A. V.; Zaitseva, G. S.; Karlove, S. S., *Main Group Met. Chem.* **2014**, 37, 67-74.

76. Leigh, W. J.; Harrington, C. R.; Vargas-Baca, I.; *J. Am Chem Soc.* **2004**, 126, 16105-16116.

77. Billone, P. S.; Beleznay, K.; Harrington, C. R.; Huck, L. A.; Leigh, W. J., *J. Am Chem. Soc.* **2011**, 133 (27), 10523-10534.

78. Mochida, K.; Yoneda, I.; Wakasa, M., *J. Organomet. Chem.* **1990**, 399 (1-2), 53-62.

79. Lesbre, M.; Mazerolles, P.; Satgé, J., *The organic compounds of germanium*. Interscience Publishers: London, New York, **1971**, 701.

80. Baines, K. M.; Cooke, J. A.; Dixon, C. E.; Liu, H. W.; Netherton, M. R., *Organometallics* **1994**, 13, 631–634.

81. Huck, L. A.; Leigh, W. J., *Can. J. Chem.* **2011**, 89, 241–255.

82. Hardwick, J. A.; Pavelka, L. C.; Baines, K. M.; *Dalton Trans.* **2012**, 41, 609– 621.

83. Ando, W.; Tsumuraya, T., *J. Chem. Soc., Chem. Commun.* **1987**, 1514–1515.

84. Mochida, K.; *Main Group Met. Chem.* **1994**, 17, 25–31.

85. Mochida, K.; Chiba, H.; Okano, M., *Chem. Lett.* **1991**, 109–112.

86. Mochida, K; Chiba, H.; *J. Organomet. Chem*. **1994**, 473, 45–54.

87. Tsumuraya, T.; Kabe, Y.; Ando, W., *J. Organomet. Chem*. **1994**, 482, 131– 138.

88. Ohshita, J.; Toyoshima, Y.; Iwata, A.; Tang, H.; Kunai, A., *Chem. Lett.* **2001**, 886–887.

89. Azemi, T.; Yokoyama, Y.; Mochida, K., *J. Organomet. Chem*. **2005**, 690, 1588– 1593.

90. Tashkandi, N. Y.; Parsons, F.; Guo, J.; Baines, K. M., *Agnew. Chem. Int. Ed.* **2015**, 54, 1612-1615.

91. Glockling, F.; Hooton, K. A., *J. Chem. Soc.* **1963**, 1849-1854.

92. Riviere, P.; Satgé, J., *Synth. Inorg. Metallorg. Chem.* **1971**, 13-20.

93. Riviere, P.; Satgé, J.; Soula, D., *J. Organomet. Chem.* **1974**, 72, 329-338.

94. Glockling, F.; Light, J. R. C.; Strafford, R. G.; *J. Chem. Soc*. **1970**, 426-432.

95. F. Glockling, J.R.C. Light, J. Walker, *Chem. Commun.* **1968**, 1052-1053.

96. Samanamu, C. R.; Materer, N. R.; Weinert, C. S., *J. Organomet. Chem.* **2012**, 698, 62-65.

97. Amadoruge, M. L.; Golen, J. A.; Rheingold, A. L.; Weinert, C. S., *Organometallics* **2008**, 27, 1979-1984.

98. Samanamu, C. R.; Amadoruge, M. L.; Yoder, C. H.; Golen, J. A.; Moore, C. E.; Rheingold, A. L.; Materer, N. F.; Weinert, C. S., *Organometallics* **2011**, 30 1046-1058.

99. Samanamu, C. R.; Amadoruge, M. L.; Schrick, A. C.; Chen, C.; Golen, J. A.; Rheingold, A. L.; Materer, N. F.; Weinert, C.S., *Organometallics* **2012**, 31, 4374-4385.

100. Hlina, J.; Zitz, R.; Wagner, H.; Stella, F.; Baumgartner, J.; Marschner, C., *Inorg. Chim. Acta.* **2014**, 422, 120-133.

101. Hlina, J.; Baumgartner, J.; Marschner, C., *Organometallics* **2010**, 29, 5289-5295.

102. Schrick, E. K.; Forget, T. J.; Roewe, K. D.; Schrick, A. C.; Moore, C. E.; Golen, J. A.; Rheingold, A. L.; Materer, N. F.; Weinert, C. S., *Organometallics* **2013**, 32 2245-2256.

103. Zaitsev, K. V.; Lermontova, E. K.; Churakov, A. V.; Tafeenko, V.A.; Tarasevich, B. N.; Poleshchuk, O. K.; Kharcheva, A. V.; Magdesieva, T. V.; Nikitin, O. M.; Zaitseva, G. S.; Karlov, S. S., *Organometallics* **2015**, 34, 2765-2774.

104. Roewe, K. D.; Golen, J. A.; Rheingold, A. L.; Weinert, C. S., *Can. J. Chem.* **2014**, 92, 533-541.

105. Roewe, K. D., Rheingold, A. L., Weinert, C. S., *Chem. Commun*. **2013**, 49, 8380-8382.

106. Zaitsev, K. V.; Lam, K.; Zhanabil, Z.; Suleimen, Y.; Kharcheva, A. V.; Tafeenko, V. A.; Oprunenko, Y. F.; Poleshchuk, O. K.; Lermontova, E. K.; Churakov, A. V., *Organometallics* **2017**, 36, 298-309.

107. Weinert, C. S., ISRN Spectroscopy **2012**, Article ID 718050, 718018.

108. Wilkins, A. L.; Watkinson, P. J.; Mackay, K. M., *J. Chem. Soc., Dalton Trans*. **1987**, 2365-2372.

109. MacKay, K. M.; Thomson, R. A., *Main Group Met. Chem.* **1987**, 10, 83-108.

110. Takeuchi, Y.; Takayama, T., *Annu. Rep. NMR Spectro*. **2005**, 54, 155-200.

111. Amadoruge, M. L.; Yoder, C. H.; Conneywerdy, J. H.; Heroux, K.; Rheingold, A. L.; Weinert, C. S., *Organometallics* **2009**, 28, 3067-3073.

112. Komanduri, S. P.; Schrick, A. C.; Feasley, C. P.; Dufresne, C. P.; Weinert, C. S., *Eur. J. Inorg. Chem.* **2016**, 3196-3203.

113. Fa, W.; Zeng, X., *C. Chem. Commun*. **2014**, 50, 9126.

114. Huo, Y.; Berry, D. H., *Chem. Mater.* **2005,** 17, 157.

115. Kobayashi, S.; Cao, S., *Chem. Lett.* **1993**, 22, 1385.

116. Miller, R. D.; Sooriyakumaran, R., *J. Polym. Sci., Part A: Polym. Chem.* **1987**, 25, 111.

117. Mochida, K.; Hata, R.; Chiba, H.; Seki, S.; Yoshida, Y.; Tagawa, S., *Chem. Lett*. **1998**, 27, 263.

118. Samanamu, C. R.; Amadoruge, M. L.; Schrick, A. C.; Chen, C.; Golen, J. A.; Rheingold, A. L.; Materer, N. F.; Weinert, C. S., *Organometallics* **2012**, 31, 4374.

119. Anderson, H. H., *J. Am. Chem. Soc.* **1953**, 75, 814.

120. Rochow, E. G.; Didtschenko, R.; West, R., *J. Am. Chem. Soc*. **1951**, 73, 5486.

121. Poskozim, P. S., *J. Organomet. Chem*. **1968**, 12, 115.

122. Castel, A.; Riviere, P.; Satge, J.; Ko, H. Y., *Organometallics* **1990**, 9, 205.

123. Burge, D. E., *J. Chem. Educ.* **1970,** *47* (2).

124. Katz, S. M.; Reichl, J. A.; Berry, D. H., *J. Am. Chem. Soc.* **1998**, 120, 9844

125. Heath, J. R.; Shiang, J. J.; Alivisatos, A. P., *J. Chem. Phys*. **1993**, 101, 1607.

126. Poskozim, P. S., *J. Organomet. Chem.* **1968**, 12, 115.

127. Carrick, A.; Glockling, F., *J. Chem. Soc.* **1966**, 623

128. Taylor, B. R.; Kauzlarich, S. M.; Delgado, G. R.; Lee, H. W. H., *Chem. Mater.* **1999**, 11, 2493.

129. Taylor, B. R.; Kauzlarich, S. M.; Lee, H. W. H.; Delgado, G. R., *Chem. Mater*. **1998**, 10, 22.

130. Mochida, K.; Hodota, C.; Hata, R.; Fukuzumi, S., *Organometallics* **1993**, 12, 586.

131. Okano, M.; Mochida, K., *Chem. Lett*. **1990**, 19, 701.

132. Kashimura, S.; Ishifune, M.; Yamashita, N.; Bu, H.-B.; Takebayashi, M.; Kitajima, S.; Yoshiwara, D.; Kataoka, Y.; Nishida, R.; Kawasaki, S.; Murase, H.; Shono, T., *J. Org. Chem*. **1999**, 64, 6615.

133. Okano, M.; Takeda, K.; Toriumi, T.; Hamano, H., *Electrochim. Acta* **1998**, 44, 659.

134. Brown, P.; Mahon, M. F.; Molloy, K. C., *J. Organomet. Chem.* **1992**, 435 265-273.

135. Simons, J. K., Wagner, E. C., Muller, J. H., *J. Am. Chem. Soc.* **1933**, 55, 3705-3712.

136. Gynane, M. J. S.; Lappert, M. F., *J. Organomet Chem.* **1977**, 142 (1), 9-11.

137. Cooke, J. A.; Dixon, C. E.; Netherton, M. R.; Kollegger, G. M.; Baines, K. M., *Synthesis and Reactivity in Inorganic and Metal-organic Chemistry* **1996**, 26 1205-1217.

138. Chaubon, M. A.; Dittrich, B.; Escudie, J.; Ramdane, H.; Ranaivonjatovo, H.; Satge, J., *Synth. React. Inorg. Met. -Org. Chem*. **1997**, 27, 519-533.

139. Samanamu, C. R.; Anderson, C. R.; Golen, J. A.; Moore, C. E.; Rheingold, A. L.; Weinert, C. S., *J. Organomet. Chem.* **2011**, 696, 2993-2999.

140. Morgan, G. T.; Drew, H. D. K., *J. Chem. Soc. Trans.* **1925**, 127, 1760-1768.

141. Kraus, C. A.; Foster, L. S., *J. Am. Chem. Soc.* **1927**, 49, 457-467.

142. Harris, D. M.; Nebergall, W. H.; Johnson, O. H., *Inorg. Synth*. **1957**, 5, 70-72.

143. Wolf, M.; Falk, A.; Flock, M.; Torvisco, A.; Frank, U., *J. Organomet. Chem.* **2017**, 851, 143-149.

144. Johnson, O. H.; Harris, D. M., *J. Am. Chem. Soc.* **1950**, 72, 5564-5566.

145. Thornton, P., *Sci. Synth.* **2003**, 5, 55-73.

146. Glockling, F., Hooton, K. A., *J. Chem. Soc.* **1962**, 3509-3512.

147. Cerveau, G.; Chuit, C.; Corriu, R. J. P.; Reye, C., *Organometallics* **1991**, 10, 1510-1515.

148. U. Krueerke, E. Wittouck, *Chem. Ber.* 1**962**, 95, 174-182.

149. Gilman, H.; Schwebke, G. L., *J. Organomet. Chem.* **1964**, 3, 382-393.

150. Gilman, H.; Peterson, D. J.; Jarvie, A. W.; Winkler, H. J. S., *Tetrahedron Lett.* **1960**, 1 (44), 5-7.

151. Kipping, F. S.; Sands. J. E.; *J. Chem. Soc., Trans.* **1921**, 119 (0), 830-847.

152. Jarvie, A. W. P.; Winkler, H. J. S.; Peterson, D. J.; Gilman, H., *J. Am. Chem. Soc.* **1961**, 83 (8), 1921-1924.

153. Gilman, H.; Schwebke, G. L., *J. Am. Chem. Soc.* **1964**, 86 (13), 2693-2699.

154. Winkler, H.; Jarvie, A.; Peterson, D. J.; Gilman, H., *J. Am. Chem. Soc.* **1961**, 83(19), 4089-4093.

155. Goto, M.; Tokura, S.; Mochida, K., *Nippon Kagaku Kaishi* **1994**, (3), 202-207.

156. Roewe, K. D.; Golen, J. A.; Rheingold, A. L.; Weinert, C. S., *Can. J. Chem.* **2014**, 92(6), 533-541.

157. Rupar, P. A.; Jennings, M. C.; Baines, K. M., *Organomet.* **2008**, 27, 5043.

# APPENDICES

**Table A.1.** Crystal data and structure refinement for $HPh_2GeGePh_2GePh_2H$ (**3**).

| | **3** | |
|---|---|---|
| Empirical formula | $C_{36}H_{32}Ge_3$ | |
| Formula weight | 682.38 | |
| Temperature (K) | 100(2) | |
| Wavelength (Å) | 0.71073 | |
| Crystal system | Triclinic | |
| Space group | *P*-1 | |
| *a,* Å | 9.6058(6) | $\alpha$ = 89.045(2) ° |
| *b*, Å | 10.9421(6) | $\beta$ = 83.682(2) ° |
| *c*, Å | 14.6843(9) | $\gamma$ = 85.038(2) ° |
| *V*, Å$^3$ | 1528.27(16) | |
| Z | 2 | |
| Density (Mg/m$^3$) | 1.431 | |
| Absorption coefficient (mm$^{-1}$) | 2.954 | |
| F(000) | 688 | |
| Crystal size (mm$^3$) | 0.220 x 0.180 x 0.100 | |
| Theta range for data collection | 2.425 to 28.334 ° | |
| Index ranges | $-12 \le h \le 12$ | |
| | $-14 \le k \le 9$ | |
| | $-19 \le l \le 19$ | |
| Reelections collected | 23524 | |
| Independent reflections | 7605 [$R_{int}$ = 0.0380] | |
| Completeness to $\theta$ = 25.000 ° | 99.9 % | |
| Absorption correction | Multi-scan | |
| Refinement method | Full-matrix least squares of $F^2$ | |
| Data/restraints/parameters | 7605/0/360 | |
| Goodness-of-fit on $F^2$ | 0.999 | |
| Final *R* indices [$I>2\sigma(I)$] | | |
| $R_1$ | 0.0302 | |
| $wR_2$ | 0.0577 | |
| *R* indices (all data) | | |
| $R_1$ | 0.0475 | |
| $wR_2$ | 0.0629 | |
| Extinction coefficient | n/a | |
| Largest diff. peak and hole (e Å$^{-3}$) | 0.654 and -0.642 | |

**Table A.2.** Atomic coordinates ( x $10^4$) and equivalent isotropic displacement parameters ($Å^2$ x $10^3$) for $HPh_2GeGePh_2GePh_2H$ (**3**). U(eq) is defined as one third of the trace of the orthogonalized $U^{ij}$ tensor.

| | x | y | z | U(eq) |
|---|---|---|---|---|
| Ge(2) | 71071(1) | 4290(1) | 6318(1) | 15(1) |
| Ge(1) | 4808(1) | 3804(1) | 7028(1) | 16(1) |
| Ge(3) | 9024(1) | 4322(1) | 7267(1) | 17(1) |
| C(13) | 6980(2) | 5915(2) | 5741(1) | 16(1) |
| C(19) | 7800(2) | 3046(2) | 5397(2) | 16(1) |
| C(7) | 4868(2) | 2169(2) | 7598(2) | 16(1) |
| C(1) | 4093(2) | 5030(2) | 7952(2) | 17(1) |
| C(25) | 8706(2) | 5628(2) | 8174(2) | 18(1) |
| C(14) | 5627(2) | 6623(2) | 5816(2) | 19(1) |
| C(6) | 4970(3) | 5440(2) | 8559(2) | 24(1) |
| C(31) | 9518(2) | 2747(2) | 7835(2) | 18(1) |
| C(24) | 7967(2) | 3300(2) | 4454(2) | 20(1) |
| C(20) | 8091(2) | 1836(2) | 5684(2) | 19(1) |
| C(29) | 8456(2) | 6343(2) | 9748(2) | 26(1) |
| C(28) | 8265(2) | 7543(2) | 9443(2) | 27(1) |
| C(4) | 3120(3) | 6865(2) | 9229(2) | 25(1) |
| C(12) | 5190(2) | 1101(2) | 7081(2) | 20(1) |
| C(32) | 8527(2) | 2144(2) | 8407(2) | 22(1) |
| C(30) | 8678(2) | 5389(2) | 9114(2) | 21(1) |
| C(33) | 8892(3) | 1027(2) | 8810(2) | 24(1) |
| C(16) | 6671(3) | 8264(2) | 4955(2) | 22(1) |
| C(18) | 8077(2) | 6411(2) | 5269(2) | 19(1) |
| C(15) | 5502(2) | 7788(2) | 5421(2) | 21(1) |
| C(26) | 8494(2) | 6847(2) | 7883(2) | 22(1) |
| C(2) | 2721(2) | 5546(2) | 8013(2) | 22(1) |
| C(8) | 4605(2) | 2061(2) | 8551(2) | 21(1) |
| C(5) | 44977(3) | 6350(2) | 9188(2) | 29(1) |
| C(3) | 2223(2) | 6461(2) | 8647(2) | 26(1) |
| C(17) | 7962(2) | 7573(2) | 4879(2) | 22(1) |
| C(36) | 10880(2) | 2179(2) | 7682(2) | 23(1) |
| C(23) | 8397(2) | 2366(2) | 3824(2) | 25(1) |
| C(9) | 4673(3) | 911(2) | 8974(2) | 25(1) |
| C(11) | 5258(2) | -43(2) | 7503(2) | 24(1) |
| C(22) | 8653(3) | 1173(2) | 4126(2) | 27(1) |
| C(34) | 10246(3) | 475(2) | 8644(2) | 27(1) |
| C(21) | 8501(2) | 906(2) | 5057(2) | 23(1) |
| C(27) | 8275(2) | 7799(2) | 8512(2) | 25(1) |
| C(10) | 5004(2) | -138(2) | 8452(2) | 26(1) |
| C(35) | 11245(3) | 1054(2) | 8077(2) | 26(1) |

**Table A.3.** Bond lengths (Å) and angles (°) for $HPh_2GeGePh_2GePh_2H$ (**3**)

| | | | |
|---|---|---|---|
| Ge(2) – C(19) | 1.958(2) | C(24) – C(23) | 1.395(3) |
| Ge(2) – C(13) | 1.960(2) | C(20) – C(23) | 1.386(3) |
| Ge(2) – Ge(3) | 2.4308(3) | C(29) – C(28) | 1.384(3) |
| Ge(2) – Ge(1) | 2.4338(3) | C(29) – C(30) | 1.397(3) |
| Ge(1) – C(1) | 1.951(2) | C(28) – C(27) | 1.391(3) |
| Ge(1) – C(7) | 1.962(2) | C(4) – C(3) | 1.382(3) |
| Ge(3) – C(31) | 1.947(2) | C(4) – C(5) | 1.388(3) |
| Ge(3) – C(25) | 1.951(2) | C(12) – C(11) | 1.387(3) |
| C(13) – C(14) | 1.391(3) | C(32) – C(33) | 1.384(3) |
| C(13) – C(18) | 1.399(3) | C(33) – C(34) | 1.384(3) |
| C(19) – C(20) | 1.397(3) | C(16) – C(15) | 1.386(3) |
| C(19) – C(24) | 1.402(3) | C(16) – C(17) | 1.390(3) |
| C(7) – C(12) | 1.398(3) | C(18) – C(17) | 1.386(3) |
| C(7) – C(8) | 1.399(3) | C(26) – C(27) | 1.390(3) |
| C(1) – C(2) | 1.3931(3) | C(2) – C(3) | 1.394(3) |
| C(1) – C(6) | 1.395(3) | C(8) – C(9) | 1.394(3) |
| C(25) – C(26) | 1.398(3) | C(36) – C(35) | 1.386(3) |
| C(25) – C(30) | 1.399(3) | C(23) – C(22) | 1.383(3) |
| C(14) – C(15) | 1.394(3) | C(9) – C(10) | 1.386(3) |
| C(6) – C(5) | 1.383(3) | C(11) – C(10) | 1.391(3) |
| C(31) – C(36) | 1.395(3) | C(22) – C(21) | 1.388(3) |
| C(31) – C(32) | 1.400(3) | C(34) – C(35) | 1.388(3) |

| | | | |
|---|---|---|---|
| C(19) – Ge(2) – C(13) | 110.29(9) | C(25) – Ge(3) – Ge(2) | 112.64(7) |
| C(19) – Ge(2) – Ge(3) | 103.66(6) | C(14) – C(13) – C(18) | 118.25(19) |
| C(13) – Ge(2) – Ge(3) | 106.42(6) | C(14) – C(13) – Ge(2) | 121.40(16) |
| C(19) – Ge(2) – Ge(1) | 108.78(6) | C(18) – C(13) – Ge(2) | 120.30(16) |
| C(13) – Ge(2) – Ge(1) | 108.54(6) | C(20) – C(19) – C(24) | 118.0(2) |
| Ge(3) – Ge(2) – Ge(1) | 118.943(13) | C(20) – C(19) – Ge(2) | 118.80(16) |
| C(1) – Ge(1) – C(7) | 109.33(9) | C(24) – C(19) – Ge(2) | 123.11(17) |
| C(1) – Ge(1) – Ge(2) | 109.63(7) | C(12) – C(7) – C(8) | 118.6(2) |
| C(7) – Ge(1) – Ge(2) | 112.15(6) | C(12) – C(7) – Ge(1) | 121.94(16) |
| C(31) – Ge(3) – C(25) | 111.12(9) | C(8) – C(7) – Ge(1) | 119.42(17) |
| C(31) – Ge(3) – Ge(2) | 113.77(7) | C(2) – C(1) – C(6) | 117.9(2) |
| C(2) – C(1) – Ge(1) | 121.36(17) | C(15) – C(16) – C(17) | 119.8(2) |
| C(6) – C(1) – Ge(1) | 120.72(17) | C(17) – C(18) – C(13) | 121.0(2) |
| C(26) – C(25) – C(30) | 118.3(2) | C(16) – C(15) – C(14) | 119.9(2) |
| C(26) – C(25) – Ge(3) | 119.52(17) | C(27) – C(26) – C(25) | 120.9(2) |
| C(30 – C(25) – Ge(3) | 122.17(17) | C(1) – C(2)) – C(3) | 121.2(2) |
| C(13) – C(14) – C(15) | 121.1(2) | C(9) – C(8) – C(7) | 120.5(2) |
| C(5) – C(6) – C(1) | 121.4(2) | C(6) – C(5) – C(4) | 119.9(2) |
| C(36) – C(31) – C(32) | 117.8(2) | C(4) – C(3) – C(2) | 119.8(2) |
| C(36) – C(31) – Ge(3) | 120.78(17) | C(18) – C(17) – C(16) | 120.0(2) |
| C(32) – C(31) – Ge(3) | 121.46(17) | C(35) – C(36) – C(31) | 121.4(2) |
| C(23) – C(24) – C(19) | 120.8(2) | C(22) – C(23) – C(24) | 120.0(2) |
| C(21) – C(20) – C(19) | 121.2(2) | C(10) – C(9) – C(8) | 120.1(2) |
| C(28) – C(29) – C(30) | 119.6(2) | C(23) – C(22) – C(21) | 120.1(2) |
| C(29) – C(28) – C(27) | 120.3(2) | C(23) – C(22) – C(21) | 120.0(2) |

| | | | |
|---|---|---|---|
| C(3) – C(4) – C(5) | 119.9(2) | C(33) – C(34) – C(35) | 119.6(2) |
| C(11) – C(12) – C(7) | 120.8(2) | C(20) – C(21) – C(22) | 120.0(2) |
| C(33) – C(32) – C(31) | 120.9(2) | C(26) – C(27) – C(28) | 119.9(2) |
| C(29) – C(30) – C(25) | 121.0(2) | C(9) – C(10) – C(11) | 119.9(2) |
| C(34) – C(33) – C(32) | 120.4(2) | C(36) – C(35) – C(34) | 119.9(2) |

**Table A.4.** coordinates (x $10^4$) and isotropic displacement parameters ($Å^2$ x $10^3$) for $HPh_2GeGePh_2GePh_2H$ (**3**).

| | x | y | z | U(eq) |
|---|---|---|---|---|
| H(14) | 4824 | 6306 | 6141 | 23 |
| H(6) | 5912 | 5086 | 8538 | 28 |
| H(24) | 7786 | 4117 | 4242 | 24 |
| H(20) | 8006 | 1648 | 6321 | 22 |
| H(29) | 8436 | 6168 | 10385 | 31 |
| H(28) | 8127 | 8195 | 9872 | 33 |
| H(4) | 2794 | 7496 | 9657 | 30 |
| H(12) | 5364 | 1159 | 6433 | 24 |
| H(32) | 7591 | 2508 | 8520 | 26 |
| H(3) | 8811 | 4566 | 9325 | 25 |
| H(33) | 8210 | 637 | 9203 | 29 |
| H(16) | 6590 | 9060 | 4687 | 27 |
| H(18) | 8963 | 5945 | 5215 | 23 |
| H(15) | 4617 | 8256 | 5472 | 25 |
| H(26) | 8499 | 7027 | 7248 | 27 |
| H(2) | 2090 | 5270 | 7616 | 26 |
| H(8) | 4377 | 2778 | 8912 | 25 |
| H(5) | 5113 | 6621 | 9591 | 34 |
| H(3A) | 1277 | 6805 | 8679 | 31 |
| H(17) | 8765 | 7897 | 4560 | 26 |
| H(36) | 11572 | 2572 | 7300 | 27 |
| H(23) | 8514 | 2550 | 3187 | 30 |
| H(9) | 4493 | 847 | 9622 | 30 |
| H(11) | 5478 | -762 | 7411 | 28 |
| H(22) | 8933 | 535 | 3696 | 32 |
| H(34) | 10491 | -297 | 8916 | 32 |
| H(21) | 8678 | 86 | 5265 | 28 |
| H(27) | 8133 | 8623 | 8305 | 30 |
| H(10) | 5058 | -922 | 8741 | 31 |
| H(35) | 12176 | 680 | 7960 | 31 |
| H(1) | 3790(20) | 3870(20) | 6348(16) | 27(7) |
| H(3) | 10260(30) | 4580(2) | 6614(19) | 49(8) |

VITA

Sangeetha P. Komanduri

Candidate for the Degree of

Doctor of Philosophy

Dissertation: SYNTHETIC, PHYSICAL, AND PHOTOLYTIC PROPERTIES OF LINEAR, BRANCHED, AND CYCLIC OLIGOGERMANES

Major Field: Chemistry

Biographical:

Education:

Completed the requirements for the Doctor of Philosophy in Chemistry at Oklahoma State University, Stillwater, Oklahoma in Aug, 2018.

Completed the requirements for the Bachelor of Science in Chemistry at University of Illinois at Urbana-Champaign, Urbana-Champaign, Illinois in 2013.

Publications:

- Hayatifar, A.; Shumaker, A. F.; Komanduri, S. P.; *et al.*, *J. Organomet. Chem.* **2018**, 37 (12), 1852-1859.
- Komanduri, S. P.; Schrick, A. C.; Daley, C. J. A.; Rheingold, A. L.; Weinert, C. S., *Main Group Chem.* **2017**, 16 (3), 217-225.
- Komanduri, S. P.; Shumaker, A. F.; *et al.*, *J. Organomet. Chem.* **2017**, 848, 104-113.
- Komanduri, S. P.; Shumaker, A. F.; Roewe, K. D.; Wolf, M.; Uhlig, F.; Moore, C. E.; Rheingold, A. L.; Weinert, C.S.; *Organomet.* **2016**, 35(18), 3240-3247.
- Komanduri, S. P.; Schrick, A. C.; Feasley, C. L.; Dufresne, C. P.; Weienrt, C.S.; *Eur. J. Inorg. Chem.* **2016**, 19, 3196-3203.

Professional Memberships:

- American Chemical Society